ROBUST OPTIMAL DESIGN AND ONLINE OPTIMAL CONTROL OF ZERO/LOW ENERGY BUILDINGS

HANGXIN LI

PhD

The Hong Kong Polytechnic University

2020

Temporary Binding for Examination Purposes

The Hong Kong Polytechnic University

Department of Building Services Engineering

ROBUST OPTIMAL DESIGN AND ONLINE OPTIMAL CONTROL OF ZERO/LOW ENERGY BUILDINGS

HANGXIN LI

A thesis submitted in partial fulfillment of the requirements for the degree

of Doctor of Philosophy

October 2019

CERTIFICATE OF ORIGINALITY

I hereby declare that this thesis is my own work and that, to the best of my knowledge and belief, it reproduces no materials previously published or written, nor material that has been accepted for the award of any other degree or diploma, except where due acknowledgement has been made in the text.

_____(Signed)

Hangxin Li (Name of student)

ABSTRACT

Abstract of thesis entitled: Robust Optimal Design and Online Optimal Control of Zero/Low Energy Buildings

Submitted by: Hangxin Li

For the degree of: Doctor of Philosophy

at The Hong Kong Polytechnic University in October, 2019

Energy conservation and environmental protection are among the most critical issues faced by the sustainable development of human societies. Zero and low energy buildings, as efficient means, are attracting increasing attentions from the society, government and professionals. Design and control play significant roles in achieving the zero/low energy goal and high energy efficiency for zero/low energy buildings. However, an effective design optimization method is still absent to identify global optimal design solutions for the entire zero/low energy buildings, including building envelope and energy systems, when a large number of design variables are involved. The impacts of uncertainties, which exist throughout building life cycle and probably lead to the failure of achieving zero/low energy goal, are ignored in current design practice. In addition, real-time multi-objective optimal control of energy systems is seldom studied. An effective approach is needed to achieve online multi-objective optimization for online multi-objective optimal controls.

This study therefore aims to develop an effective and comprehensive optimal design method

for zero/low energy buildings concerning uncertainties, and to develop an online multi-objective optimal control strategy for energy systems in zero/low energy buildings.

A coordinated optimal design method is proposed for the entire zero/low energy buildings on the basis of the existing multi-stage design optimization methods to effectively identify the global optimal design solutions, which need to consider the design optimization of building envelope and energy systems as a whole. It considers the interactions between design optimizations of building envelope and energy systems using an iterative approach. The results and experiences of the case studies show that the proposed coordinated design method can provide global optimal designs with robust performance efficiently. The life cycle "cost" of the optimal designs is 4% less and unmet cooling load is over 22% less compared with that given by existing multi-stage design optimization methods.

The impacts of alternative objective functions for robust optimal design concerning uncertainties are studied. A proper objective function for robust design optimization in building energy field is identified by analyzing and comparing the commonly-used objective functions in pioneer fields. Results show that the commonly-used objective functions in pioneer fields are not suitable if applied in building energy field directly without proper revisions. Revisions to objective functions, particularly the involvement of variance of performance indicator, are proposed for robust design optimization of buildings.

A coordinated robust design optimization method is proposed for the entire zero/low energy buildings by considering uncertainties and the interactions between robust design

optimizations of building envelope and energy systems, based on the coordinated optimal design method and robust optimal design method proposed. Point estimate method is used to quantify the uncertainties in the design inputs. The results of the case study show that the coordinated robust optimal design method is most robust in sustaining possible uncertainties in operation followed by coordinated optimal design method, compared with the existing multi-stage design methods. The coordinated robust optimal design achieved has 97% less accumulated unmet cooling load and 42% less system design objective value in average under possible uncertain scenarios, compared with that given by existing multi-stage design optimization methods.

A coordinated online multi-objective optimal control strategy consisting of two control optimization schemes are proposed for the predictive scheduling and real-time optimal control of energy systems in zero/low energy buildings. A cooperative game theory-based method is adopted for the online multi-objective optimizations. The control strategy and schemes are tested and evaluated on the energy systems with battery storage in the reference building. The test results show that it is essential and beneficial to coordinate the predictive scheduling and real-time optimal control in actual operation. The cooperative game theory-based method is effective for the online multi-objective optimization without the need of setting weights of different objectives.

PUBLICATIONS ARISING FROM THIS THESIS

Journal Papers published

[1] **Li, H.X.**, and S.W. Wang. 2017. Probabilistic optimal design concerning uncertainties and on-site adaptive commissioning of air-conditioning water pump systems in buildings. *Applied Energy* 202: 53-65.

[2] **Li, H.X.**, S.W. Wang, and H. Cheung. 2018. Sensitivity analysis of design parameters and optimal design for zero/low energy buildings in subtropical regions. *Applied Energy* 228, 1280-1291.

[3] **Li, H.X.**, S.W. Wang, and R. Tang. 2019. Robust optimal design of zero/low energy buildings in subtropical regions considering uncertainties and the impacts of objective functions. *Applied Energy* 254. (Online)

[4] Tang, R., **H.X. Li**, and S.W. Wang. 2019. A game theory-based decentralized control strategy for power demand management of building cluster using thermal mass and energy storage. *Applied Energy* 242: 809-820.

[5] Tang, R., S.W. Wang, and **H.X. Li**. 2019. Game theory based interactive demand side management responding to dynamic pricing in price-based demand response of smart grid. *Applied Energy* 250: 118-130.

[6] **Li, H.X.**, and S.W. Wang. 2019. Coordinated optimal design of zero/low energy buildings and their energy systems based on multi-stage design optimization. *Energy* 189: 116202.

[7] **Li, H.X.**, and S.W. Wang. 2019. A systematic and probabilistic approach for

optimal design and on-site adaptive commissioning of building central cooling systems concerning uncertainties. *Science and Technology for the Built Environment*, under second review.

[8] **Li, H.X.**, and S.W. Wang. 2019. Model-based multi-objective predictive scheduling and real-time optimal control of energy systems in zero/low energy buildings using a game theory approach. Automation in Construction, under review.

Journal papers in preparation

[1] **Li, H.X.**, and S.W. Wang. 2019. Coordinated robust optimal design of building envelope and energy systems considering uncertainties. recommended for Applied Energy.

Conference papers

[1] **Li, H.X.**, S.W. Wang, and F. Xiao. 2019. Probabilistic optimal design and on-site adaptive commissioning of building air-conditioning systems concerning uncertainties. *Energy Procedia* 158: 2725-2730.

[2] **Li, H.X.**, S.W. Wang, and H. Cheung. 2018. Sensitivity analysis and probabilistic optimal design of zero/low energy buildings in subtropical regions. *Proceeding of Building Simulation and Optimization 2018*, Cambridge, UK, September 10-12.

[3] **Li, H.X.**, and Wang, S.W. 2019. A modified multi-stage design optimization approach for zero energy buildings considering uncertainties. *Proceeding of ICAE 2019--The 11th International Conference on Applied Energy 2019,* Västerås, Sweden, August 12-15.

ACKNOWLEDGEMENTS

I would like to express my sincerest appreciation to Professor Shengwei Wang, my supervisor, for his patient supervision, valuable suggestions, encouragement and continuous support during the period of my Ph.D study. Also, I would like to thank Professor Fu Xiao**,** for her valuable suggestions and support.

I would also like to thank all teammates in the Building Energy and Automation Research Laboratory, especially Dr. Howard Cheung, Dr. Rui Tang, Dr. Maomao Hu and Dr. Kui Shan. Their talents and diligence always inspire and encourage me to be better.

Finally, I am truly grateful for the love and support from my family and friends. Without them, I would not have been able to thrive in some hard time during my doctoral program.

TABLE OF CONTENTS

LIST OF FIGURE

LIST OF TABLE

NOMENCLATURE

A	area (m^2)
C	optimization constraints for predictive scheduling
C'	optimization constraints for real-time optimal control
Cap	design capacity (kW/kWh)
COP	coefficient of performance of chiller
D	infeasible performance
E	energy (kWh)
$E(\cdot)$	weighted average
F	combined objective
$\tilde{F}$	combined objective for robust optimization
FC	fuel consumption (kW)
GII	grid impact index
H	total number of control action time intervals concerned in one day
IC	initial cost (USD)
K	temperature coefficient of the maximum generation power of PV panels (1/K)
L	total length of linear thermal transmittance (m)
M	number of uncertain inputs concerned
N	number of optimization objectives concerned
NCC	number of charge cycles
OC	operation cost (USD)
P	power (kW)
PMV	predicted mean vote
$Prb(\cdot)$	probability of occurrence
Q	thermal load (kW)
RC	replacement cost (USD)

RPC	rotor power coefficient
S	coordinating design/control variables
T	temperature (°C)
TC	total cost (USD)
U	U value
X	vector of design/control variables
Z	supercriterion
a	penalty ratio for infeasible performance of building
a'	penalty ratio for infeasible performance of energy systems
a1	penalty ratio for unmet power
a2	penalty ratio for unmet cooling load
a3	penalty ratio for grid impact
c	unit price
f	performance/objective concerned
$g(\cdot)$	equality design constraints
$h(\cdot)$	inequality design constraints
k	years in building life cycle
l	partial load
m	flow rate (m^3/s)
n	number
p	vector of design/control inputs
r	solar radiation (kW/m^2)
s	scaling factor
t	time
v	velocity (m/s)
w	weight
x	variable

Greek letters

γ	the coefficient of skewness
ξ	standard location
η	efficiency
μ	mean
ρ	air density (kg/m^3)
σ	standard deviation
χ	point thermal transmittance (W/K)
ψ	linear thermal transmittance (W/(m·K))
Δt	time interval
ΔT	time interval

Subscripts

AC	absorption chiller
AHU	air handling units
AL	standalone
CG	co-generators
CL	cooling load
CT	cooling tower
EC	electric chiller
EL	electrical power load
GC	grid-connected
PS	predictive scheduling
PV	photovoltaic
RT	real-time optimal control
WT	wind turbine
air	air
amb	ambient

bat	battery
cell	cell
ch	battery charge
clp	cooling water pumps
cw	chilled water
cwp	chilled water pumps
dch	battery discharge
dem	demand
design	design value
dis	thermal discomfort
ele	electricity
env	envelope
ex	export
fuel	fuel
grid	power grid
hr	heat recovery
hub	hub of wind turbine
i	count number
im	import
inv	inverter
j	count number
max	the maximum value
min	the minimum value
ni	normalized value of the *i*th (objective)
op	*in operation*
ref	reference
sa	sensitivity analysis

sup	supply
sys	system
tif	feed in tariff
tot	total
umt	unmet
wst	the worst value

CHAPTER 1 INTRODUCTION

1.1 Background and Motivation

Energy conservation and environmental protection are among the most critical issues faced by the sustainable development of human societies. The concerns about the increase in energy consumption and its adverse impacts on the environment are even growing since the global energy consumption keeps increasing. Between 1971 and 2016, the world total primary energy supply increased by almost 2.5 times, and the world carbon dioxide (CO_2) emissions from fuel combustion rose by 1.3 times (from 13.9 to 32.3 billion tonnes). Energy-related air pollution keeps leading to millions of premature deaths each year. The early data in 2018 indicate a continued growth, which makes a trajectory far from climate goals. Among these countries, China is the largest energy consumer since 2009. During 1971-2016 the total final energy consumption in China increased markedly from 0.34 to 1.98 billion tonnes (an average annual increase of 10.7%), and the total CO_2 emissions from fuel combustion increased from 0.79 to 9.10 billion tonnes (International Energy Agency, 2018). The energy and environmental issues would be more critical if there were no continued improvements in energy efficiency and powerful policies (Li et al., 2013).

Buildings account for a significant proportion of the energy consumption and CO_2 emissions. Buildings consumes over 40% of the total end-use energy and account for one-third of CO_2 emissions (International Energy Agency, 2017) globally. In Hong Kong, buildings consume 80% of end-use energy and 90% of electricity (EMSD, 2016). The proportion even keeps growing in response to the warmer climate, higher expectations for thermal comfort and more applications of computing and communication systems (EMSD, 2016; Yan et al., 2012). It is widely accepted that the greatest scope for the reduction of energy demand and CO_2 emission lay in improving the building stock (Clift,

2007). As the zero/low energy consumption principle is viewed as an efficient means to reduce carbon emissions and dependence on fossil fuels, zero/low energy buildings are gaining increasing attentions from the society, government and professionals (Kolokotsa et al., 2011; Torcellini et al., 2006; Rodriguez-Ubinas et al., 2014).

A low energy building is a building which enables to provide high living standards and comfort with low energy consumption through energy-efficient design and technical measures (Sartori and Hestnes, 2007). A zero energy building (ZEB) is a building with greatly reduced energy needs through efficiency gains such that the balance of energy needs can be supplied with renewable technologies (Torcellini et al., 2006). The reason why zero/low energy buildings are efficient means or the major benefits of zero/low energy buildings are that building energy demand is largely reduced through energy efficiency strategies, and CO_2 emissions is also significantly reduced by fully using renewable energy resources. In addition, the concept of zero/low energy encourages the immediate awareness and better understanding of energy use for the occupants in buildings.

Many countries have adopted policies or regulations to promote the development of zero/low energy buildings. For instance, in European Union (EU), an Energy Performance of Buildings Directive (EPBD) is proposed to meet the target for energy efficiency improvements. It requires that all new buildings must be net zero energy buildings by 2021. Nowadays, there are quite a number of zero/low energy buildings in the worldwide already. Examples include the Beddington Zero Energy Development (BedZED) in the UK, the Zero Energy Building of BCA Academy in Singapore, Samsung's Green Tomorrow of Korea, Magic School of Green technology in National Cheng Kung University in Taiwan, Zero Energy Office Building developed by the

National Institute of Environmental Research of Korea, the Cascadia Centre for Sustainable Design and Construction in USA, and the Hong Kong Zero Carbon Building (ZCB). The numbers of zero/low energy buildings could be increased significantly in the future since the progress made in new technologies and the increased costs of traditional fossil fuels make the development of zero/low energy buildings more possible and easier. However, there are still some big technical challenges faced by the development of zero/low energy buildings:

Firstly, the design optimization of the entire zero/low energy buildings (including building envelope and energy systems) generally involves a large number of design variables, which poses a big challenge in searching the global optimal design solution. It is very difficult to obtain the global optimal design solution when the number of design variables to be optimized is too large. An effective design optimization method is needed to identify the global optimal design solutions for zero/low energy buildings.

Secondly, most of the existing design methods are performed under presumed and fixed design conditions, which probably leads to the failure of achieving zero/low energy goal. Existing design methods consider the uncertain nature of design/operation condition by assigning a safety factor blindly. It very likely overestimates the energy demand and generation, which may lead to low energy efficiency and failure of achieving zero energy goal in operation (Gang et al., 2016; Zhang et al., 2016; Tian and Wilde, 2011). The development of design (optimization) method considering uncertainties based on a quantitative approach is essential to assure high energy efficiency and the achievement of zero/low energy goal for zero/low energy buildings.

Thirdly, renewable energy generation systems such as wind turbines and solar photovoltaics (PV) bring a major source of affordable electricity with low-emissions, but

create additional requirements for the reliable operations/control of power and building energy systems. Online optimal control of energy systems plays a significant role in improving energy efficiency and assuring reliable operations of zero/low energy buildings. However, increasing concerns on different performance indicators pose more challenges to the online optimal control of building energy systems. The development of an effective online multi-objective optimal control strategy including both predictive scheduling and real-time optimal control is needed.

1.2 Aim and Objectives

The aim of this PhD study is to develop an effective and comprehensive optimal design method for zero/low energy buildings concerning uncertainties, and an online multi-objective optimal control strategy for energy systems in zero/low energy buildings. It is accomplished by addressing the following objectives:

1. Develop a building simulation platform consisting of building performance model and energy system models. The building performance model and energy system models are used for the test and validation of the proposed (robust) optimal design methods and online optimal control strategy.
2. Develop a holistic sensitivity analysis method and perform sensitivity analysis to investigate the impacts of design parameters and uncertain design inputs on the performance of zero/low energy buildings in the specific regions concerned (i.e., subtropical regions in this study). The intention is to identify the key design parameters and main uncertain design inputs of zero/low energy buildings in subtropical regions for the test and validation of the proposed (robust) optimal design methods.

3. Develop a coordinated optimal design method for the entire zero/low energy buildings, including building envelope and energy systems. The method is expected to obtain the global optimal design solution, which needs to consider building envelope and building energy systems as a whole in the optimization, with much less computing cost.
4. Study the robust optimal envelope design of zero/low energy buildings and evaluate the existing objective functions for robust design optimization concerning uncertainties. The performance of optimal design solutions obtained using different objective functions is compared to identify the proper objective function for the robust design optimization in building energy field.
5. Develop a coordinated robust optimal design method for the entire zero/low energy buildings including building envelope and energy systems concerning uncertainties. The method is expected to effectively achieve the solutions with best performance even under uncertain operation conditions.
6. Develop an online multi-objective optimal control strategy for the predictive scheduling and real-time optimal control of energy systems in zero/low energy buildings. The strategy is expected to provide optimal schedules and control decisions effectively without the need of specifying weights for different optimization objectives.

1.3 Organization of the thesis

This thesis consists of 9 chapters, which is organized as follows.

Chapter 1 presents the background and motivations for developing zero/low energy buildings. The technical challenges faced by the development of zero/low energy buildings are discussed. Then the aim and objectives of this study are presented as well

as the organization of this thesis.

Chapter 2 presents an overview of zero/low energy buildings, and a comprehensive literature review on the optimal design and control issues of zero/low energy buildings as well as the uncertainty analysis and its applications in building energy field. Design optimization is reviewed in terms of the impacts of climate/site on building design, design optimization methods, optimization algorithms, and design objectives. The review on the optimal control of energy systems covers optimal control methods, online control optimization methods, and control objectives. Uncertainty analysis is reviewed in terms of uncertainty quantification methods, robust optimal design methods concerning uncertainties and robust optimal design in building energy field. The research gaps in the above subject areas are summarized.

Chapter 3 presents an overview of the passive and active design strategies used in the reference building and the building simulation models. The Zero Carbon Building (ZCB), a ZEB developed in Hong Kong, is selected as the reference building to develop the simulation platform for the test and validation of the proposed design optimization methods and optimal control strategy. The simulation platform consists of building performance models and energy system models.

Chapter 4 presents the identification of key envelope design parameters and main uncertain design inputs which have significant impacts on the performance of zero/low energy buildings in subtropical regions. A multi-stage sensitivity analysis method is proposed and used to identify the key envelope design parameters that significantly affects the building performance. Key system design parameters are selected. The main uncertain design inputs, which have significant impacts on building performance, is also identified through sensitivity analysis.

Chapter 5 presents the procedure and methods of the proposed coordinated design optimization method for the entire zero/low energy buildings. An artificial neural network (ANN) building performance model is used to reduce computing time, which is trained and validated prior to being used. Three case studies, involving a case of standalone low energy buildings, a case of grid-connected low energy buildings and a case of grid-connected ZEBs, are conducted to validate the coordinated optimal design method.

Chapter 6 presents the procedure and methods of the robust design optimization for zero/low energy buildings considering uncertainties, and the impacts of the alternative optimization objective functions on robust design optimization. Three case studies using different objective functions are conducted to study the robust optimal envelope design of zero/low energy buildings using the ANN model as the building performance model. The performance of optimal building design obtained using different optimization objective functions are compared to identify the proper objective function for the applications in building energy field.

Chapter 7 presents the procedure and methods of the coordinated robust design optimization method for entire zero/low energy buildings concerning uncertainties. Point estimate method is adopted for uncertainty quantification to largely reduce the uncertain scenarios which need to be considered. One case study is conducted to test and validate the coordinated robust design optimization method.

Chapter 8 presents a coordinated online multi-objective optimal control strategy for energy systems in zero/low energy buildings based on a game theory approach. The control strategy consists of a multi-objective predictive scheduling scheme and a real-time multi-objective optimal control scheme. A cooperative game theory-based method is adopted for the online multi-objective optimizations of predictive scheduling and real-

time optimal control. Two case studies are conducted to test and evaluate the control strategy.

Chapter 9 summarizes the main contributions and conclusions of the work conducted in this PhD project, and gives recommendations for future research on the research subjects concerned.

CHAPTER 2 LITERATURE REVIEW

A comprehensive literature review on the concept, optimal design and control of zero/low energy buildings is conducted to provide the research background and a clear picture of what have been done and what needs to be done (i.e., the research gaps) in the research domain of this study.

Section 2.1 presents an overview of zero/low energy buildings, including the definitions and energy calculation methods, the regulations/policies, and the worldwide development. *Section 2.2* presents a review on the design optimization of zero/low energy buildings, including the impacts of main design parameters and climate/site, design optimization methods, optimization algorithms and the design objectives. *Section 2.3* presents a review on the optimal control of energy systems in zero/low energy buildings. *Section 2.4* presents a review on the uncertainty analysis and its applications in building energy field. *Section 2.5* presents a summary of the research gaps in the above research areas.

2.1 An overview of zero/low energy buildings

2.1.1 Definitions and the zero energy calculation methods

Low energy buildings are broadly defined, but are generally known as buildings which enables to provide high living standards and comfort with low energy consumption through energy-efficient design and technical measures (Sartori and Hestnes, 2007). They have lower energy demand than common buildings regulated by national building codes. "Low energy buildings" may refer to a specific type of buildings in some countries or buildings with lower energy demand such as passive houses and zero energy buildings in general in other countries.

Similarly, ZEBs are defined using a wide range of terms and expressions in the existing literature, but are generally known as buildings with greatly reduced energy needs through efficiency gains such that the balance of energy needs can be supplied with renewable technologies (Torcellini et al., 2006). Most of the existing "zero energy" calculation methods are developed just for a specific ZEB case, on the basis of the methodologies proposed by the researchers participating in the IEA SHC Task 40/ECBCS Annex 52 'Towards Net Zero Energy Solar Building' or the methodology suggested by Hernandez and Kenny (2010). A commonly agreed definition and a standard calculation method of zero energy balance is still absent for ZEBs. Detailed review on the existing studies on the definitions and zero energy calculation methods of zero energy buildings are presented as follows.

Torcellini et al. (2006) summarized four commonly-used definitions of ZEBs including: "net zero site energy", "net zero source energy", "net zero energy costs", and "net zero energy emissions". A net zero site energy building produces at least as much energy as it uses in a year, when accounted for at the site. A net zero source energy building produces at least as much energy as it uses in a year, when accounted for at the source. The source energy refers to the primary energy used to generate and deliver the energy to the site. To calculate the total source energy of a building, the energy consumed at the site should be multiplied by a corresponding site-to-source conversion factor. In a cost ZEB, the amount of money the utility pays the building owner for the energy exported to the grid is at least equal to the amount the owner pays the utility for the energy imported from the grid over a year. A net-zero emissions building produces at least as much emissions-free renewable energy as it uses from emissions-producing energy sources in a year.

Hernandez and Kenny (2010) proposed a definition of life cycle zero energy buildings.

The definition of zero energy building is extended to include the embodied energy of buildings and their components. The REHVA Task Force proposed a technical definition for nearly net ZEBs, which is required in the implementation of the EPBD recast (Kurnitski et al., 2011). Based on the definition in the directive, net ZEB is a building using 0 kWh/(m²·a) primary energy. Based on the cost-optimality principle of the directive, nearly net ZEB is defined as a building with national cost optimal energy use of > 0 kWh/(m² a) primary energy.

Marszal et al. (2011) discussed several important issues for developing a new ZEB definition and the associated zero energy calculation method. These issues include the metric of balance, the balance period, the type of energy use included in the balance, the type of energy balance, the accepted renewable energy supply options, the connection to the energy infrastructure, and the requirements for energy efficiency, indoor climate and building-grid interactions.

Sartori et al. (2012) proposed a consistent framework of developing a definition for ZEBs. The framework involves five main criteria, including: building system boundary, weighting system, net zero energy balance, temporal energy match characteristics, and measurement and verification. Building system boundary includes physical boundary, balance boundary and boundary conditions. Weighting system includes metrics, symmetry and time dependent accounting. Net zero energy balance includes balancing period, type of balance, energy efficiency, and energy supply. Temporal energy match characteristics includes load matching and grid interaction.

2.1.2 Regulations/policies

The goals for implementing zero/low energy buildings are discussed and proposed in many countries. For instance, in the USA, the Energy Independence and Security Act of

2007 authorizes the Net-Zero Energy Commercial Building Initiative to support the goal of net zero energy for all new commercial buildings by 2030. Besides, it specifies a zero-energy target for 50% of U.S. commercial buildings by 2040 and a zero-energy target for all U.S. commercial buildings by 2050 (Crawley et al., 2009). In Canada, the Government released Build Smart (i.e., Canada's Buildings Strategy), which seeks to significantly increase the energy efficiency of Canadian buildings in pursuit of a net zero energy ready level of performance (Natural Resources Canada, 2017).

In Europe, the Energy Performance of Buildings Directive recast (EPBD recast) establishes the 'nearly zero energy building' as the building target from 2018 for all public owned buildings or buildings occupied by public authorities and from 2020 for all new buildings (Official Journal of the European Union, 2010). In UK, the BC Energy Step Code has entered into legal force in British Columbia, which is designed as a technical roadmap to help the province to reach its target that all new buildings will attain a net zero energy ready level of performance by 2032 (Province of British Columbia, 2018).

In Japan, the government sets the goal of ZEB to be the standard of new constructions by 2020 ("Zero-energy building," n.d.). In Malaysia, the Sustainable Energy Development Authority Malaysia started a voluntary initiative called Low Carbon Building Facilitation Program in 2016 to support the current low carbon cities program (Lojuntin, 2018). In Singapore, a climate action plan specifies a goal of green building for 80% of the buildings by 2030 to combat climate change (National Climate Change Secretariat, 2016).

In China, the central government sets the target to achieve peak carbon dioxide emission around 2030, and increase non-fossil fuel usage to 20% of total energy share (NDRC, 2015). In Hong Kong, the SAR government sets the target to reduce the carbon intensity by 65–67% by 2030 using 2005 as the baseline, which is equivalent to an absolute

reduction of 26%-36% or a reduction of 3.3-3.8 tonnes per capita (Environment Bureau, 2017).

2.1.3 Worldwide development

Communities, governments and construction industries in many countries and regions have taken many efforts to develop new zero/low energy buildings and low energy retrofit for existing buildings to combat climate change and energy crisis. There are quite a number of zero/low energy buildings in the world already. Most of them are in Europe and USA. The examples include: the BedZED in the UK, the Zero Energy Building of BCA Academy in Singapore, Samsung's Green Tomorrow of Korea, Magic School of Green technology in National Cheng Kung University in Taiwan, Zero Energy Office Building developed by the National Institute of Environmental Research of Korea, the Cascadia Centre for Sustainable Design and Construction in USA, the Zero Carbon Building in Hong Kong SAR, and the Pearl River Tower in Guangzhou of China.

Besides the demonstration projects, many studies have been conducted in different countries to support the development of zero/low energy buildings. Between 2008 and 2013, researchers from the United Kingdom, the United States and 17 other countries were working together in a joint research program "Towards Net Zero Energy Solar Buildings" in order to bring the net zero energy concept to market viability. The objective of the joint research program was to develop a common understanding, a harmonized international applicable definition framework, advanced building design and technology solutions, and industry guidelines for ZEBs. The scope covers new and existing buildings located within the climate zones of the participating countries.

2.2 Design optimization of zero/low energy buildings

2.2.1 Impacts of main design parameters and climate/site

The impacts of the main building design parameters on building performance in different climates/sites have been studied by many researchers (Sanchez et al., 2014; Yang et al., 2016; Tian, 2013; Bernal-Agustín and Dufo-Lopez, 2009; Li et al., 2013; Chen et al., 2017; Singh et al., 2016; Dall'O' et al., 2013; Kurnitski et al., 2011). The results show that the highly-sensitive parameters of building performance are different in different climate regions as listed in Table 2.1 (Yildiz and Arsan, 2011; Yu et al., 2013; Lam and Hui, 1996; Zhao et al., 2015; Heiselberg et al., 2009; Corrado and Mechri, 2009; Mechri et al., 2010; Spitz et al., 2012). The internal loads, infiltration and temperature set-point of heating, ventilation and air-conditioning (HVAC) systems were proven to be the highly-sensitive parameters in all climate regions (Yildiz and Arsan, 2011; Yu et al., 2013; Lam and Hui, 1996; Sanchez et al., 2014). Thermal insulation of external walls is important for buildings in the climate regions with cold winter (Yu et al., 2013; Sanchez et al., 2014; Zhao et al., 2015), while window area, glazing and solar protection are very influential to building energy consumption in the climate regions with hot summer (Yildiz and Arsan, 2011; Yu et al., 2013; Lam and Hui, 1996; Zhao et al., 2015). For buildings in the climate regions with mild seasons, natural ventilation can make a great contribution to reducing the building cooling demands (Heiselberg et al., 2009). However, there are two limitations in the existing studies. First, single sensitivity analysis method is usually adopted to assess the design parameters which may lead to the missing of important design parameters. Yang et al. (2016) recommended that at least two fundamentally different sensitivity analysis methods should be performed to provide more robust results. Second, current sensitivity analysis does not comprehensively address design parameters

and the identification of key design parameters since many other non-design parameters are involved.

Table 2.1 Summary of sensitivity analysis in previous studies

Reference	Analysis method	Site/climate region	Performance objectives	Highly-sensitive (envelope) parameters
Yildiz and Arsan (2011)	Regression (SRRC)	Hot-humid	Cooling load & heating load	Total window area, window U value and window solar heat gain coefficient
Yu et al. (2013)	Local sensitivity analysis	Hot summer and cold winter	Cooling load & heating load	Wall U value and window to wall ratio (WWR)
Lam and Hui (1996)	Local sensitivity analysis	Hong Kong (Hot humid summer and mild winter)	Annual energy consumption, peak design loads and load profiles	Shading coefficient, WWR, space air temperature, equipment load, lighting load and occupancy density
Zhao et al. (2015)	Local sensitivity analysis	Severe cold, cold, hot summer and cold winter, hot summer and warm winter, mild	Annual energy consumption	Infiltration rate and wall insulation thickness (climate regions with cold seasons); shading coefficient, window solar heat gain coefficient and wall insulation thickness (climates with hot/warm seasons);
Heiselberg et al. (2009)	Morris	Denmark (cool summer and mild winter)	Annual energy consumption	Lighting control and ventilation rate in winter
Corrado and Mechri (2009)	Morris	Turin (humid subtropical climate)	Cooling load, heating load, heating degree days etc. (14 objectives)	Indoor temperature, air change rate, number of occupants, metabolism rate, and equipment heat gains
Mechri et al. (2010)	FAST	Italy (three climate zones)	Cooling load & heating load	Envelope transparent surface ratio and compactness ratio
Spitz et al. (2012)	Sobol	France (hot summer and cold winter)	Indoor air temperature	Infiltration rate, internal gains, window U value, capacity of electric heating and heat exchanger efficiency

Note: SRRC refers to standardized rank regression coefficient. FAST refers to Fourier amplitude sensitivity testing.

2.2.2 Design optimization methods

The parameters or design are generally optimized using two approaches. The typical approach adopted in the old days can be regarded as "local design optimization" which optimizes individual design parameter one-by-one (Baker, 1987). The typical approach adopted in recent years can be regarded as "global design optimization" which optimizes all the concerned design parameters at the same time (or optimizes the design parameters group by group) to identify the optimal set of the design parameters. The first approach has its limitation that the obtained design options may not be the global optimum since it ignores the correlations and interactions between the design parameters. The second approach can overcome this drawback. So far, most of the building design optimization studies focus on the regions with cold winters. This is probably due to the government policy (e.g. European initiatives) and the urgency for the cold regions to reduce building energy consumption. The envelope design optimization of zero/low energy buildings without heating in subtropical regions is seldom studied. Most studies on the design optimization for zero/low energy buildings in subtropical regions focused on building energy systems (Lu et al., 2015; Sun, 2015; Fong and Lee, 2012; Kumar et al., 2009; Lu et al., 2015; Liu et al., 2015). In addition, the design parameters are determined mainly based on experiences and previous impact studies in similar climate regions. Very few researchers addressed sensitivity analysis on design parameters and design optimization comprehensively.

Previous studies about the "global design optimization" of zero/low energy buildings mainly addressed three tasks, including: *i*. design optimization of building envelope only (Li et al., 2018; Thalfeldt et al., 2013), *ii*. design optimization of building energy systems only (Lu et al., 2015; Kaabeche and Ibtiouen, 2014; Ismail et al., 2012; Lu et al., 2015; Lu et al., 2015; Daud and Ismail, 2012; José and Rodolfo, 2009; Diaf et al., 2008; Zhang

et al., 2016), and *iii*. design optimization of the entire building including both building envelope and energy systems (Marszal and Heiselberg, 2011; Georges et al., 2012; Ferrara et al., 2014; Hamdy et al., 2012; Kapsalaki et al., 2012; Hamdy et al., 2013; Kurnitski et al., 2011; Rysanek and Choudhary, 2012; D'Agostino and Parker, 2018). For the task *i*, Thalfeldt et al. (2013) identified the cost optimal façade solutions for nearly ZEBs in Estonia. For the task *ii*, Lu et al. (2015) optimized renewable energy systems of standalone and grid-connected ZEBs using single-objective optimization and multi-objective optimization methods respectively. Kaabeche and Ibtiouen (2014) adopted an iterative approach to optimize the sizing of various standalone PV/wind/diesel/battery hybrid system components for zero load energy deficit. Ismail et al. (2012) optimized a PV/diesel/battery standalone hybrid system to minimize its cost.

The methods presented in the literature for design optimization of both building envelope and energy systems (i.e., the task *iii*) can be classified as two main categories. The first category is “simultaneous design optimization method”. The methods in this category aim at optimizing design variables of building envelope and energy systems simultaneously (Marszal and Heiselberg, 2011; Georges et al., 2012; Ferrara et al., 2014; Hamdy et al., 2012; Kapsalaki et al., 2012). Marszal and Heiselberg (2011) explored the cost optimal design for a residential net ZEB in Denmark by searching among three levels of building envelope design and three alternatives of energy system design. Georges et al. (2012) investigated a single-family dwelling in Belgium by analyzing the combinations of sixteen heating systems and five building designs. Optimal designs were selected among limited number of possible design solutions in these studies (Marszal and Heiselberg, 2011; Georges et al., 2012; Hamdy et al., 2013). More effective optimization tools/algorithms were introduced for effective search among wider search spaces with lower computation cost. Ferrara et al. (2014) optimized 10 design variables of building

envelope and the associated technical system using Genopt as the optimizer and TRNSYS as the simulation tool. More than 6×10^3 simulations were performed in order to find the optimal design solution among 14×10^9 possible design solutions. Hamdy et al. (2012) optimized 9 design variables of building envelope and energy supply system for a nearly ZEB using GenOpt. 18,000 - 400,000 evaluations were performed to identify the cost optimal design solution among 1,306,368 possible design solutions using three different optimization algorithms. It is found that the computation costs of these methods highly depend on the settings of the optimization algorithms and the number of variables to be optimized. For example, the computation cost of genetic algorithm (GA) generally increases exponentially with the increased number of design variables to be optimized. In addition, the use of simulation software tools for evaluating building envelope and energy systems can further increase the computation cost and complexity of design optimization. In fact, as stated by Ting (2005), it is extremely difficult to achieve the optimal design using simultaneous optimization methods when the number of design variables is too large.

The second category is “multi-stage design optimization method”. Most methods in this category break down the whole design optimization task into several subtasks and effective optimization algorithms/tools are adopted to speed up the search in each of the subtasks (Hamdy et al., 2012; Kurnitski et al., 2011; Rysanek and Choudhary, 2012; D'Agostino and Parker, 2018). For example, Hamdy et al. (2013) proposed a multi-stage optimization method. In the first stage, design variables of building envelope and heat recovery unit are optimized to minimize the primary energy consumption of a building. In the second stage, optimal heating/cooling system is identified by assessing the financial and environmental viability of the combinations of heating/cooling systems and the selected building envelope designs. In the third stage, renewable energy system is

optimized for the objective of cost minimization while subject to sufficient energy production. After breaking down the optimization task into three subtasks, optimization was achieved by only 3,200 evaluations to optimize 11 design variables, which would need to evaluate more than 3×10^9 design options if exhaustive search was applied. Kurnitski et al. (2011) proposed a seven-step procedure to minimize the life cycle cost of nearly ZEBs. Where, 7 design variables were optimized in 2 stages. Rysanek and Choudhary (2012) decoupled the whole-building optimization of 17 variables into three stages for expedient exhaustive search of low-carbon and low-energy building refurbishment options. Ascione et al. (2016; 2017; 2019) proposed multi-stage design optimization methods for building design and retrofitting respectively. The whole design optimization task was divided into two main stages: envelope design optimization and energy system design optimization. The multi-stage design optimization methods reduce computation cost greatly by avoiding unfeasible combinations of building envelope and energy system designs (Hamdy et al., 2013). However, these existing multi-stage optimization methods assume no impacts of energy system design optimization on the optimal envelope design and ignore the possible interactions between building envelope and building energy systems. The optimal solutions achieved are "local optimal solutions" of building envelope and energy systems separately rather than "global optimal solutions" considering the building envelope and the energy system as a whole.

Different design solutions were identified using different methods for different climate requirements and design goals as introduced above. However, these designs are identified under presumed and fixed design conditions. This kind of design methods are generally termed as "deterministic design optimization". It is probable to fail to achieve zero/low energy goal using deterministic design optimization method, as the energy demand may be underestimated and the energy system may be oversized/undersized by ignoring

uncertain nature of design condition (Gang et al., 2016; Zhang et al., 2016; Tian and Wilde, 2011). Zhou et al. (2016) investigated the actual operational performance of a ZEB in Tianjin. The actual power consumption was 30.9% higher than that predicted at the design stage, and the actual PV power generation was only 36.8% of the amount predicted at the design stage. As a result, the electricity generated from the PV system could meet 29.5% of the actual building energy demand only, though a safety factor of 1.2 was considered in the design of the PV system. Therefore, it is necessary to consider the uncertainties in the design of zero/low energy buildings.

2.2.3 Design optimization algorithms

The optimization algorithms for building envelope design mainly includes the direct search method and stochastic population-based search method (Huang and Niu, 2016). The direct search method searches around the current/initial solution point. In general, an initial point is defined at first. A series of points are then searched, and their objective function values are evaluated and compared. If the objective function value of a point is closer to the optimization target compared with other points, this point is updated as the current point. These steps are repeated until reaching the optimization target (Hooke and Jeeves, 1961). There are two types of direct search methods: the gradient-deterministic method and the gradient-free method. The gradient-deterministic search is the most straightforward optimization method. In a gradient-deterministic problem, the optimal solution can be easily obtained by going in the direction that has a reducing gradient. It is found that the gradient-deterministic search method was adequate to solve the building design optimization problem concerning energy conservation (Asadi et al., 2014). But it may be inadequate for solving other building design optimization problems such as the design concerning thermal comfort (Adamski, 2007). The gradient-free search method

does not require any information about the gradient of the objective function. Different searching rules are used by this method to search the optimal solution until no further increase or decrease in the objective value is observed.

The most popular stochastic population-based search method is evolutionary algorithm (Huang and Niu, 2016). The typical process of searching the optimal solution(s) using the evolutionary algorithm includes selection, crossover and mutation. A series of points are generated randomly as the initial population at first. The objective value of each point is then evaluated and compared. The points which best fit the optimal solution are selected as the parents, which are used to reproduce the children through crossover and mutation. The parents and their children constitute the new population, which would go through a new round of selection and reproduction. These steps are repeated until the termination condition of the algorithm is satisfied (Back, 1996). Compared with the direct search method, the evolutionary algorithm has better accuracy and higher adaptability. Genetic algorithm, as an evolutionary algorithm, is the most favorable optimization method in optimal design of building envelope (Huang and Niu, 2016).

Similarly, the main optimization techniques for building energy system design include genetic algorithm, particle swarm optimization, linear programming, and stochastic approach. Other techniques are also adopted, such as simulated annealing, neural networks, simplex algorithm, dynamic programming, iterative and probabilistic approaches, design space based approach, etc. (Erdinc and Uzunoglu, 2012). Among them, genetic algorithm is also the most widely used for the design cases of building energy systems. Compared with the building envelope design optimization, the design optimization of building energy systems often involves both continuous and discrete design variables, especially when the number of the system components need to be

optimized. In this situation, mixed-integer nonlinear programming is preferred. In MATLAB, genetic algorithm is integrated with the mixed integer nonlinear programming, which enables optimizing the continuous and discrete design variables at the same time.

2.2.4 Design objectives

The main objectives concerned in the design optimization of building envelope include energy performance index, life cycle cost index, thermal comfort index and visual comfort index (Huang and Niu, 2016). The energy performance index includes total building energy consumption, space heating load, space cooling load, and HVAC system energy consumption. The life cycle cost index mainly includes life cycle cost and life cycle CO_2 emission. Thermal comfort index includes the thermally comfortable hours, mean predicted mean vote (PMV) level, space temperature, mean PPD level and operative temperature. Visual comfort index includes the illumination uniformity, illumination level, daylight factor, useful daylight illuminance and daylight autonomy. Huang and Niu (2016) summarized 70 optimization cases. The results show that over 80% of the cases minimized the energy consumption or life cycle cost, 5.5% minimized thermal comfort, while 12.3% of optimization objective is visual comfort.

The main objectives for design optimization of building energy systems are the net present cost and the levelized cost of energy (Bernal-Agustín and Dufo-López, 2009). The net present cost is the sum of the investment cost and the discounted present values of all future costs in the life cycle of the system. The levelized cost of energy is the total cost divided by the energy supplied by the energy system. Besides the cost and energy consumption, a few researchers also considered the CO_2 emission, thermal comfort and the stress of power import and export on the power grid. For instance, Lu et al. (2015)

considered three objectives when optimizing the renewable energy system of a zero carbon building, including total cost, carbon dioxide emissions and grid interaction index. Sun et al. (2015) optimized the design of energy systems in a ZEB considering three objectives, involving initial cost, indoor thermal comfort and power mismatch. Besides the design objectives, restrictions are usually considered in the design optimization, such as loss of load probability, loss of power supply probability and unmet load (Bernal-Agustín and Dufo-López, 2009). Loss of load probability is obtained by dividing the accumulated power failure time by the time period concerned. Loss of power supply probability is the probability of insufficient power supply when the energy system is unable to satisfy the load demand. Unmet load refers to the non-served load.

2.3 Optimal control of energy systems in zero/low energy buildings

2.3.1 Optimal control methods

The online control of energy systems in buildings mainly includes online predictive scheduling, real-time optimal (or supervisory) control and real-time process control (Wang and Ma, 2008), as shown in Table 2.2. Both online predictive scheduling and real-time optimal control might be, in fact, considered as online optimal control in the literature. Online predictive scheduling optimizes the operation schedule of the energy systems by taking account into (predicted) future operation conditions or/and events, which is particularly essential for energy systems involving energy storages. The schedule of energy systems in buildings should be optimized in a relatively large time interval, i.e., typically hour(s) and day(s). For example, the predictive control strategies can make decisions well ahead to shift the load at the high electricity price to be at the low electricity price by using energy storage systems to reduce the operation energy cost, which cannot be realized by real-time optimal control or process control. Real-time optimal control and real-time process control are activated at much shorter time intervals. The control interval

of real-time optimal control is typically minute(s), which normally addresses the optimal operation of systems without energy storage while having the objective to optimize the system energy and/or environmental performance (Wang and Ma, 2008). The control interval of real-time process control is typically second(s) in buildings, with the objective to maintain the controlled variables at their desired set points (Wang and Ma, 2008). Process control is essential for the normal operation of energy systems in order to provide the expected building services. Previous studies related to the optimal control of energy systems in zero/low energy buildings mainly focus on predictive scheduling (Martirano and Giuseppi, 2018; Zhao et al., 2015; Lu et al., 2015; Yang et al., 2011; Martirano and Greco, 2017; Huang and Sun, 2019; Ma et al., 2016; Odonkor and Lewis, 2015; Fan et al., 2018; Shaikh et al., 2016; Schirrer et al., 2016; Yu et al., 2007). Few studies addressed the real-time optimal (or supervisory) control problems. For example, Zhao et al. (2015) proposed a model predictive control-based strategy to optimize the schedules of energy systems in a ZEB day-ahead under time-sensitive electricity pricing. Lu et al. (2015) proposed an optimal scheduling strategy for the energy systems in a ZEB to minimize the operation cost day-ahead using the mixed-integer nonlinear programming approach. More serious efforts on real-time optimal control of energy systems in zero/low energy buildings are needed. How to coordinate real-time optimal control with predictive scheduling remains to be addressed.

Table 2.2 Typical online controls in buildings and their optimization/control intervals

Control type	**Typical interval**
Online predictive scheduling	hour(s), day(s)
Real-time supervisory/optimal control	minute(s)
Real-time process control	second(s)

2.3.2 Online control optimization methods

For the optimal control of building energy systems, nonlinear optimization methods are usually used since most of the problems are highly nonlinear and constrained optimization problems. Nonlinear optimization methods include nonlinear local optimization methods and nonlinear global optimization methods (Wang and Ma, 2008). The nonlinear local optimization methods likely provide local (i.e. not global) optimums, while the nonlinear global optimization methods give global optimums with high computing cost. The direct search methods introduced before is one kind of nonlinear local optimization techniques. Nonlinear global optimization methods include evolutionary algorithm, branch and bound, simulated annealing, tabu search, etc. For online predictive scheduling, as the time allowance is longer, most of the nonlinear optimization techniques are applicable. For real-time supervisory control, as the optimal control decisions need to be provided instantly, nonlinear local optimization techniques are generally used.

2.3.3 Control objectives

Selection of optimization objectives is another important issue for optimal control problems. 60% of the studies in building applications consider single objective involving only one performance indicator (Shaikh et al., 2014). Since multiple objectives are often concerned to evaluate the performance of building energy systems in practice, more and more studies are conducted on the multi-objective optimal control in recent years. Weighted sum method is commonly used for the multi-objective control problems by transforming a multi-objective optimization problem into a single objective optimization problem (Shaikh et al., 2014). For example, Stadler et al. (2011) proposed an optimal control strategy to minimize the weighted average of annual energy costs and CO_2 emissions of buildings. Martirano and Giuseppi (2018) proposed an optimal predictive

control strategy for a heating system to optimize the energy consumption while satisfying the individual needs of residents. The objective function used is the weighted sum of the operation cost, the deviation of indoor temperature from its reference value and the deviation of water temperature in the central heating system from its reference value. Yang et al. (2011) developed a Graphical User Interface (GUI) to manage various comfort demands in buildings using a multi-agent control system. Particle Swarm Optimization (PSO) was used to minimize the objective function, which is the weighted sum of energy demand and users' comfort. However, it is difficult to determine proper weights for different objectives based on the preferences and it is even impractical to assign preferences to different objectives in some cases. Though multi-objective optimization algorithm like multi-genetic algorithm can provide pareto-optimal solutions to choose from, such choice needs to be selected manually by an expert or the decision-maker and it is not practical in online optimal control which requires instant and automatic decisions. A proper and effective approach is needed to achieve online multi-objective optimization for online optimal controls involving multiple objectives.

2.4 Uncertainty analysis and its applications in building energy field

2.4.1 Uncertainty quantification methods

The widely accepted definition of uncertainty is "any deviation from the unachievable ideal of completely deterministic knowledge of the relevant system" (Walker et al., 2003). Uncertainty quantification methods could be classified into two categories: forward uncertainty propagation method and inverse uncertainty quantification method (Tian et al., 2018). Forward uncertainty propagation quantifies the output uncertainty by propagating from uncertain input variables according to their probability density distributions, while inverse uncertainty quantification determines unknown variables

from measured data. Forward uncertainty propagation methods based on probabilistic approaches are considered as the most rigorous approaches for uncertainty analysis in engineering design due to its consistency with the theory of decision analysis. However, its robustness depends on the accuracy of the probability distribution functions assumed for the uncertainty sources. Monte-Carlo based uncertainty analysis method is the most widely used forward uncertainty analysis method (Tian et al., 2018). A number of studies have been conducted to investigate its sampling efficiency and sampling convergence (Janssen, 2013). It is widely understood that Latin hypercube sampling method (LHS), among a number of alternative Monte-Carlo-based methods, outperforms random sampling method in most applications (McKay et al., 1979; Stein, 1987; Helton and Davis, 2002; Helton and Davis, 2003; Helton et al., 2005).

2.4.2 Robust optimal design methods concerning uncertainties

Design optimization concerning uncertainties is usually called "robust design optimization" when the variance of performance indicator is concerned as an optimization objective. Robust design was introduced around 1940s to improve the quality of manufactured goods (Yao et al., 2011; Park et al., 2006). There are different definitions for robust design. It is widely accepted that robust design is a design insensitive to variations (Yao et al., 2011; Park et al., 2006; Nguyen et al., 2014). It aims not only to make the mean value close to the target value, but also to minimize the variation produced by uncertain factors. The original robust design method is called Taguchi method. It is only applicable to unconstrained design problem and the input variables should be discrete (Park et al., 2006). Robust design optimization, which integrates the robustness concept with conventional design optimization, well solves these problems. Unlike deterministic design optimization, robust design optimization uses quantitative

approaches to assess and consider the effects of uncertainties (Yao et al., 2011; Park et al., 2006; Nguyen et al., 2014).

Many studies have been conducted on robust design optimization in the pioneer fields, such as engineering fields and finance field (Nguyen et al., 2014; Mulvey et al., 1995). In general, the mean and standard deviation of the performance indicators under uncertain design scenarios are considered as the design objectives for robust design optimization. The typical formulation of the optimization objective is a weighted sum of the mean and standard deviation (Yao et al., 2011; Nguyen et al., 2014). In 1950, Mulvey et al. (1995) proposed another objective function for robust design optimization of large scale systems, which consists of three terms: mean of performance indicator, variance of performance indicator and an infeasibility/performance penalty. The infeasibility penalty was proposed in cases when some of the constraints for robust optimization cannot be satisfied under all uncertain scenarios. These two types of optimization objectives are widely used in structural engineering and aerospace engineering fields, which have stringent requirements on the variation of the performance and are risk-averse (Yao et al., 2011; Nguyen et al., 2014).

2.4.3 Robust optimal design in building energy field

The concept of uncertainty has been introduced to building performance model development and validation since the early 1980s. In 2000s, researchers started to apply uncertainty quantification in model application contexts, such as building design (Sun, 2014). For instance, Macdonald and Strachan (2001) integrated the uncertainty quantification with ESP-r to analyze the influence of uncertainty on the building design. De Wit and Augenbroe (2002) integrated the uncertainty quantification with risk analysis in the decision-making for building design. In recent years, robust optimal design or

uncertainty-based optimal design has been attracting increasing attention in the building energy field. These studies show the necessity of uncertainty analysis in building energy field and how a different decision would be made if the decision makers were informed of uncertainties in the predictions.

Uncertainties in building energy field

Uncertainties arise in a number of ways and for a variety of reasons. Uncertainties are divided into two categories in most of the literature: aleatoric and epistemic (Matthies, 2007). The aleatoric uncertainty is also known as statistical uncertainty. It represents unknowns that differ each time we run the same experiment, which is irreducible. The epistemic uncertainty is also known as systematic uncertainty. It is due to lack of knowledge about fundamental phenomena, which is reducible. This uncertainty typology has some theoretical merits but is of limited value in the applications of uncertainty analysis for decision-making, since most of uncertainties are the combinations of aleatoric and epistemic uncertainties (Sun, 2014).

A few researchers investigated particularly on the sources of uncertainty in building performance modelling and simulation. Morgan (2009) suggested to divide the uncertainty in modeling and simulation into two categories: the uncertainty about the parameters in modeling systems, and the uncertainty about the model functional form. Sun (2014) divided the sources of uncertainty in building modeling and simulation into five categories, including: meteorological, urban, building, systems, and occupants. Gang et al. (2016) classified the uncertainty sources of cooling load into three groups, including: outdoor weather, building design/construction and indoor conditions. Chen et al. (2017) divided the uncertainties in HVAC field into two types: design uncertainties and operation uncertainties. Operation uncertainties mainly refer to information

uncertainty and system reliability. Design uncertainties are mainly related to the cooling load uncertainty, involving the epidemic uncertainty (such as heat transfer performance of building envelopes and efficiency of system components) and variability (such as the number of occupants and weather conditions). Li and Wang (2017) classified the sources of uncertainties, associated to the pressure head of water pump systems, into two categories, i.e. model uncertainties and construction uncertainties. Model uncertainties refer to that exist in the parameters of models used for pressure loss calculation. Construction uncertainties refer to that caused by deviations of site-construction from design and the manufacturing tolerances of devices used.

Robust and uncertainty-based optimal design of buildings and their energy systems

In recent years, robust and uncertainty-based optimal design of building and energy systems is attracting increasing attention. Hoes et al. (2011) used the ratio of standard deviation to the mean of performance indicator under uncertainty scenarios to quantify the negative effect of performance indicator variation. Rezvan et al. (2012) performed robust design optimization of distributed generation systems in buildings using the objective function including three terms proposed by Mulvey et al. (1995) and further revised by Yu et al. (2000). Gelder et al. (2014) proposed two new objectives for robust design optimization of building envelopes including: effectiveness (ε) and robustness (R_P). Where, ε is used to assure good average performance and R_P is used to assure a small variance of annual performance under different scenarios. Sun et al. (2015) used the mean of performance indicator only to optimize the energy system (i.e., heating, ventilation and air-conditioning (HVAC) system and renewable energy system) for a ZEB. De Wit and Augenbroe (2002) evaluated the optimal design solution alternatives according to the mean of the performance under the predicted uncertainty and the risk of

extreme situations (such as high peak cooling load). Gang et al. (2016) used the mean of total annual cost only to optimize district cooling systems. Both the uncertainties at the design stage and the reliability of the cooling systems in operation were considered for the robust design optimization.

Though previous studies have covered robust design optimization of generic buildings and their energy systems as well as robust design optimization of energy systems for zero/low energy buildings, no study has been found on robust optimal envelope design for zero/low energy buildings and robust optimal design of the entire zero/low energy buildings. In addition, the objective functions for robust design optimization in pioneer fields were used directly in the building field in many previous studies and other studies used the mean performance indicators without considering their variances. The applicability and needs of using these optimization objectives for robust design optimization in building energy field have not been analyzed and discussed in these studies. In fact, Nguyen et al. (2014) has raised their doubt on the necessity of robust design optimization in building energy field concerning the needs and applicability of using the commonly-used objective functions, particularly the involvement of the standard deviation of performance indicators. They also suggested that more serious investigations on this fundamental issue are needed.

2.5 Summary on research gaps identified

This chapter provides a comprehensive review on the optimal design and control of zero/low energy buildings as well as uncertainty analysis and its applications in building energy field. From the above review, the research gaps can be summarized as follows:

- Single sensitivity analysis method is usually adopted to assess the impacts of design parameters on building performance, which may lead to the missing of important

design parameters. Current sensitivity analysis often does not comprehensively address design parameters and the identification of key design parameters since many other non-design parameters are involved.

- The envelope design optimization of zero/low energy buildings without heating provision in subtropical regions is seldom studied. Very few researchers addressed sensitivity analysis on design parameters and design optimization comprehensively.
- An efficient design optimization method for the entire zero/low energy buildings, which can achieve the global optimum with less computing cost, is needed. The current multi-stage design optimization methods can reduce computing time, but the design solution achieved may be local optimum since they assume no impacts of energy system design optimization on the envelope design optimization and ignore the possible interactions between design optimizations of building envelope and building energy systems.
- Robust optimal envelope design for zero/low energy buildings and robust optimal design of the entire zero/low energy buildings are seldom studied. In addition, the objective functions for robust design optimization in pioneer fields were used directly in the building field in most previous studies without analyzing their applicability.
- More serious studies on the online optimal control of energy systems in zero/low energy buildings are needed. How to coordinate real-time optimal control with predictive scheduling remains to be addressed. A proper and effective approach is needed to achieve online multi-objective optimizations for online multi-objective optimal controls, particularly when it is impractical to assign preferences to different objectives.

CHAPTER 3 REFERENCE BUILDING AND BUILDING SIMULATION MODELS

This chapter presents an overview of the passive design and energy system design strategies used in the reference building Hong Kong "Zero Carbon Building" (ZCB) and the building simulation models in this study. The building simulation models, including building performance models and energy system models, are developed on the basis of the ZCB and used for the test and validation of the proposed methods in this PhD study.

3.1 An overview of Hong Kong Zero Carbon Building

The Zero Carbon Building is the first and the only zero carbon building in Hong Kong, which is completed in June 2012. Figure 3.1 shows the aerial view of ZCB. It is developed by the Construction Industry Council (CIC) in collaboration with the HKSAR Government (CIC, 2018). The ZCB covers a total building area of 1,380 m^2. The building consists of two indoor exhibition areas, an eco-home, an eco-office, a multi-purpose hall, two executive rooms, a meeting room and a guest room. ZCB is to serve as an exhibition, education and information center for zero/low carbon building design and technologies and for promoting low carbon living in Hong Kong. It is also to serve as a platform for the construction industry to share knowledge and expertise in low/zero carbon building design and technologies, and to help to raise community awareness of low carbon living. A number of passive design and energy system design strategies are used in ZCB, which are presented as follows.

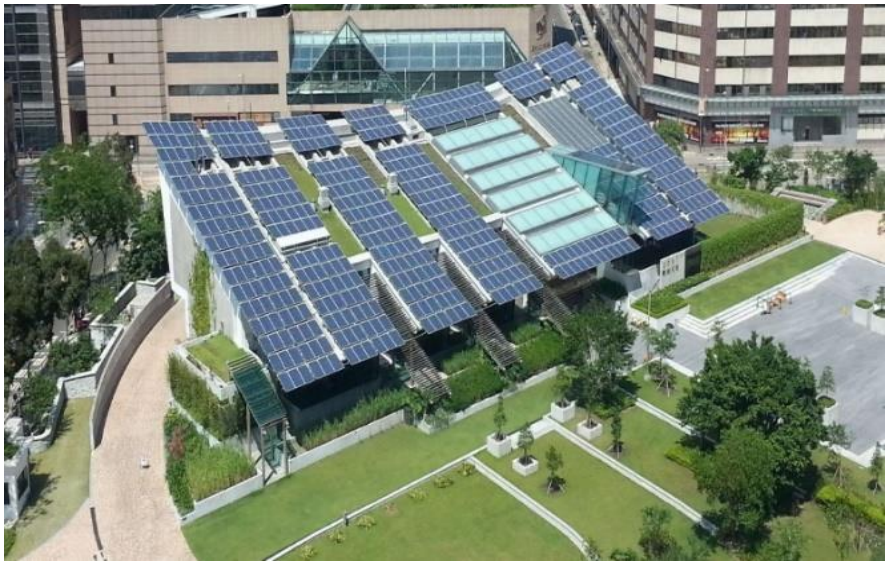

Figure 3.1 Aerial view of ZCB in Hong Kong

3.1.1 Passive design

Passive design approaches include the structure of the building itself (such as building orientation, window placement, skylight installation, insulation and building materials) and specific elements of a building (such as windows and window shades). In the ZCB, various passive design measures are adopted, including: cross-ventilated layout, high performance glazing, north glazing, insulated roof, external shading, heat reflecting shade, wind catcher, earth cooling tube, light shelves and light pipes. The main measures or measures associated to this study are elaborated below.

Cross-ventilated layout

The climate in Hong Kong is characterized by two distinct seasons, i.e., winter and summer. Summer days are long and tend to be hot and humid. Winter days are short but are cool and dry. On the cool days, there is a good potential for buildings to be naturally ventilated, which can significantly reduce the use of mechanical ventilation and cooling systems. The ZCB is positioned to maximize this potential by orienting its main facade to southeast, since the prevailing wind direction in the area of ZCB is southeast throughout the year.

High performance glazing

The high performance glass wall system offers good thermal and optical performance, which reduces the cooling load and the reliance on artificial lighting and hence reduces the energy consumption.

External shading

The glazed external walls of ZCB are protected by external shading of different types. The shading on the walls of different sides varies to suit different solar conditions.

3.1.2 Active systems and renewable energy

Active systems refer to the electrical and mechanical systems, such as the HVAC systems and lighting systems. Renewable energy is energy collected from renewable resources, which are naturally replenished on a human timescale. The main active systems and renewable energy adopted in the ZCB include:

High temperature cooling system

The high temperature cooling system comprises underfloor displacement cooling, radiant cooling and desiccant dehumidification. The cooling system does not need to overcool the air to achieve the comfort humidity level, which saves the energy for air conditioning, since a separate cooling and humidity removal system is used.

Adsorption chiller

The adsorption chiller uses water as refrigerant, a silica gel as adsorbent, and hot water as main power source. The evaporator section cools the chilled water through adsorption of the silica gel, while the hot water regenerates ("dries") the silica gel.

Intelligent lighting management

Integrated system comprising zone control, dimmable energy-efficient light fittings,

preset scenes for multi-purpose room, time-clock and occupancy sensing, daylight harvest and responsive control, automatic shade for glare control, individual control and BMS integration.

Biodiesel tri-generation

A biofuel tri-generator is used in the ZCB to generate the heat and electricity. Biofuel is a type of fuel derived from organic matter (obtained directly from plants, or indirectly from agricultural, commercial, domestic, and/or industrial wastes) instead of from fossil products.

Photovoltaics

Three types of PV panels have been chosen for various locations. A study has been carried out to assess the solar irradiance levels at various parts of the site, to determine the viability and layout of PV panels.

3.2 Building performance model

Two kinds of building performance models are developed for the test and validation of the proposed design methods and control strategy. One is EnergyPlus model, the other is ANN (artificial neural network) model. EnergyPlus model is built referring to the layout and design condition (e.g., occupancy density and equipment load) of the reference building ZCB. It is used for sensitivity analysis in Chapter 4, training/test data preparation for ANN models, and building performance simulation for online optimal control in Chapter 8. ANN model is used for building performance evaluation to reduce computing cost. This is because it requires much less time for building simulation than EnergyPlus, and also requires much less times of simulation to prepare the training/test data than to search optimal design solutions in design optimization especially when different settings in the optimization algorithms need to be tested. It is used for coordinated optimal design

in Chapter 5, robust optimal design in Chapter 6, and coordinated robust optimal design in Chapter 7. Different ANN models are built for these three different applications as different inputs are concerned. It is worth noticing that only one ANN model is needed if the ANN model is trained to cover the variations in all the design inputs concerned in these three cases.

3.2.1 EnergyPlus models

EnergyPlus (Crawley et al., 2001), as a commonly-used building simulation software, is used for building performance simulation in this study. Two EnergyPlus building performance models are built for building performance evaluation and training/test data preparation for ANN models, based on the two base architectures shown in Figure 3.2 respectively, using the OpenStudio Sketchup Plug-in (Guglielmetti et al., 2011) and EnergyPlus. Architecture 1, as shown in Figure 3.2A, is built by following the reference building ZCB exactly. The EnergyPlus model of this architecture is used for building performance simulation in sensitivity analysis in Chapter 4, training/test data preparation for ANN model in robust optimal envelope design in Chapter 6 and building performance simulation for online optimal control in Chapter 8. Architecture 2 shown in Figure 3.2B is revised based on the Architecture 1 by simplifying the thermal zones and changing windows from the longer side walls to the shorter side walls, in order to better investigate the need of coordinated optimal design and coordinated robust optimal design. The EnergyPlus model of this architecture is used for training/test data preparation for ANN models in coordinated optimal design in Chapter 5 and coordinated robust optimal design in Chapter 7. For Architecture 2, only one thermal zone is considered. PV panels are fixed on the slope roof of the building. The internal loads assumed for building performance simulation in sensitivity analysis, coordinated optimal design and online optimal control are listed in Table 3.1, which are the design assumptions of the ZCB. Schedules of these

internal loads at different time are also assumed, which are proportions of the design values. These settings in robust optimal design and coordinated robust design are introduced in Chapter 4 as uncertainties are considered for these parameters.

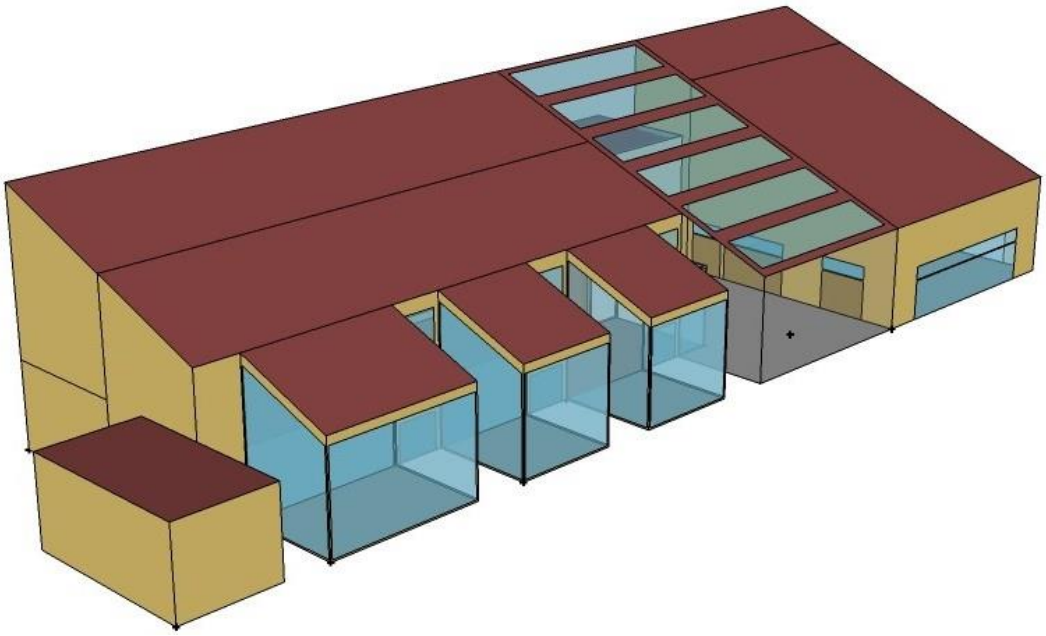

(A) Architecture 1

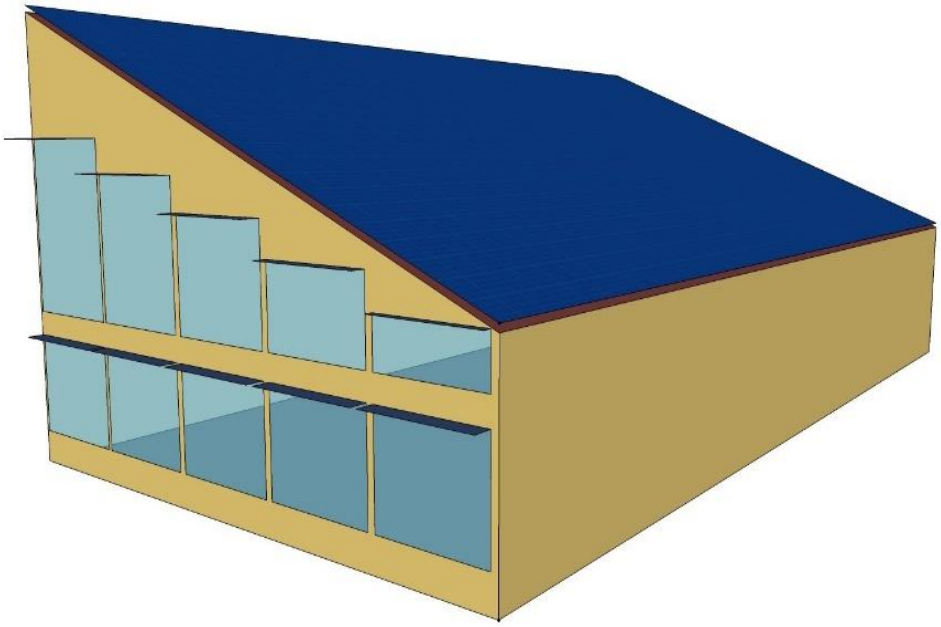

(B) Architecture 2

Figure 3.2 Base architectures for building performance simulation in different case studies

Table 3.1 Design assumptions of internal loads for building performance simulation in sensitivity analysis, coordinated optimal design and online optimal control

Feature		**Design value**
Lighting load	Office	6 (W/m^2)
	Exhibition area	6 (W/m^2)
	Multi-purpose room	6 (W/m^2)
Equipment load	Office	20 (W/m^2
	Exhibition area	10 (kW)
	Multi-purpose room	5 (W/m^2)
People load	Office	130 (W/person)
	Exhibition area	130 (W/person)
	Multi-purpose room	95 (W/person)
Occupant density	Office	8 (m^2/person)
	Exhibition area	4.7 (m^2/person)
	Multi-purpose room	300 (person)
Fresh air		4.3 (L/s/person)

In general, free energy sources, such as natural ventilation and daylight, are taken into full consideration in zero/low energy buildings in practice in order to satisfy the low energy requirement. Therefore, the control logic, adopted by EnergyPlus for the building performance simulation in this study, is set to maximize natural ventilation and daylight in order to minimize building energy consumption while maintaining an acceptable thermal comfort as far as possible. These simulated control logics concerning the uses of natural ventilation and daylight are described as below.

The “hybrid ventilation availability manager” in EnergyPlus is used and set to maximize

the use of natural ventilation in order to reduce the cooling loads of buildings, as illustrated in Figure 3.3. The blue columns are the inputs and outputs of this manager. “Operative temperature control using adaptive comfort 90% acceptability limits” is selected as the ventilation control mode (i.e. criteria) of the hybrid ventilation availability manager in order to maximize the use of natural ventilation while maintaining an acceptable thermal environment as far as possible. First, the natural ventilation test is conducted at the beginning of each simulation time step based on the inputs of weather data, maximum window/door opening settings, internal loads, etc. The zone operative temperature is calculated and examined to assess whether it is favorable for the use of natural ventilation, i.e. whether it is within the comfortable zone based on ASHRAE standard (ASHARE, 2010). This standard sets the range of comfortable zone air operative temperature within the lower and upper adaptive comfort 80%/90% acceptability limits while 90% acceptability is adopted in this study. If the indoor environment can be controlled within the comfortable zone, natural ventilation is allowed and no cooling/heating is needed and the mechanical ventilation is off. Otherwise, natural ventilation is not applicable and will be shut off. Under this condition, if it is in the system operation hour, the mechanical ventilation will be switched on for the intake of the minimum outdoor air needed for acceptable indoor air quality. Otherwise, both mechanical ventilation and air-conditioning systems are shut off. In operation hour, if the zone air temperature is higher than its (cooling) set-point, the air-conditioning system operates and the indoor air temperature will be controlled at its set-point whilst the calculated cooling demand will be used for further performance assessment. If zone air temperature is equal to or lower than the indoor set-point, the air-conditioning system is switched off and the indoor air temperature will be lower than its set-point as no heating is available whilst the calculated PMV (Fanger, 1972) of the zone is used for further

performance assessment.

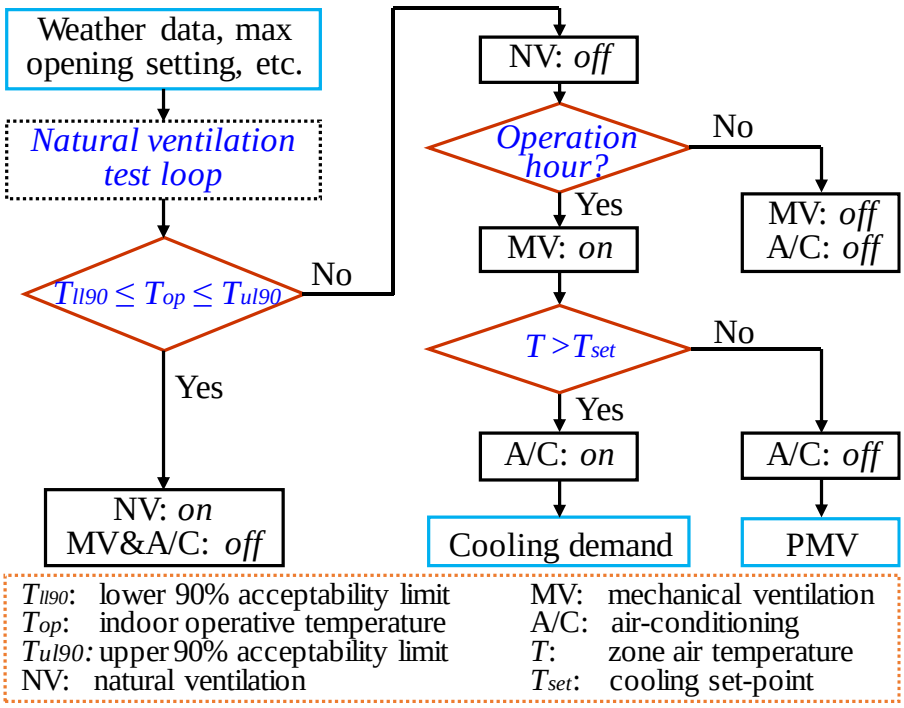

Figure 3.3 Hybrid control logic of natural ventilation and air-conditioning operation in building performance simulation

The artificial lighting output in a zone is adjusted based on the daylight illuminance at the reference point in the simulation according to the lighting control set-point. In this study, the reference points are chosen at the center of each room at the height of 0.8m. The lower and upper limit for daylight illuminance are set as 100lux and 500lux, respectively. A simplified daylight dimming control logic is illustrated in Figure 3.4. When the daylight illuminance is lower than the lower limit, the lighting power input equals to the design (full) lighting load. When the daylight illuminance increases between the lower and upper limits, the lighting power input decreases linearly with the increased daylight illuminance until 10% of the design lighting load. If the daylight illuminance reaches or exceeds the upper limit, the lighting system will be switched off and the lighting power input becomes zero.

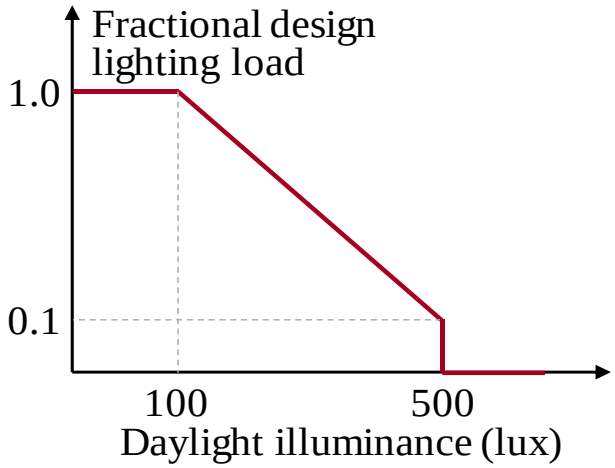

Figure 3.4 Daylight dimming control logic

3.2.2 ANN models and their training method

Three ANN models are developed and used for building performance evaluation in coordinated optimal design in Chapter 5, robust optimal design in Chapter 6, and coordinated robust optimal design in Chapter 7, respectively. The detailed training and validation results are shown in the corresponding chapters. This subsection introduces the configuration of the ANN models used and the training method.

The multi-layer feed-forward neural network is selected and used in this study since the feed-forward neural network, trained using a back-propagation learning algorithm, is the most commonly-used neural network in the building design applications (Svozil et al., 1997). This type of neural network generally consists of one input layer, one output layer and several hidden layers. The number of hidden layers, the number of neurons in each hidden layer and the weights between different neurons in adjacent layers need to be adjusted based on the actual case, to ensure the ANN model outputs are as close to the actual building performance data (i.e., the simulation data from EnergyPlus Model in this study) as possible. The training process is illustrated in Figure 3.5 and explained as follows.

In this study, the ANN model structure and model parameters (weights) are both optimized in the training process. Improper (too simple or too complex) model structures and non-optimal weights can reduce the accuracy of the ANN model and may lead to overfitting. The procedure of the ANN model optimization thus involves three steps: *preparation of training and test data, model structure optimization* and *model parameter optimization*, as illustrated in Figure 3.5. The mean squared error (MSE) is used to evaluate the performance of the ANN model in this study.

In the first step, the training and test datasets are prepared. The input scenarios (i.e., combinations of different model inputs) are generated by sufficient sampling of the ANN model inputs (according to their ranges or probability distributions) using the LHS (Latin hypercube sampling) method. The building performance of each input scenario over the period concerned is then simulated using EnergyPlus. The corresponding performance values of each input scenario are obtained and used as the training/test targets.

In the second step, the optimal ANN model structure is identified using 10-fold cross-validation (Kohavi, 1995). Different numbers of hidden layers and different numbers of neurons in different hidden layers are tested for the ANN model. The performance (MSE) of ANN models with different structures is assessed using 10-fold cross-validation n times with the training data prepared in the first step. The ANN model structure with the minimum average MSE from the 10-fold cross-validations is identified as the optimal ANN model structure.

In the third step, the parameters (weights) of the ANN model with the optimal model structure are optimized to eventually obtain the optimal ANN model for the design optimization. The same training datasets prepared in the first step are used to train the ANN model, and the test dataset is then used to evaluate the accuracy of the ANN model

obtained. The ANN model with the optimal structure is trained and tested *m* times, to eliminate the impact of the random initialization of the model training process. Out of the *m* models, the model giving the minimum MSE (highest accuracy) in the model test is eventually selected as the optimal ANN model for design optimization.

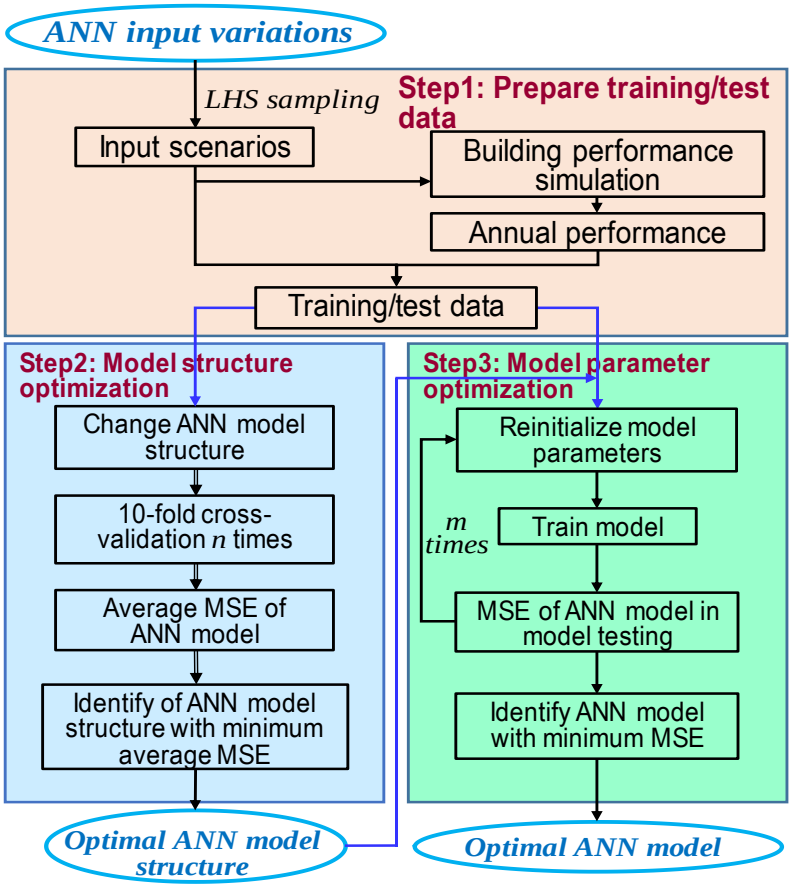

Figure 3.5 Procedure of ANN model training and optimization

3.3 Building energy system configuration and energy system models

3.3.1 Configuration of building energy systems

A typical energy system configuration is considered for the test and validation of the coordinated optimal design in Chapter 5, coordinated robust optimal design in Chapter 7 and online optimal control in Chapter 8 (but simplified by excluding wind turbines), as shown in Figure 3.6. The energy systems mainly consist of three parts: power generation systems, air-conditioning systems and energy storage system. The power generation

systems include PV panels, wind turbines and co-generators. The air-conditioning systems mainly consist of absorption chillers, electric chillers, air handling units (AHU), cooling towers, cooling water circulation system and chilled water distribution system. The absorption chillers are used to replace the adsorption chillers in ZCB and considered in this study, since the absorption chillers are more widely-used in practice. Battery constitutes the energy storage system to store abundant electricity generated by the power generation system and supply electricity when needed. Due to the facts that heating is not provided in most subtropical regions, only cooling supply is considered in the case studies, which is provided only in the working hours (8:00-19:00, except Wednesday). Where, Saturdays and Sundays are working days due to the demonstration purpose of the reference building. The main differences of energy systems in the grid-connected buildings compared with that in the standalone buildings are that the abundant electricity can be exported to the grid when there is still abundant electricity after the building energy demand is satisfied and the battery is charged to its maximum limit, and electricity can also be imported into buildings when the electricity generation cannot satisfy the electricity demand.

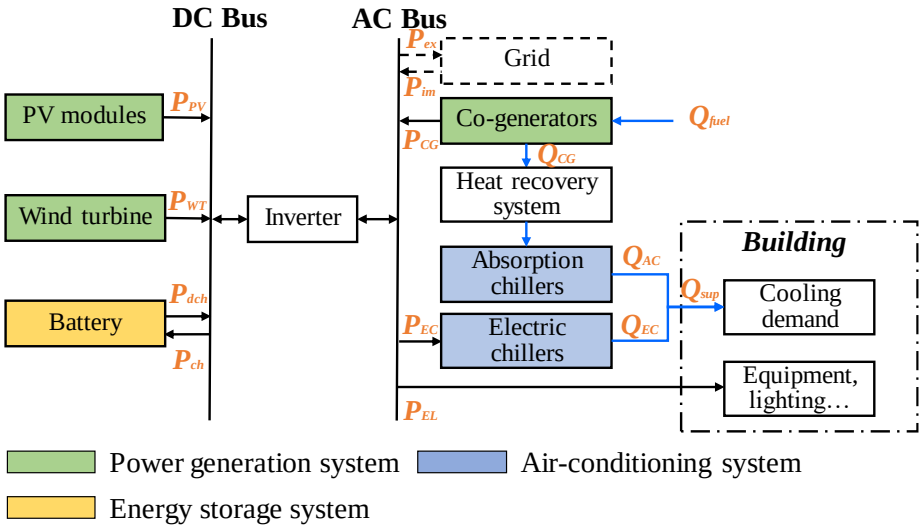

Figure 3.6 Energy system configuration concerned

3.3.2 Energy system models

Mathematical models are developed for energy system components to simulate their performance. The detailed models for the system components are presented as follows. The basic information for the energy system models are listed in Table 3.2.

Power generation systems

PV model: The power supplied by PV panels is calculated using Eq. (3.1) (Daud et al., 2012). It is determined mainly by the solar radiation, PV area and cell temperature. The cell temperature is calculated by Eq. (3.2) (Daud et al., 2012). Where, P_{PV} is the power (kW) generated by PV panels. r is the solar radiation (kW/m^2). A_{PV} is the total area of PV panels (m^2). η_{PV} is the overall efficiency of PV panels. K is temperature coefficient (1/K) of the maximum generation power of PV panels. In this study, K is set as -3.7×10^{-3}. T_{cell} is cell temperature (°C) of PV panels. T_{ref} is cell temperature (°C) at reference condition, which is set as 25°C in this study. T_{amb} is the ambient temperature (°C).

$$P_{PV} = r \times A_{PV} \times \eta_{PV} \times (1 + K(T_{cell} - T_{ref})) \quad (3.1)$$

$$T_{cell} = T_{amb} + 0.0256 \times r \quad (3.2)$$

Wind turbine model: The power generated by a wind turbine is calculated by Eq. (3.3-3.4) (Maheri, 2014). Where, P_{WT} is the power produced (kW) by a wind turbine. ρ is air density (kg/m^3). v_{hub} is wind speed (m/s) at the hub elevation of the wind turbine. A_{WT} is rotor area (m^2). RPC is rotor power coefficient. η_{WT} is the overall efficiency of the wind turbine. This model is valid when $3 \leq v_{hub} \leq 25$ m/s, and the power generated by the wind turbine is 0 when v_{hub} is out of this range.

$$P_{WT} = 0.5 \times \rho \times v_{hub}^3 \times A_{WT} \times RPC \times \eta_{WT} \quad (3.3)$$

$$RPC = (-2.025 \times 10^{-7} \times v_{hub}^{6} + 1.926 \times 10^{-5} \times v_{hub}^{5} - 7.421 \times 10^{-4} \times v_{hub}^{4} + 1.483 \times 10^{-2} \times v_{hub}^{3} - 0.162 \times v_{hub}^{2} + 0.887 \times v_{hub} - 1.508) \times 10^{-3} \quad (3.4)$$

Table 3.2 Basic data of energy system models

Parameter	**Symbol**	**Value**	**Unit**
Unit price of PV	-	229.72	USD/m²
Unit price of wind turbine	-	2000	USD/kW
Unit price of co-generator	-	2400	USD/kW
Unit price of battery	-	213	USD/kWh
Unit price of diesel oil (fuel)	c_{fuel}	1.3	USD/L
Unit price of electricity	c_{ele}	0.1472	USD/kWh
Feed in tariff	c_{tif}	0.065	USD/kWh
Interest rate	-	8	%
Lifetime of PV	-	20	year
Lifetime of wind turbines	-	20	year
Lifetime of co-generators	-	24000	hour
Lifetime of battery	-	10	year
Lifetime of electric chillers	-	15	year
Lifetime of absorption chillers	-	15	year
Overall efficiency of PV	η_{PV}	0.12	-
Efficiency of wind turbines	η_{WT}	0.9	-
Efficiency of heat recovery system	η_{hr}	0.8	-
Charge efficiency of battery	η_{ch}	0.85	-
Discharge efficiency of battery	η_{disch}	0.85	-
Efficiency of inverter	η_{inv}	0.92	-
Heat value of diesel oil	-	39	MJ/L

Co-generator model: The electricity and heat produced by a co-generator are calculated using Eq. (3.5) and Eq. (3.6) (Liu et al., 2012), respectively. Where, P_{CG} is the electricity (kW) produced by a co-generator. FC_{CG} is fuel consumption (kW). Q_{CG} is the heat (kW) generated by the co-generator. η_{CG} is the co-generator efficiency. The efficiency varies with partial electric load of the co-generator (l_{CG}), which is calculated by Eq. (3.7-3.8) (Liu et al., 2012).

$$P_{CG} = FC_{CG} \times \eta_{CG} \tag{3.5}$$

$$Q_{CG} = FC_{CG} \times (1 - \eta_{CG}) \tag{3.6}$$

$$\eta_{CG} = -0.2 \times l_{CG}^2 + 0.4 \times l_{CG} + 0.1 \tag{3.7}$$

$$l_{CG} = \frac{P_{CG}}{P_{CG,design}} \tag{3.8}$$

Air-conditioning systems

Electric chiller model: The electricity required by electric chillers (P_{EC}) is calculated using Eq. (3.9), which is mainly determined by the cooling load (Q_{EC}) which needs to be supplied using electric chillers, and their COP (COP_{EC}). A lower COP_{EC} would lead to more electrical energy demand of electric chillers. COP_{EC} is assumed as a variable of partial load of chillers (l_{EC}), as Eq. (3.10-3.11) (Gang et al., 2015). Where, n_{op} is the number of electric chillers in operation.

$$P_{EC} = \frac{Q_{EC}}{COP_{EC}} \tag{3.9}$$

$$COP_{EC} = -6.563 \times l_{EC}^2 + 10.714 \times l_{EC} + 1.0794 \tag{3.10}$$

$$l_{EC} = \frac{Q_{EC}}{n_{op} \times Cap_{EC}} \tag{3.11}$$

Absorption chiller model: The cooling supplied by absorption chillers (Q_{AC}) depends on the heat generated by the co-generators (Q_{CG}), heat recovery efficiency (η_{CG}) of the heat

recovery unit and the COP of absorption chillers (COP_{AC}). It is calculated using Eq. (3.12-3.13) (Liu et al., 2012). A constant COP is used for absorption chillers in this study, which is set as 0.7.

$$Q_{AC} = Q_{hr} \times COP_{AC} \tag{3.12}$$

$$Q_{hr} = Q_{CG} \times \eta_{hr} \tag{3.13}$$

Other air-conditioning system models: The energy models of chilled water pumps (*cwp*), cooling water pumps (*clp*), AHUs and cooling towers (*CT*) are revised on the basis of the models fitted using the operation data of the corresponding energy devices in the ZCB, as shown in Eq. (3.14-3.17) (Lu et al., 2015). Where, P is the power electricity (kW). m is the flow rate (m^3/s). The subscript *cw* represents the chilled water, while the subscript *air* represents air. Q_{CT} is the cooling load of cooling tower (kW).

$$P_{cwp} = 10 \times \frac{m_{cw}}{m_{cw,design}} - 1 \times (\frac{m_{cw}}{m_{cw,design}})^2 \tag{3.14}$$

$$P_{clp} = constant \tag{3.15}$$

$$P_{AHU} = 8 \times \frac{m_{air}}{m_{air,design}} + 12 \times (\frac{m_{air}}{m_{air,design}})^3 \tag{3.16}$$

$$P_{CT} = P_{CT,design} \times (\frac{Q_{CT}}{Q_{CT,design}})^{1.5} \tag{3.17}$$

Energy storage system

Battery model: The energy storage in the battery (E_{bat}) is limited within a range in order to prolong the lifetime of battery. Its minimum limit is set to be 20% of the battery capacity in this study, while its maximum limit is set to be 80% of the battery capacity. In addition, battery has its maximum limit for charging and discharging power. The maximum hourly power charging rate is set as 20% of the battery capacity, while the maximum hourly power discharging rate is 50% of the battery capacity. Charge efficiency

(η_{ch}) and discharge efficiency (η_{dch}) are considered when the battery charges and discharges, respectively.

Modelling of equipment lifetime and degradation

When the performance of energy systems are simulated over the building life cycle, the lifetime and performance degradation of system components are considered because of aging. Once an energy system component reaches its lifetime during the building life cycle, it needs to be replaced. The lifetime of battery is determined by its calendar life and the number of charge cycles (NCC). Calendar life is the lifetime of battery even when it has never been put into operation, which is assumed to be 10 years in this study. NCC has a maximum limit, as frequent charging and discharging can significantly reduce the lifetime of battery. It is calculated by Eq. (3.18) (Nottrott et al., 2013). Once NCC or calendar life reaches its maximum limit in the building life cycle, battery is replaced. Besides lifetime, degradation is considered in this study for PV panels in the coordinated optimal design and coordinated robust optimal design. The overall efficiency of PV panels is assumed to degrade by 0.8% (Huang et al., 2018) each year in their lifetime. The degradation is not considered in the online optimal control as the period concerned is short.

$$NCC(t) = NCC(t-1) + 0.5 \times \left|\frac{E_{bat}(t) - E_{bat}(t-1)}{E_{bat,max} - E_{bat,min}}\right| \quad (3.18)$$

3.4 Summary

This chapter presents an overview of the passive design and energy system design strategies used in the reference building (i.e., Hong Kong "Zero Carbon Building" (ZCB)) and the building simulation models used in this study. Two EnergyPlus building performance models for building performance simulation are built referring to the ZCB for different uses of building performance simulation. Three ANN building performance

models are developed and used to reduce the computation time of building performance evaluation for coordinated optimal design, robust optimal envelope design and coordinated robust optimal design, respectively. A typical energy system configuration is considered and mathematic models for each system component are formulated for the test and validation of the proposed design and control methods.

CHAPTER 4 IDENTIFICATION OF KEY DESIGN PARAMETERS AND MAIN UNCERTAIN DESIGN INPUTS FOR ZERO/LOW ENERGY BUILDINGS IN SUBTROPICAL REGIONS

Hong Kong, as a city in a subtropical region, is selected and considered in the case studies for the test and validation of the proposed design methods and control strategy. This chapter therefore presents the typical climate conditions in Hong Kong, the building performance objective for sensitivity analysis, identification of key envelope design parameters in subtropical regions, selection of key system design parameters, and identification of main uncertain design inputs of significant impacts in subtropical regions. A multi-stage sensitivity analysis method is proposed for the identification of the key envelope design parameters to avoid the missing of important parameters. Sensitivity analysis is performed to study the impacts of envelope design parameters and uncertain design inputs on the performance of zero/low energy buildings in subtropical regions.

4.1 The climate conditions in Hong Kong

The Hong Kong climate is subtropical, tending towards temperate for nearly half the year. Between 1981 and 2010, the mean monthly temperature in Hong Kong ranged from 18.6°C to 31.4°C, and the mean monthly relative humidity ranged from 71% to 83% (Hong Kong Observatory, 2015). It is not uncommon for the ambient temperature to drop below 10°C in urban areas for a short period in winter. Figure 4.1 shows the daily maximum/minimum dry-bulb temperatures, daily mean dew point and daily maximum global horizontal radiation of the typical meteorological year (TMY) weather data (Wilcox and Marion, 2008) in Hong Kong, which is derived from historical weather data of many years.

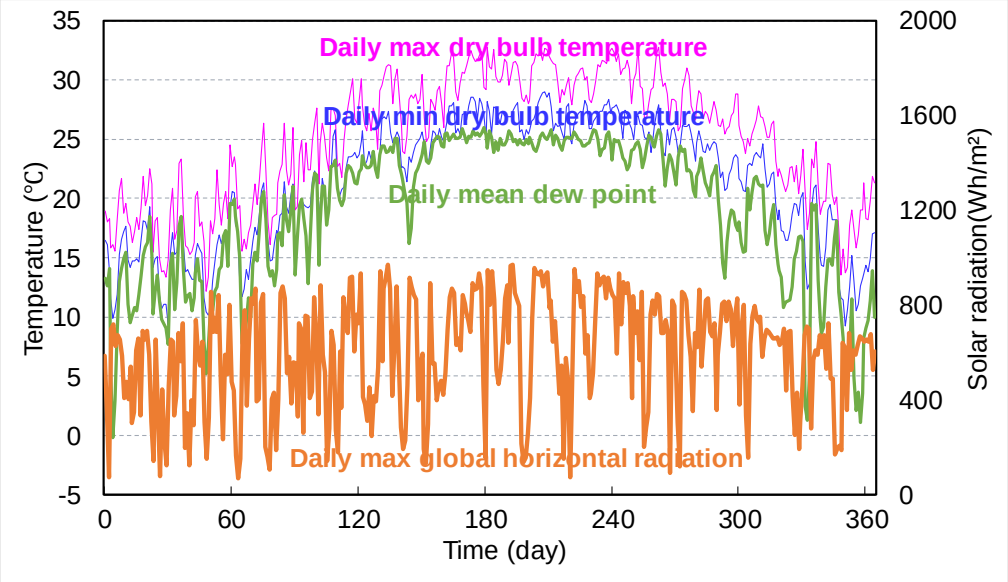

Figure 4.1 Daily max/min dry bulb temperatures, mean dew point and maximum global horizontal radiation of TMY weather data in Hong Kong

4.2 Performance objective for sensitivity analysis

An important issue concerning envelope design of buildings without heating provision in subtropical regions is that discomfort may occur in cold seasons since no heating is provided. If the thermal comfort issue in cold seasons is not taken into consideration when selecting optimal design option for zero/low energy buildings in subtropical regions, the obtained optimal design may cause severe cold indoor environment in the winter season. In order to reduce building energy demands while maintaining an acceptable indoor thermal comfort as far as possible, a comprehensive objective, which integrates building performance indictor (i.e., annual building electricity consumption) and performance penalty (i.e., penalty for winter thermal discomfort), is defined for building performance assessment in the sensitivity analysis in Section 4.3 and 4.5. The objective function is defined as Eq. (4.1) – (4.4). A discomfort index is introduced to quantify the building thermal discomfort in cold winter days. It is obtained by normalizing the hourly PMV value to a value between 0 and 1. The value 1 of the discomfort index represents the case when PMV is -3, which means cold. The value 0 of the discomfort index represents the

case when PMV is -0.5 or more, which means not cool. In order to consider building thermal discomfort and energy consumption comprehensively, a penalty ratio (a) is assigned to the discomfort index accumulated over the period concerned. a indicates the energy that owners would like to pay to mitigate the discomfort, and is significantly affected by the size of buildings. The penalty ratio can be determined based on the weighting of thermal comfort in the mind of owners. In the study, a is set at 100 kWh per unit of thermal discomfort, which is a typical hourly electricity consumption for cooling the reference building in a typical summer day, since there is data of cooling provision only in this study. It is based on the assumption that the owner likes to pay the same amount of electricity used in summer to heat the building in winter when its indoor PMV reaches -3. It is worth noticing that heating load should also be included for the regions where heating is provided. Summer thermal discomfort also needs to be considered if there is no cooling provision in summer in heating dominated regions.

$$F_{sa} = f + a * D \tag{4.1}$$

$$f = \sum E_{tot} = \sum (E_{EL} + E_{CL}/\mathrm{COP}) \tag{4.2}$$

$$\mathrm{D} = \sum D_{dis} \tag{4.3}$$

$$D_{dis} = \begin{cases} \frac{\text{-PMV-0.5}}{2.5} & \text{PMV<-0.5} \\ 0 & \text{PMV}\geq\text{-0.5} \end{cases} \tag{4.4}$$

where, F_{sa} is the performance objective used in sensitivity analysis (kWh). f is building performance indicator concerned. D is the infeasible performance. a is the penalty ratio (kWh) for the infeasible performance. E_{tot} is the hourly total electricity consumption (kWh), including the electricity consumption of equipment, lighting and air-conditioning (cooling) system. D_{dis} is hourly discomfort index. E_{EL} is hourly electricity consumption (kWh) of lighting and other equipment. E_{CL} is hourly cooling demand of building (kWh). COP is the overall coefficient of performance of air-conditioning system, which is set as

a typical value of 3 in this study since the design of energy systems is unknown before the design parameters of building envelope are determined and it is the easiest way to convert the cooling demand to electricity demand. PMV is the hourly PMV value (Fanger, 1972).

4.3 Identification of key envelope design parameters

4.3.1 Procedure and methods of sensitivity analysis

A multi-stage sensitivity analysis approach is proposed in this study to identify the key envelope design parameters for building design optimization. The multi-stage approach involves two stages of sensitivity analysis. The magnitudes of the effects of the main envelope design parameters on the performance objective are assessed at the first stage while, at the second stage, the directions of the effects of highly-sensitive design parameters, which are selected at the first stage, on the thermal discomfort and the energy consumption are assessed respectively.

At the first stage, three global sensitivity analysis methods, namely the regression method, Morris method (Morris, 1991) and FAST method (McRae et al., 1982), are adopted to assess the impacts of the main design parameters. The highly-sensitive design parameters are identified based on the results of the sensitivity analysis using the three methods. At first, highly-sensitive parameters (usually the top parameters with obviously higher sensitivity measures) of individual methods are identified and ranked respectively. Then top 5 highly-sensitive parameters of individual methods and the other highly-sensitive parameters (but not top 5) of 2 or 3 sensitivity analysis methods are finally identified as the highly-sensitive parameters to be considered at later stage. Note, the proper numbers of highly-sensitive design parameters to be selected could be different for different building applications.

At the second stage, the highly-sensitive envelope design parameters identified at the first stage are further assessed with the local sensitivity analysis method (Tian, 2013) to select the key design parameters. The impacts (in percentage) on annual discomfort index and annual total electricity consumption of each highly-sensitive envelope design parameter are assessed (compared to a base case) when other parameters remain unchanged. The envelope parameters with opposite effects on annual discomfort index and annual total electricity consumption (i.e. the change of the parameter in one direction results in the changes of discomfort index and consumption in opposite directions, one increases and the other decreases) are identified as the key envelope design parameters which need to be optimized eventually.

For the implementation of simulation-based sensitivity analysis, one of the main challenges is that a large number of building performance simulations are required and each simulation run requires a new building model description (e.g. input data files (IDF) in EnergyPlus) since the envelope parameters are changed. In this study, jEplus (jE+) (Zhang, 2009) and EnergyPlus (E+) are adopted to achieve the automatic process of numerous new building design establishment and building performance simulation. jEplus is a parametric study software, which can automatically change the parameter values in building simulation model and call EnergyPlus to do the building performance simulation. Apart from jEplus and EnergyPlus, SimLab (JRC, 2011) is also adopted for sensitivity analysis at a higher level. The process of each sensitivity analysis is illustrated in Figure 4.2. Firstly, SimLab generates the input scenarios based on the defined main design parameters and selected sensitivity analysis method, and a job list is also created based on the input scenarios for jEplus. Secondly, jEplus changes the corresponding parameter values in the building model based on the job list and generates a set of the corresponding building simulation model descriptions (IDF files) for EnergyPlus.

EnergyPlus will automatically run the simulations of all the scenarios using the weather data input (TMY weather data in Hong Kong in this section). Finally, jEplus collects all the simulation results and a simple calculation is conducted to obtain the corresponding objective values using the outputs of the performance simulations. With the input scenarios and the corresponding objective values, SimLab can calculate the sensitivity measures based on the selected sensitivity analysis method.

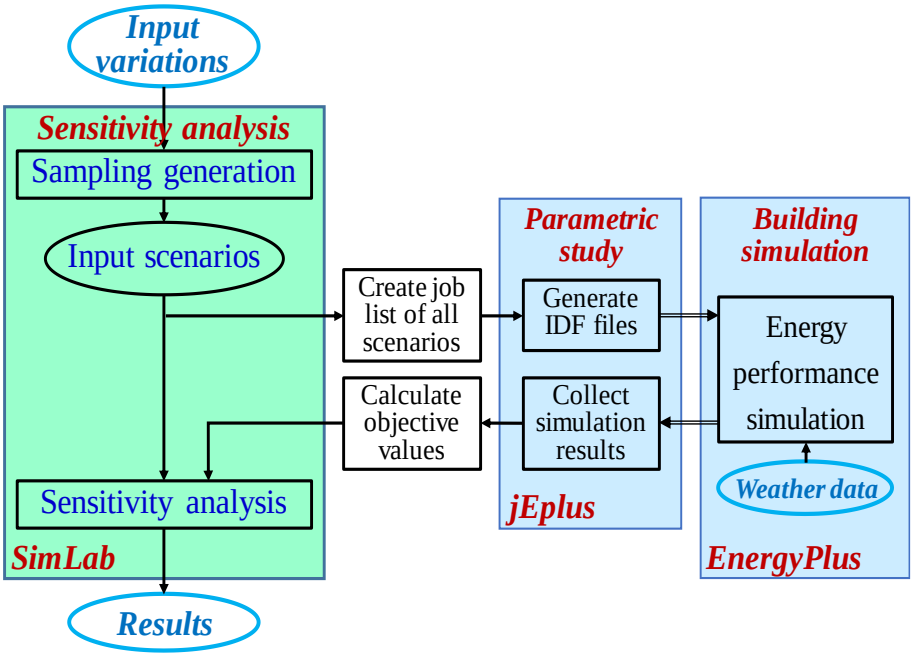

Figure 4.2 Procedures of sensitivity analysis for identification of key envelope design parameters

4.3.2 Selection of main design parameters

The main building design parameters can be classified into 5 categories: *building layout*, *envelope thermal characteristics, energy efficiency measures, energy system design parameters* and *construction quality*. In total, 29 main design parameters of these 5 categories are considered for sensitivity analysis of the reference building. Among the 29 parameters, a few parameters which are not envelope parameters are also included in the sensitivity analysis in order to identify, comparatively, the key envelope design parameters which have significant influence on building performance. For the sensitivity

analysis, all 29 design parameters are treated as continuous variables having a uniform distribution over their preset ranges. Their typical ranges are determined based on a few previous publications (Lam and Hui, 1996; Bernal-Agustín and Dufo-Lopez, 2009; Li et al., 2013; Ge and Baba, 2015; Tavares and Martins, 2007; Schnieders et al., 2016; Johnson et al., 2012) and summarized in Table 4.1. All the doors (including the windows on the top of the doors) and interior windows remain unchanged. Thermal bridge and thermal characteristics of skylight and ground slab, which were seldom considered in previous studies, are assessed in this study. In addition, the parameters influencing thermal bridge and natural ventilation are used directly instead of using global parameters to avoid the double-counting of their impacts. For instance, the impact of thermal bridge is determined by thermal transmittance and length of building connection. The common use of a thermal loss percentage will double-count the impacts of building shape if the impacts of building shape are also assessed. In this study, an overall wall U value is used to integrate the thermal bridge in the building simulation, as shown in Eq. (4.4) (Morrison Hershfield Limited, 2016).

$$U_{tot} = \frac{\Sigma(\psi \cdot L) + \Sigma(\chi)}{A_{tot}} + U \tag{4.4}$$

where, U_{tot} is the overall wall U value including the effects of thermal bridge (W/(m^2·K)). U is the wall U value (W/(m^2·K)). A_{tot} is the total opaque wall area (m^2). ψ is the linear thermal transmittance (W/(m·K)) representing the additional heat transfer of a linear thermal bridge, which is not included in the wall U value. L is the total length of linear thermal transmittance (m). χ is the point thermal transmittance (W/K) representing the additional heat transfer of a point thermal bridge, which is not included in the wall U value.

Table 4.1 Main design parameters concerned to identify key envelope design parameters

Category	Parameter	Abbreviation	Distribution	Range	Units
Layout	Building orientation	BO	Uniform	0-360	^{o}
	Window to wall ratio	WWR	Uniform	0.045-0.9	-
	Skylight to roof ratio	SRR	Uniform	0-0.9	-
Envelope thermal characteristics	Wall U value	WU	Uniform	0.09-11.1	W/(m^2·K)
	Wall specific heat	WSH	Uniform	800-2000	J/(kg·K)
	Wall solar absorptance	WSA	Uniform	0.1-0.9	-
	Ground slab U value	GSU	Uniform	0.15-2.27	W/(m^2·K)
	Ground slab specific heat	GSSH	Uniform	800-2000	J/(kg·K)
	Roof U value	RU	Uniform	0.09-4.8	W/(m^2·K)
	Roof specific heat	RSH	Uniform	450-1400	J/(kg·K)
	Roof solar absorptance	RSA	Uniform	0.1-0.9	-
	Window U value	WinU	Uniform	0.2-9	W/(m^2·K)
	Window solar heat gain coefficient	WSHGC	Uniform	0.1-0.9	-
	Window visible transmittance	WVT	Uniform	0.06-0.81	-
	Skylight U value	SU	Uniform	0.2-9	W/(m^2·K)
	Skylight solar heat gain coefficient	SSHGC	Uniform	0.1-0.9	-
	Skylight visible transmittance	SVT	Uniform	0.06-0.81	-
Construction quality	Infiltration air mass flow rate	AMFR	Uniform	0.01-0.03	kg/(s·m)
	Floor slab linear transmittance	FSLT	Uniform	0.007-1.842	W/(m·K)
	Glazing transition linear transmittance	GLT	Uniform	0.03-1.058	W/(m·K)
	Parapet linear transmittance	PLT	Uniform	0.056-1.06	W/(m·K)
	Corner linear transmittance	CLT	Uniform	0.036-0.684	W/(m·K)
	Interior wall intersection linear transmittance	IWLT	Uniform	0.039-1.15	W/(m·K)
System design	Indoor set-point	IS	Uniform	22-26	^{o}C
	Outdoor air flow rate	OA	Uniform	0-0.02	m^3/s/psn
Energy efficient measures	Overhang projection ratio	OPR	Uniform	0.2-3	-
	Discharge coefficient (natural ventilation)	DC	Uniform	0.6-1	-
	Sensible heat recovery effectiveness	SHR	Uniform	0-0.9	-
	Latent heat recovery effectiveness	LHR	Uniform	0-0.9	-

4.3.3 Results of sensitivity analysis

Results of first-stage sensitivity analysis

The results of sensitivity analysis using three different methods are presented and compared as below. The main design parameters concerned are sufficiently sampled to assure the reliability of the sensitivity analysis. The highly-sensitive parameters, which have significant impacts the building performance, are identified by holistic consideration on the outputs of three sensitivity analysis methods.

Sensitivity analysis results using regression method: LHS (Latin hypercube sampling) method is used for sampling the 29 selected design parameters within their ranges and a total number of 1000 samples are generated by SimLab for the sensitivity analysis using regression method. Two indicators, i.e. standardized rank regression coefficient (SRRC) and partial rank correlation coefficient (PRCC), are used as the sensitivity measures. SRRC measures the linear impacts of design parameters, while PRCC provides a sensitivity analysis excluding the correlation impacts between the design parameters (Yildiz and Arsan, 2011). A positive value of the indicators means that an increase of a design parameter results in an increase of performance objective. A negative value means that the changes in a design parameter and the consequential performance objective go in opposite directions.

The results are shown in Figure 4.3. It can be seen that the sensitivity ranking of the two indicators are the same although the values of the sensitivity measures are different. The values of PRCC are obviously larger than that of SRRC, which indicates that non-linear impacts exist. The skylight to roof ratio (SRR) and skylight solar heat gain coefficient (SSHGC) have the most significant influence on the building performance. The parameters of system design and construction quality (i.e. air flow rate (OA), indoor set-

point (IS) and infiltration air mass flow rate (AMFR)) have higher impacts on building performance compared with the envelope design parameters except two parameters (i.e. SRR and SSHGC). This means a higher indoor set-point within the acceptable comfort zone and a good construction quality with high air tightness can contribute significantly to the performance objective reduction (improvement). The thermal bridge has little impact in subtropical regions. The sensitivity measure of latent heat recovery effectiveness (LHR) is larger than that of sensible heat recovery effectiveness (SHR), which was not addressed in previous studies. So latent heat recovery is more important than sensible heat recovery in subtropical regions with high relative humidity. Among the envelope thermal parameters, roof solar absorptance (RSA), window solar heat gain coefficient (WSHGC), ground slab U value (GSU), roof U value (RU) and wall solar absorptance (WSA) have more significant impacts on the building performance compared with the U value of wall (WU), skylight (SU) and window (WinU). Natural ventilation is mainly determined by WWR and building orientation (BO) and the impacts of discharge coefficient (DC) are very low. Eventually, 12 highly-sensitive parameters are identified based on the sensitivity analysis results using regression method, including SRR, SSHGC, OA, IS, AMFR, WWR, LHR, RSA, WSHGC, GSU, RU and WSA.

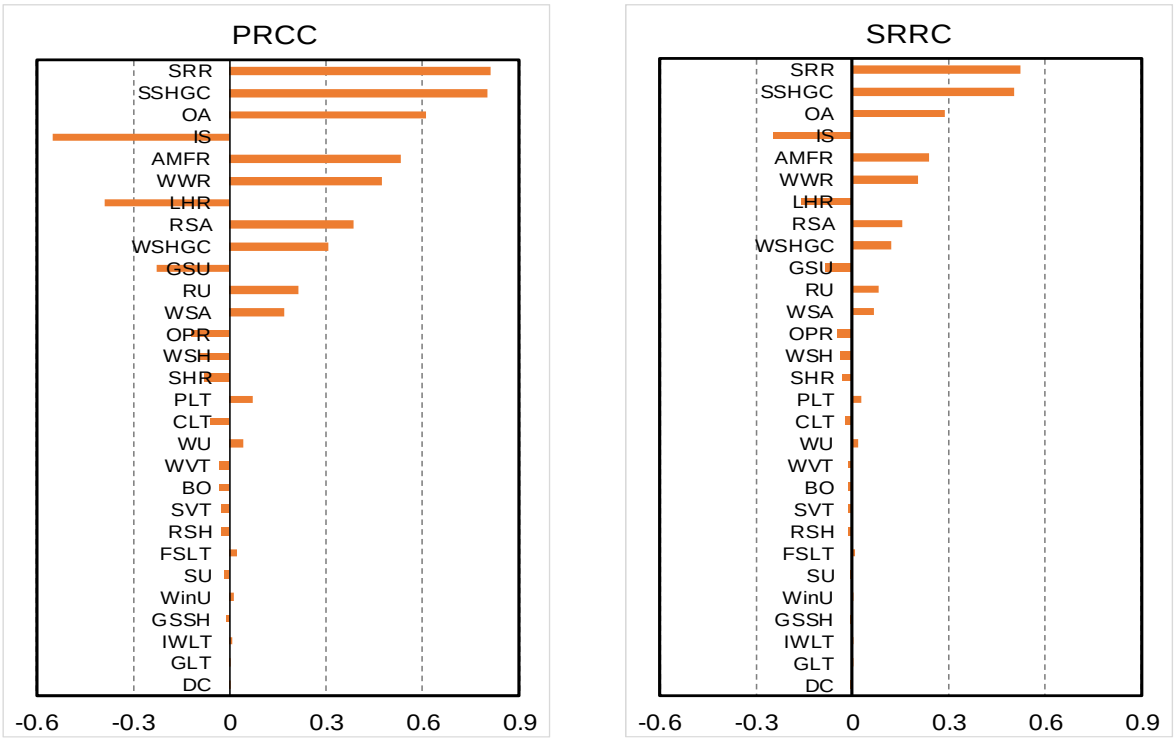

(A) Partial rank correlation coefficient (B) Standardized rank regression coefficient

Figure 4.3 Regression/correlation coefficients of all parameters concerned using regression method

Sensitivity analysis results using Morris method: 240 simulations (the number of elementary effects per parameter is set as 8), obtained by sampling all the 29 design parameters within their ranges, are conducted for sensitivity analysis using the Morris method and the sensitivity analysis results are shown in Figure 4.4. A μ value on the x–axis represents the absolute value of elementary effects of a parameter, which reflects the importance of this parameter. A σ value in y–axis is an indicator that measures the non-linear effects of a parameter and its interactions with other parameters. If a point is within the wedge (i.e. the shadowed area between the two dotted lines), the represented parameter mainly has a non-linear or/and a correlated impact on the performance objective. If a point is outside and far from the wedge, the represented parameter mainly has a linear impact on the performance objective. If a point is near to the lines of the

wedge, the represented parameter has both linear and non-linear/correlated impacts. It can be seen that most of the parameters have both linear and non-linear/correlated impacts on the performance objective, while SRR, SSHGC, OA, IS, AMFR and WWR mainly have linear effects. If parameters are ranked based on their μ values, the top 11 highly-sensitive parameters identified using Morris method are the same as that using regression method but with different orders. The biggest difference between results of the two sensitivity analysis methods is that building orientation is found to be very important when using Morris method and overhang projection ratio (OPR) and SHR are also rather influential to the performance objective. Eventually, 15 highly-sensitive parameters are identified using Morris method, including SRR, IS, OA, SSHGC, AMFR, WWR, RSA, LHR, WSHGC, RU, GSU, OPR, BO, WSA and SHR.

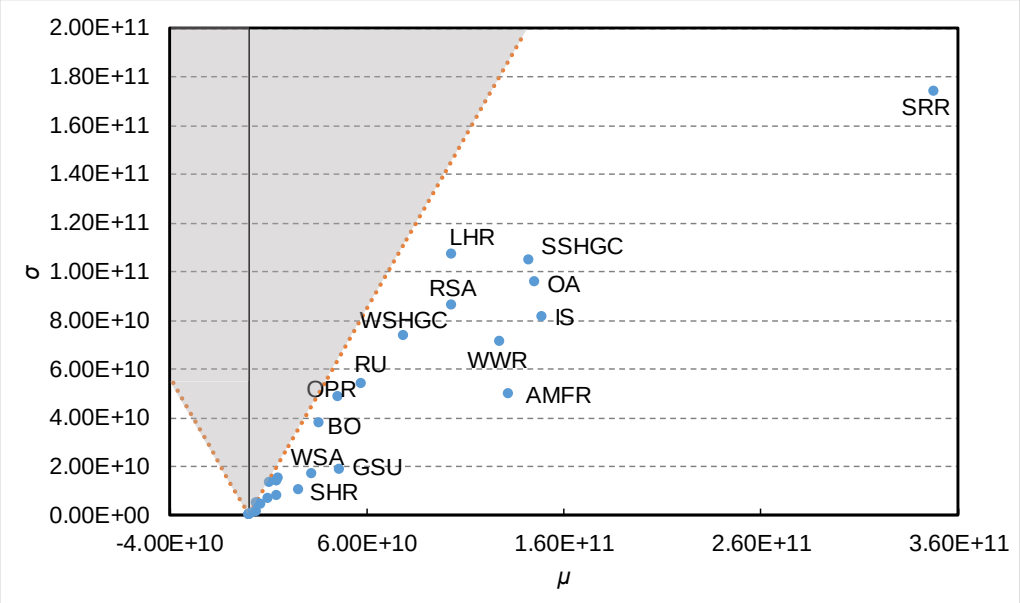

Figure 4.4 Mean and standard deviation of all parameters concerned using Morris method

(Note: only highly-sensitive parameters identified are named)

Sensitivity analysis results using FAST method: 1885 simulations (minimum sufficient samples for 29 parameters), obtained by sampling all the 29 parameters within their

ranges, are performed for sensitivity analysis using the FAST method and the sensitivity analysis results are shown in Figure 4.5. Two sensitivity measures, i.e. the first order and the total order, are used to assess the parameters. The first order of a parameter reflects its main effects, while its total order reflects its main effects and correlated effects. Figure 4.5 shows that most of the parameters have correlations with other parameters, while the main effects of IS, WWR, SSHGC and AMFR dominant indicating they have little correlation with other parameters. This result is consistent with that of Morris method. The sensitivity order given by FAST method is very different from that given by regression method and Morris method, which may be due to that the FAST method measures the linear and nonlinear impacts while the regression method and the μ of Morris method measure the linear impacts only. SRR, SSHGC, OA, IS, AMFR, WWR, LHR, RSA and RU are the common recognized highly-sensitive parameters by the three sensitivity analysis methods. Parapet linear transmittance (PLT) and wall specific heat (WSH) are identified as highly-sensitive parameters by FAST method, which is very different from the results of the former two methods. The performance objective is proven to be very sensitive to BO and OPR, which is in consistent with the results of Morris method. The highly-sensitive parameters identified based on first order and total order are a bit different. 11 highly-sensitive parameters can be identified based on the first order. They are SRR, AMFR, SSHGC, WWR, IS, RU, OPR, BO, OA, RSA and LHR. Two more highly-sensitive parameters are identified based on the total order, i.e. PLT and WSH.

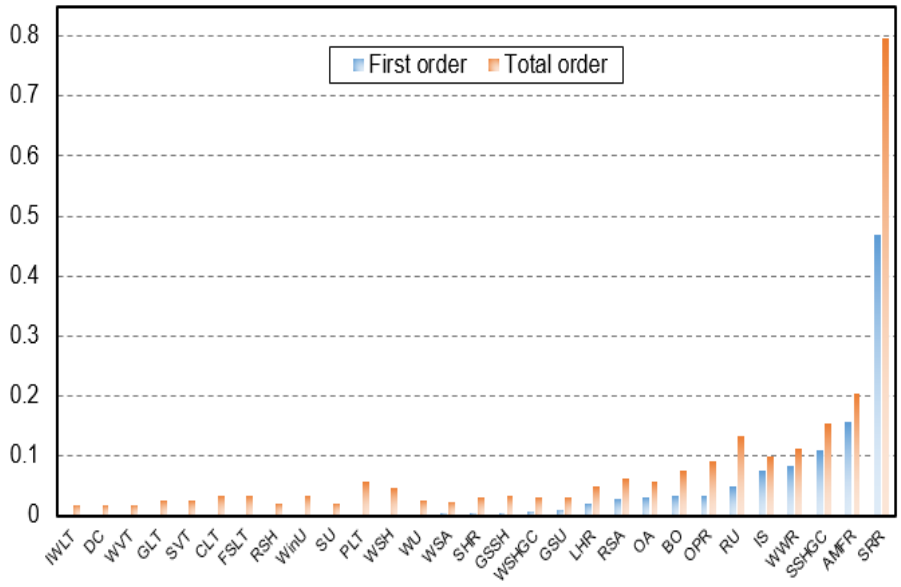

Figure 4.5 First and total order of all parameters concerned using FAST method

Identification of highly-sensitive parameters by holistic consideration: The ranking orders of the highly-sensitive parameters using the three different sensitivity analysis methods are presented in Table 4.2. The results of Morris method are highly consistent with the results of regression method and rather consistent with the results of FAST method. The ranking order using FAST method are very different from that using regression method. Therefore, identifying key design parameters using a single sensitivity analysis method likely results in missing important parameters. For instance, the use of regression method can lead to missing OPR and BO, which are commonly recognized as highly-sensitive parameters in hot climate regions.

Eventually, a total number of 14 highly-sensitive parameters are identified using the three methods collectively including: SRR, SSHGC, OA, IS, AMFR, WWR, LHR, RSA, RU, WSHGC, GSU, WSA, OPR and BO. Among these parameters, OA, IS, AMFR, WWR, WSHGC, OPR and BO are highly-sensitive parameters commonly considered in previous studies (as shown in Table 2.1). WSA and GSU are considered as important parameters of buildings without heating in subtropical regions in terms of energy consumption and

winter thermal discomfort, which are seldom considered in previous studies. This inconsistency may result from the consideration of winter thermal discomfort in performance objective, which can be deduced from the comparison with the identified highly-sensitive parameters when annual energy consumption is the only concern as shown in Table 4.3.

Results of second-stage sensitivity analysis

A second-stage sensitivity analysis is conducted on the identified 14 highly-sensitive parameters to further select the key envelope design parameters which need to be optimized, since there is no need to optimize all the highly-sensitive parameters (e.g., some parameters are obviously the higher the better or the lower the better). At this stage, the local sensitivity analysis method is used to assess the directions of the effects of the parameters on annual electricity consumption and annual discomfort index respectively. The reason not to assess the directions of the effects on the combined optimization objective is that its change direction is affected by the preset penalty ratio for the discomfort, leading to potentially missing key design parameters.

Only the highly-sensitive envelope design parameters are assessed at this stage. The parameters related to building operation, i.e., OA, IS, AMFR, are not considered although they are included in the first-stage sensitivity analysis due to the reason explained earlier. In addition, the skylight (windows) is not considered for design optimization since the skylight is not used for the indoor spaces in this study. A few selected main results of the local sensitivity analysis are presented in Figure 4.6. It can be seen that WSA and RSA have the opposite impacts on the annual electricity consumption and annual discomfort index. It means that they need to be optimized in order to minimize the performance objective. The impacts of GSU and RU on both annual discomfort index and annual

electricity consumption are in the same directions. It means that their values are either the higher the better or the lower the better. Therefore, there is no need to optimize them when optimizing the building design according to the defined objective in the climate condition of concern.

Table 4.2 Ranking orders of highly-sensitive parameters based on three different sensitivity analysis methods (objective considering energy consumption and winter thermal discomfort)

Parameter	**Regression**		**Morris**	**FAST**	
	SRRC	PRCC	μ	first order	Total order
SRR	1	1	1	1	1
SSHGC	2	2	4	3	3
OA	3	3	3	9	10
IS	4	4	2	5	6
AMFR	5	5	5	2	2
WWR	6	6	6	4	5
LHR	7	7	8	11	12
RSA	8	8	7	10	9
WSHGC	9	9	9		
GSU	10	10	11		
RU	11	11	10	6	4
WSA	12	12	14		
OPR			12	7	7
WSH					13
SHR			15		
PLT					11
BO			13	8	8

Note: The parameters in bold and italic are identified as the highly-sensitive parameters.

Table 4.3 Ranking orders of highly-sensitive parameters based on three different sensitivity analysis methods (objective considering energy consumption only)

Parameter	**Regression**		**Morris**	**FAST**	
	SRRC	PRCC	μ	first order	Total order
SSHGC	1	1	2	3	3
SRR	2	2	1	1	1
OA	3	3	4	10	11
IS	4	4	3	4	7
AMFR	5	5	5	2	2
RSA	6	6	6	6	8
WWR	7	7	7	5	6
WSHGC	8	8	8	12	
LHR	9	9	9	11	12
WSA		10			
GSU		11			
RU		12		9	5
OPR		13		7	4
WSH					10
PLT					13
BO				8	9

Note: The parameters in bold and italic are identified as the highly-sensitive parameters.

Eventually, six key envelope design parameters are identified and selected for design optimizations involving envelope design, including BO, RSA, WWR, WSA, WSHGC and OPR. Table 4.4 presents these six envelope design parameters and their searching ranges considered in the design optimizations. They are assumed to be continuous in the design. It is worth noticing that four of them (i.e., BO, WWR, WSHGC and OPR) are commonly-selected design parameters for design optimization in existing studies. RSA and WSA are rarely selected as the key design parameters for design optimization except

one case (Yu et al., 2008). In this study, the sensitivity analysis results show that these two parameters should be considered when thermal comfort issue is concerned in the situation without heating provision in subtropical regions. The U values or thermal inertia of building envelope components, which also have impacts on building performance, are not considered for design optimization in this study since the results of the sensitivity analysis show that the selected design variables have more significant impacts on building performance than the U values and thermal inertia in subtropical regions. A similar conclusion was also made by Chen et al. (2018), which also shows that the U value of wall has much less impacts on building performance than other parameters like building orientation, solar heat gain coefficient and overhang projection ratio in Hong Kong.

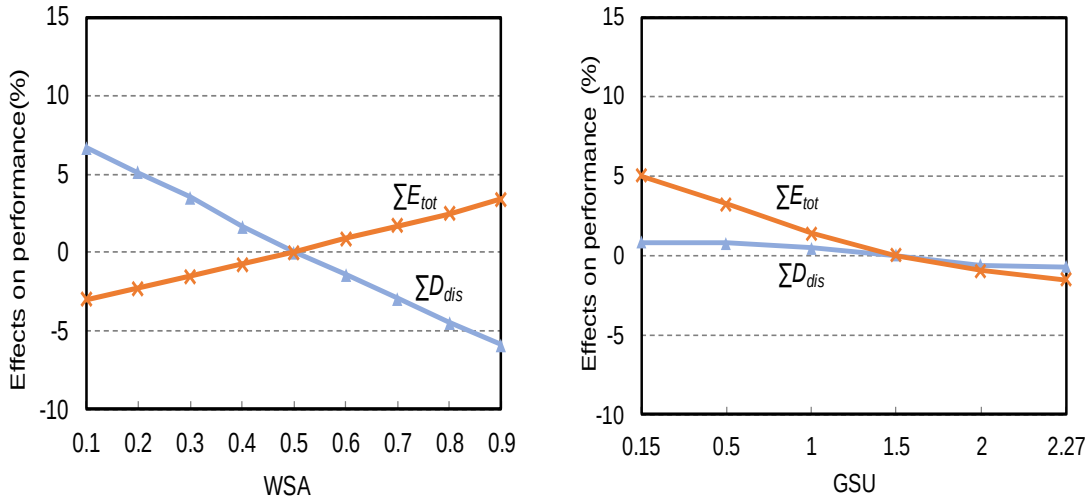

(A) Wall solar absorptance (WSA) (B) Ground slab U value (GSU)

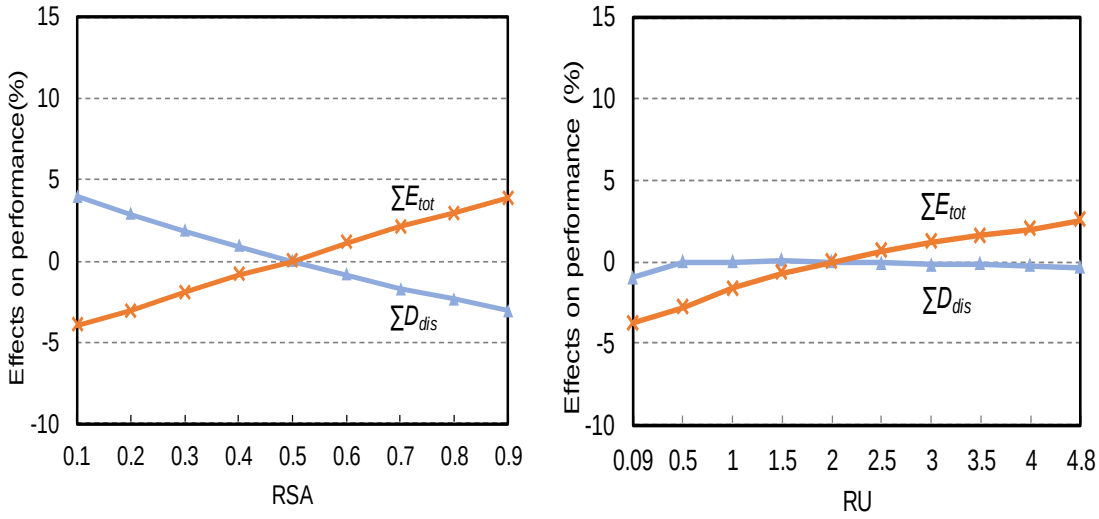

(C) Roof solar absorptance (RSA) (D) Roof U value (RU)

Figure 4.6 Effects of selected design parameters on annual discomfort index ($\sum D_{dis}$) and annual electricity consumption ($\sum E_{tot}$)

4.4 Selection of key system design parameters

The design optimization of building energy systems in this study focuses on the optimization of component size and number by assuming that the type of each system component is selected prior to design optimization. Ten design variables of building energy systems are selected and optimized. The detailed variables and their searching ranges are listed in Table 4.4. They are PV area, number and capacity of wind turbines, number and capacity of co-generators, number and capacity of electric chillers, number and capacity of absorption chillers, and capacity of battery. The minimum values of the capacities of energy system components are determined based on the minimum capacity of available devices in the market, while their maximum values are determined based on the energy demand of the reference building. It is worth noticing that, for a more complex and detailed system optimization, different efficiencies need to be considered for different types of components when the optimal choice of component types is included. Among the design variables, the number of system component is assumed to be discrete in the

design, while the capacity of the system component is assumed to be continuous.

Table 4.4 Design variables of building envelope and energy systems

Category	Design variable	Abbreviation	Searching range	Unit
Building envelope	Building orientation	BO	[0,360]	°
	Roof solar absorptance	RSA	[0.1,0.9]	-
	Window-to-wall ratio	WWR	[0.2,0.6]	-
	Wall solar absorptance	WSA	[0.1,0.9]	-
	Overhang projection ratio	OPR	[0.05,0.5]	-
Building energy systems	PV area	A_{PV}	[100,1032]	m²
	Capacity of wind turbines	Cap_{WT}	[1,40]	kW
	Number of wind turbines	n_{WT}	{0,1,2,3}	-
	Capacity of co-generators	Cap_{CG}	[30,150]	kW
	Number of co-generators	n_{CG}	{1,2,3}	-
	Capacity of absorption chillers	Cap_{AC}	[20,200]	kW
	Number of absorption chillers	n_{AC}	{1,2,3,4,5}	-
	Capacity of electric chillers	Cap_{EC}	[20,200]	kW
	Number of electric chillers	n_{EC}	{1,2,3,4,5}	-
	Capacity of battery	Cap_{bat}	[10,100]	kWh

4.5 Identification of main uncertain inputs

4.5.1 Procedure and method of sensitivity analysis

Due to the huge number of possible uncertain design scenarios, a robust design optimization that involves performance trials under all possible scenarios needs an extremely long computation time. *To reduce the computation time, the uncertain design inputs of significant impacts on the building performance in the specific climate regions concerned are identified beforehand by sensitivity analysis.* Where, single sensitivity

analysis method is effective and used as the number of uncertain design inputs considered is small. The regression method (Hygh et al., 2012) is selected for sensitivity analysis because of its simple implementation and non-inferior ability of ranking parameters than meta-model sensitivity analysis methods (Nguyen and Reiter, 2015). The standardized regression coefficient (SRC) is chosen as the sensitivity index to measure the effects of the design inputs on the building performance. A higher SRC means a more significant impact on building performance.

Three software tools are used to conduct the sensitivity analysis: MATLAB, jEplus (jE+) and EnergyPlus (E+). jEplus and EnergyPlus are used to achieve the automatic process of numerous new building design establishment and building performance simulation. In addition to jEplus and EnergyPlus, MATLAB is used at a higher level.

The process of the sensitivity analysis is shown in Figure 4.7. *First*, all possible combinations of uncertain design inputs (input scenarios) are generated by sampling sufficiently within the uncertain design inputs according to their probability distributions, using the LHS method. A job list is created according to the input scenarios for jEplus. *Second*, jEplus assigns the values of the parameters with uncertainties to the building model (base model) as specified in the job list (while keeping the design and other model parameters fixed) and generates a set of corresponding building simulation model descriptions (IDF files) for EnergyPlus. EnergyPlus then automatically runs the simulations of all of the scenarios. *Finally*, jEplus collects all of the simulation results, and a simple calculation is conducted to obtain the building performance under each input scenario using the corresponding outputs of building performance simulations. Once the input scenarios and their performance values are obtained, the SRCs of the uncertain design inputs are calculated and the design inputs are then ranked according to their SRCs.

The design inputs with higher rankings (i.e., larger SRCs) are identified as significant uncertain design inputs.

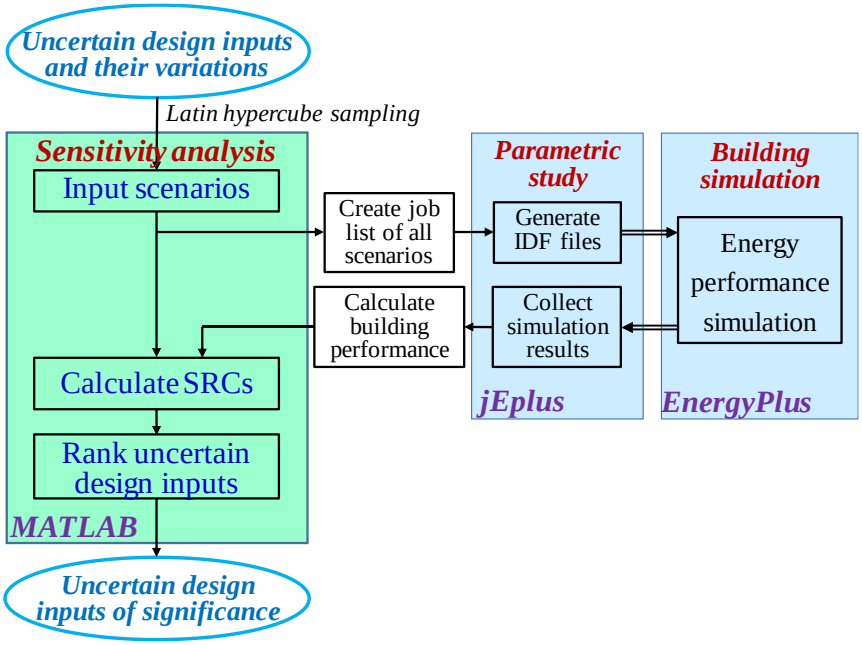

Figure 4.7 Sensitivity analysis procedure for the identification of uncertain design inputs of significant impacts using regression method

4.5.2 Uncertain design inputs considered for sensitivity analysis

The uncertain design inputs for building design optimization, are classified into four categories: *weather condition, internal loads, infiltration* and *thermal bridge*, as shown in Table 4.5. They are related to climate, building use (internal loads) and construction quality (infiltration and thermal bridge), respectively. It is worthy noticing that the uncertainties in the cost such as construction and energy prices should be also considered when cost is considered in the objective functions.

The uncertainties in theses design inputs are quantified based on a probabilistic approach. Their probability distributions are shown in Table 4.5. Where, U(a, b) refers to the uniform distribution (a and b are the minimum and maximum values respectively). Tri(a, b, c) refers to the triangular distribution (a, b, and c are the minimum, maximum and peak values, respectively). N(μ, σ) refers to the normal distribution (μ and σ are the mean and

standard deviation respectively).$TN_{(a, b)}(\mu, \sigma)$ refers to the truncated normal distribution, which is derived from a normal distribution $N(\mu, \sigma)$ by bounding the variable within (a, b).

Table 4.5 Uncertain design inputs considered in sensitivity analysis, robust optimal design and coordinated robust optimal design

Category	**Uncertain design inputs**	**Unit**	**Distribution**	**Uncertainty considered**		
				Sensitivity analysis	Robust optimal design	Coordinated robust optimal design
Weather condition	Dry bulb temperature (DB)	℃	Actual measured weather (1979-2016)	✓	✓ (Actual weather: 1979-2008)	✓ (Actual weather: 1979-2008)
	Relative humidity (RH)	%				
	Solar radiation (SR)	Wh/m²				
	Wind speed (WS)	m/s				
	Wind direction (WD)	-				
	Climate change trend	K/year	U(0,0.048)		✓	✓ $TN_{(0, 0.024)}$ (0.012,0.006)
Internal loads	Occupant density	-	Factor (ILF): Tri(0.3,1.2,0.9)	✓	✓	✓ Factor: N(1, 0.1)
	Lighting load	-				
	Equipment load	-				
Infiltration	Infiltration air mass flow rate (IAMFR)	kg/(s·m)	U(0.0025,0.0075)	✓	✓	✓ $TN_{(0.008,0.04)}$(0.024,0.008)
Thermal bridge	Interior wall intersection linear transmittance (IWLT)	W/(m·K)	U(0.039,1.15)	✓		
	Floor slab linear transmittance (FSLT)	W/(m·K)	U(0.007,1.842)	✓		
	Glazing transition linear transmittance (GLT)	W/(m·K)	U(0.03,1.058)	✓		
	Parapet linear transmittance (PLT)	W/(m·K)	U(0.056,1.06)	✓		
	Corner linear transmittance (CLT)	W/(m·K)	U(0.036-0.684)	✓		

The uncertainties in weather condition are quantified using the actual measured weather data over 38 years (i.e., between 1979 and 2016) in Hong Kong. This method of quantifying weather uncertainties has been recommended in other studies of building energy system design that consider uncertainties (Gang et al., 2016; Sun et al., 2014). The uncertainties in internal loads are quantified by assigning an uncertain factor to the design value of occupant density, lighting load and equipment loads, assuming that all of these are correlated to occupant density. The uncertain factor is assumed to follow a triangular distribution. Both the uncertainties in infiltration and the thermal bridge are assumed to follow uniform distributions. Their ranges are determined based on the best and worst cases that may occur in practice.

4.5.3 Results of sensitivity analysis

304 sets of uncertain design inputs are generated using the LHS method, in order to make sure the number is integral multiples of years of historical weather data (i.e., 38) while satisfying the requirement of the minimum sampling number using LHS method. Their corresponding annual energy consumption and annual discomfort index are obtained using EnergyPlus. The SRCs of these design inputs are calculated and the results are shown in Figure 4.8. The design inputs with uncertainties that have significant effects on annual energy consumption, are internal loads, wind direction, ambient dry-bulb temperature, infiltration and wind speed, as shown in Figure 4.8A. Those with significant effects on winter thermal discomfort are ambient dry-bulb temperature, wind direction, wind speed, solar radiation and internal loads (as shown in Figure 4.8B), whereas ambient dry-bulb temperature, wind direction, wind speed and solar radiation are the weather condition variables. Therefore, weather condition, infiltration and internal loads are eventually identified as uncertain design inputs that have significant effects on the

performance of buildings in subtropical regions. It is worth noticing that if the internal loads are stochastic with different time, the impacts of the uncertainties in the internal loads would be larger.

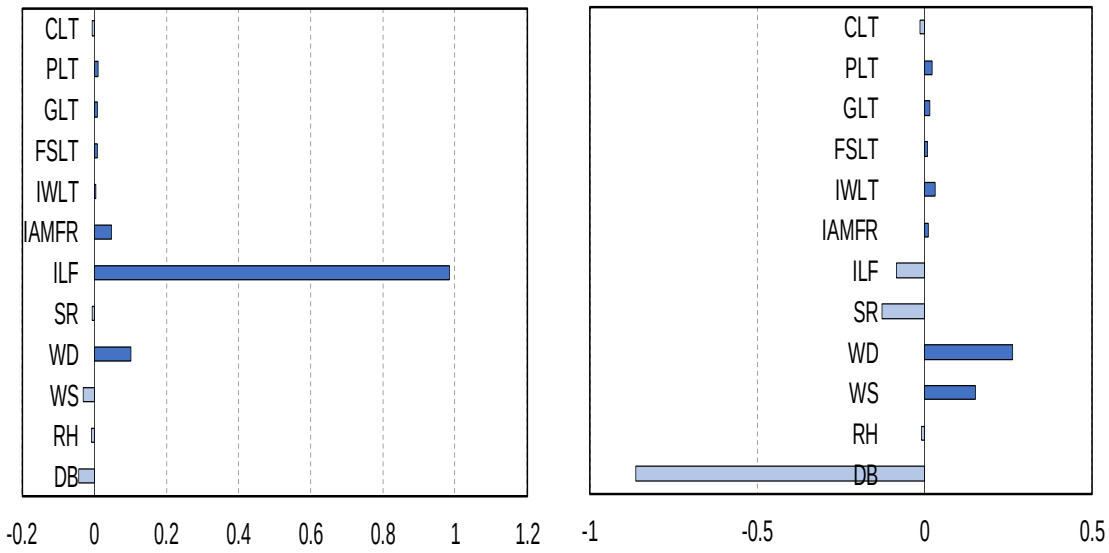

(A) Annual energy consumption (B) Annual discomfort index

Figure 4.8 Standardized regression coefficients of uncertain design inputs concerned for building energy consumption and discomfort index

The extent to which the identified uncertain design inputs affect the building optimal design is further analyzed. The impacts of uncertainties of internal loads and weather conditions on the optimal design of WWR concerning the performance objective are presented here as examples. The results show that a WWR of 0.6 is the optimum when the actual internal load is 1.2 times the design internal load, while a lower WWR of 0.45 is preferred when the actual internal load is 0.3 times the design internal load. The optimal WWR under the TMY weather condition in Hong Kong is 0.5, but the optimal WWR is lower to minimize the objective value under the actual weather condition in 2016. It is thus necessary to consider the uncertainties of design inputs in the optimal design of zero/low energy buildings.

Finally, the uncertainties in these main uncertain inputs are considered in the robust

optimal design in Chapter 6 and coordinated robust optimal design in Chapter 7, together with the uncertainty in the climate change trend over the building life cycle, as shown in Table 4.5. The distribution types and values of the main uncertain design inputs considered in robust optimal design in Chapter 6 are the same as that in sensitivity analysis, while the distribution types and values of the main uncertain design inputs considered in coordinated robust optimal design in Chapter 7 are revised on the basis of that considered in robust optimal design as listed in Table 4.5. Truncated normal distributions or normal distributions are used to quantify some of the uncertainties, since it is reasonable and easy to implement when point estimate method is used for uncertainty propagation.

It is worth noticing that building performance is evaluated over the building life cycle in the robust optimal design and coordinated robust optimal design. The weather uncertainties during building life cycle are quantified by two parts in this study, i.e., the variation of weather conditions and the climate change trend. The uncertain variations of weather condition during the building life-cycle are simulated by using the actual historical weather data (1979-2008) reorganized into a random order, which is a highly recommended method in recent years for the quantification of uncertain variations of weather condition (Gang et al., 2016; Sun et al., 2014). A climate change trend (a linear increase in dry-bulb temperature over the life-cycle) is added to the randomly-ordered historical weather data. For example, if the climate change trend is 0.01 K/year, the temperature of the randomly-ordered historical weather data in the first year is added by 0.01 K, and the temperature in the 30th year is added by 0.3 K. The magnitude of the climate change trend is assumed to be in a range between 0 and 0.048 K/year following a uniform distribution as shown in Table 4.4. This maximum value is assumed based on the actual dry bulb temperature increase of +0.012 K/year (from 1885 to 2017) as reported

by the Hong Kong Observatory, and by considering the urban island effect.

4.6 Summary

In this chapter, the impacts of envelope design parameters and uncertain design inputs on the performance of zero/low energy buildings in subtropical regions are studied. Key system design parameters are selected. A multi-stage sensitivity analysis method is implemented to identify the key envelope design parameters that significantly affects the performance objective. Sensitivity analysis is performed to identify the key envelope design parameters and main uncertain design inputs. Based on the results of sensitivity analysis, conclusions can be made as follows.

- Six key envelope design parameters, which significantly affects the performance of buildings in subtropical regions are identified. They are building orientation, roof solar absorptance, window to wall ratio, wall solar absorptance, window solar heat gain coefficient and overhang projection ratio. Ten system design parameters are selected, which are the number and capacity of the system components.
- The outputs of the sensitivity analysis using different sensitivity analysis methods can be different and using a single sensitivity analysis method to identify the key design parameters may result in missing some important design parameters. It is therefore recommended to combine more than one sensitivity analysis method to identify and determine the parameters to be optimized. For instance, the sensitivity analysis using regression method only would lead to missing two key design parameters, namely overhang projection ratio and building orientation, which are commonly considered as highly-sensitive parameters in previous studies for buildings in hot climate regions.
- The consideration of winter thermal discomfort significantly affects outputs of sensitivity analysis for buildings without heating provision in subtropical regions and

therefore the identification and selection of their key design parameters. In this study, the results of sensitivity analysis show that roof and wall solar absorptance are highly-influential parameters when winter thermal discomfort is concerned in the buildings without heating provision in subtropical regions. However, these two parameters are seldom selected as the key design parameters in previous studies, which are mainly concerned about energy consumption.

- The uncertainties in the design inputs have significant effects on the choice of optimal design for zero/low energy buildings. It is necessary to consider the uncertainties in the building design optimization. The uncertain design inputs, which have significant impacts on the performance of buildings in subtropical regions, are weather conditions, infiltration and internal loads.

CHAPTER 5 COORDINATED OPTIMAL DESIGN OF BUILDING ENVELOPE AND ENERGY SYSTEMS

This chapter presents the procedure and methods of the proposed coordinated design optimization method for the entire zero/low energy buildings including building envelope and energy systems. An ANN (artificial neural network) building performance model is trained and validated for building performance evaluation. Three case studies, including a case of standalone low energy buildings, a case of grid-connected low energy buildings and a case of grid-connected ZEBs, are conducted to validate the coordinated optimal design method.

5.1 Procedure and methods of coordinated optimal design

5.1.1 Procedure and major steps

Existing multi-stage design optimization methods (namely uncoordinated optimal design in the rest of this thesis) generally optimize the envelope and the energy systems of a building separately without considering the impacts of energy system design optimization on building envelope design optimization as shown in Figure 5.1A. At Stage 1, the design variables of building envelope are optimized within their searching ranges by considering the impacts of building envelope design optimization on energy system design optimization, since the impacts of building envelope design on the performance of building and energy systems may be adverse. At Stage 2, building loads, such as the electricity and cooling load profiles associated with the optimal envelope design, are then calculated. Based on the load profiles, design variables of the energy systems are optimized within their searching ranges. The obtained optimal envelope design and

energy system design are eventually taken as the optimal design solution for the building. As the building design and energy system design are optimized at two separate stages by ignoring the impacts of energy system design optimization on building envelope design optimization, the optimal solutions achieved are very likely to be "local" optimal solutions.

The proposed coordinated optimal design method coordinates the design optimizations of building envelope and energy systems to consider the interactions between building envelope and energy system design optimizations in order to achieve the global optimal solution or the same effect of the simultaneous optimization, as shown in Figure 5.1B. The method involves two steps, i.e., the identification of coordinating design variables and the coordinated design optimization. *At the first step*, the coordinating design variables (S) are identified. They are some of the energy system design variables, which have impacts on building envelope optimization. These variables are considered at the stage of building envelope design and optimized at the stage of system design optimization.

At the second step, an iterative approach is adopted to coordinate the multi-stage design optimizations. Each iteration (optimization loop) is, in fact, a multi-stage design optimization, consisting of building envelope design optimization and energy system design optimization. At the first stage, an initial set of values (S_i) is assumed for the coordinating design variables to be used in the performance assessment for building envelope design optimization in order to make a trade-off between building envelope and energy system design optimizations. Building envelope design optimization is conducted to identify the optimal envelope design, which minimizes the optimization objective of envelope design. At the second stage, hourly cooling load and electrical power load

(excluding electricity for cooling) profiles of the optimal envelope design are calculated using building simulation software. These profiles are used for building energy system design optimization. The optimal energy system design variables including the optimal coordinating design variables are identified to minimize the optimization objective of energy system design, subject to the satisfaction of the energy demands of the optimal envelope design. If the obtained optimal coordinating design variables given by energy system design optimization (S_i') deviates significantly from the value set in the envelope design optimization (S_i), a new trial of building envelope optimization will be performed after setting a new S_{i+1} based on the S_i and S_i' at last optimization loop. The new S_{i+1} can be determined as the S_i' at the last optimization loop or the average of the S_i and S_i' at last optimization loop in order to accelerate the convergence. A new optimization loop starts, and building envelope design optimization and energy system design optimization are conducted again under the updated setting. The optimization loop continues until the deviation between S_i and S_i' in the same loop is less than a preset threshold, ε. ε is set as 2% in this study by assuming that 2% deviation has negligible impacts on building and system performance. The finally achieved optimal envelope design and optimal energy system design constitute the optimal design solution for the building.

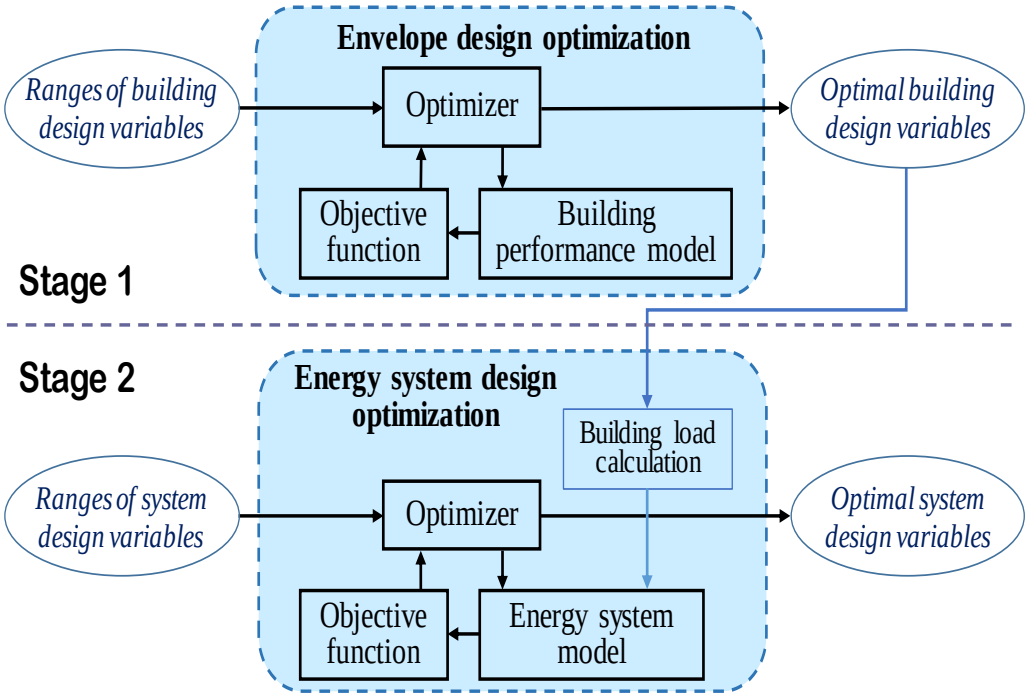

(A) Existing uncoordinated optimal design method

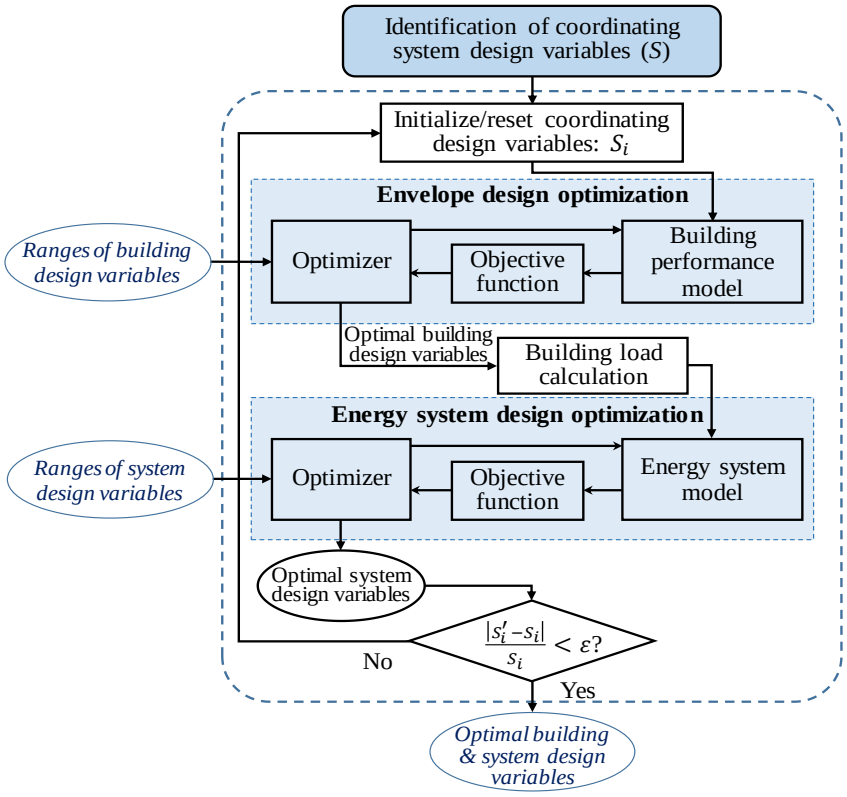

(B) Proposed coordinated optimal design method

Figure 5.1 Outline of the proposed coordinated optimal design method and the existing uncoordinated optimal design methods

5.1.2 Formulation of the optimization problems

The design optimization problems of building envelope and energy systems are formulated as Eq. (5.1) and Eq. (5.2), respectively. Where, F is the design optimization objective. X is the vector of the design variables. p is the vector of the presumed design inputs, which is fixed in the design optimization process. The subscript "*env*" refers to envelope, while subscript "*sys*" refers to energy systems. The design variables of building envelope are optimized within their searching ranges. The design variables of energy systems are optimized within their searching ranges subject to some equality and inequality design constraints.

Envelope design optimization:

$$\text{Minimize: } F_{env}(X_{env}, p_{env}, S) \tag{5.1}$$

$$\text{subject to: } X_{env,min} \leq X_{env} \leq X_{env,max}$$

System design optimization:

$$\text{Minimize: } F_{sys}(X_{sys}, p_{sys}) \tag{5.2}$$

$$\text{subject to: } X_{sys,min} \leq X_{sys} \leq X_{sys,max}$$

$$g(X_{sys}, p_{sys}) = 0$$

$$h(X_{sys}, p_{sys}) \leq 0$$

5.2 An overview of the validation case

5.2.1 Optimization objective functions and design constraints

The design optimizations of low energy buildings and zero energy buildings are both addressed in the case studies, which can be standalone or grid-connected. Different design optimization objective functions of energy systems are formulated for standalone and grid-connected buildings. The design optimization objective functions and design constraints for building envelope and energy systems are formulated and illustrated as

follows. GA (genetic algorithm) in the global optimization tool box of Matlab is used as the optimization algorithm in this study, which is able to solve the mixed integer optimization problems. A population size of 100 is set for envelope design optimization, while a population size of 200 is set for system design optimization.

Optimization objective function for building envelope design

A single objective (F_{env}) is formulated as Eq. (5.3) for building envelope design optimization, which integrates the part to consider performance objective defined in Section 4.2 and the part to consider the performance of the system component associated with the coordinating design variables *S*. In this study, the PV area is the coordinating design variable for the building concerned as identified in Section 5.3.1 in later step. Thus, the PV power generation is considered in envelope design optimization as shown in Eq. (5.4). Two weighting factors, c_{ele} and c_S, are used to integrate these two parts as a single cost function. c_{ele} is the unit price of buying electricity (USD/kWh), while c_S is the unit price of selling electricity generated by PV (USD/kWh). For standalone buildings, c_{PV} is equal to c_{ele}. For grid-connected buildings, c_{PV} is the feed in tariff. Δt is the time interval, which is set as one hour in this study. The performance is assessed throughout a typical year under the TMY (typical meteorological year) weather data in Hong Kong.

$$F_{env} = c_{ele} * (f + a * D) - c_S * f_S \tag{5.3}$$

$$f_S = \sum P_{PV} * \Delta t \tag{5.4}$$

Optimization objective function for building energy systems of standalone zero/low energy buildings

The optimization objective ($F_{sys,AL}$) for building energy system design of standalone zero/low energy buildings consists of total cost (*TC*), the accumulated unmet power (ΣP_{umt}) and the accumulated unmet cooling load (ΣQ_{umt}), in the building life cycle, which

is calculated using Eq. (5.5-5.6). The total cost *TC* (USD) includes initial cost (*IC*), operation cost (*OC*) and replacement cost (*RC*) in building life-cycle. The total cost over the building life cycle is assessed as the present cost. The initial cost of a system component is calculated by multiplying the unit price of the component by its design capacity and number. An interest rate is considered, as listed in Table 3.2, to discount the operation cost in the future. The replacement cost is calculated based on the initial cost of the system component considering the interest rate. The accumulated unmet power is the sum of the hourly unmet power P_{umt} (kW) over the building life cycle, which is induced when power supply is less than power demand. Similarly, the accumulated unmet cooling load is the sum of the hourly unmet cooling load Q_{umt} (kW) over the building life cycle, which is induced when total capacity of chillers is less than the building cooling demand. Two penalty ratios, *a1* and *a2*, are assigned to unmet power and unmet cooling load respectively. *k* refers to the total years in the building life cycle.

$$F_{sys,AL} = TC + \sum_{i=1}^{k}\sum_{j=1}^{8760} a1 * P_{umt,i,j} + \sum_{i=1}^{k}\sum_{j=1}^{8760} a2 * Q_{umt,i,j} \quad (5.5)$$

$$TC = IC + OC + RC \quad (5.6)$$

Optimization objective function for building energy systems of grid-connected zero/low energy buildings

The optimization objective ($F_{sys,GC}$) for building energy system designs of grid-connected zero/low energy buildings consists of total cost (*TC*), the accumulated unmet cooling load (ΣQ_{umt}), and the accumulated grid impact index (ΣGII), in the building life cycle, which is calculated using Eq. (5.7-5.8). Gird impact index is considered to reduce the stress that the building imposes on the grid because of frequent power import and export. It is the standard deviation of the ratio of the net imported energy to the average energy demand

over a month, as shown in Eq. (5.8). Two penalty ratios, *a2* and *a3*, are assigned to unmet cooling load and grid impact index respectively. *a2* is the same as that in Eq. (5.5).

$$F_{sys,GC} = TC + \sum_{i=1}^{k}\sum_{j=1}^{8760} a2 * Q_{umt,i,j} + \sum_{i=1}^{k}\sum_{j=1}^{12} a3 * GII_{i,j} \quad (5.7)$$

$$\mathrm{GII} = \mathrm{std}\left(\frac{P_{im,i}-P_{ex,i}}{\int_{t1}^{t2} P_{dem}dt}\right) \quad (5.8)$$

Design constraints for building energy systems

The constraints for the design optimization of building energy systems include the limit for battery charge and discharge rate, and the limit for battery storage, as shown in Eq. (5.9-5.11). In addition, for the zero energy buildings, the energy generated from renewable resources over the building life cycle should be equal to or larger than the energy demand of energy systems over the building life cycle.

$$0 \le P_{ch} \le P_{ch,max} \quad (5.9)$$

$$0 \le P_{dch} \le P_{dch,max} \quad (5.10)$$

$$E_{bat,min} \le E_{bat} \le E_{bat,max} \quad (5.11)$$

5.2.2 Energy system control strategies

The following typical control strategies are implemented in an ideal control model for the performance assessment of system design optimization in this study. The priority (high to low) of power supply is: PV & wind turbines, battery, co-generators and grid. Absorption chillers have higher priority to supply cooling than electric chillers when co-generators are put into operation. At this situation, electric chillers are put into operation when cooling demand cannot be satisfied using absorption chillers only. Only electric chillers are used when co-generators are not in operation. The detailed control strategies of the entire energy system for grid-connected buildings are illustrated in Figure 5.2, including an overall control mode selection and three alternative operation modes. Where,

P_{sup} and P_{dem} are calculated using Eq. (5.12) and Eq. (5.13), respectively.

$$P_{sup} = (P_{PV} + P_{WT} + P_{dch}) \times \eta_{inv} + P_{CG} \quad (5.12)$$

$$P_{dem} = P_{EC} + P_{EL} + P_{ch} \quad (5.13)$$

Overall control mode selection: It is a step to determine the proper control mode of the system at the beginning of each time step. First, if the total capacity of electric chillers is insufficient to satisfy the total cooling demand, the "co-generator mode" will be selected. Otherwise, other modes are to be checked. Then, if the power generations of PV and wind turbines are insufficient to meet the (maximum) electricity demand when electric chillers are used only for cooling supply, the "battery discharge mode" will be selected. Otherwise, the "battery charge mode" will be selected.

Co-generator mode: Absorption chillers and electric chillers are used for cooling supply, while PV, wind turbines and co-generators are used for power supply. If the electricity supply is insufficient when running the energy generation system at its full capacity, the deficit is imported from the grid. Unmet cooling load (Q_{umt}) and grid impact index (*GII*) are computed. The state parameters (i.e., E_{bat} and NCC) of battery are updated. For standalone buildings, unmet power (P_{umt}) and unmet cooling load are computed instead in this situation. Otherwise (i.e., the electricity supply is sufficient), the optimal heat generation of co-generators is identified to satisfy both the electricity and cooling demand (i.e., to satisfy the higher one). If there is surplus electricity after satisfying electricity demand, the "battery charge mode" will be activated.

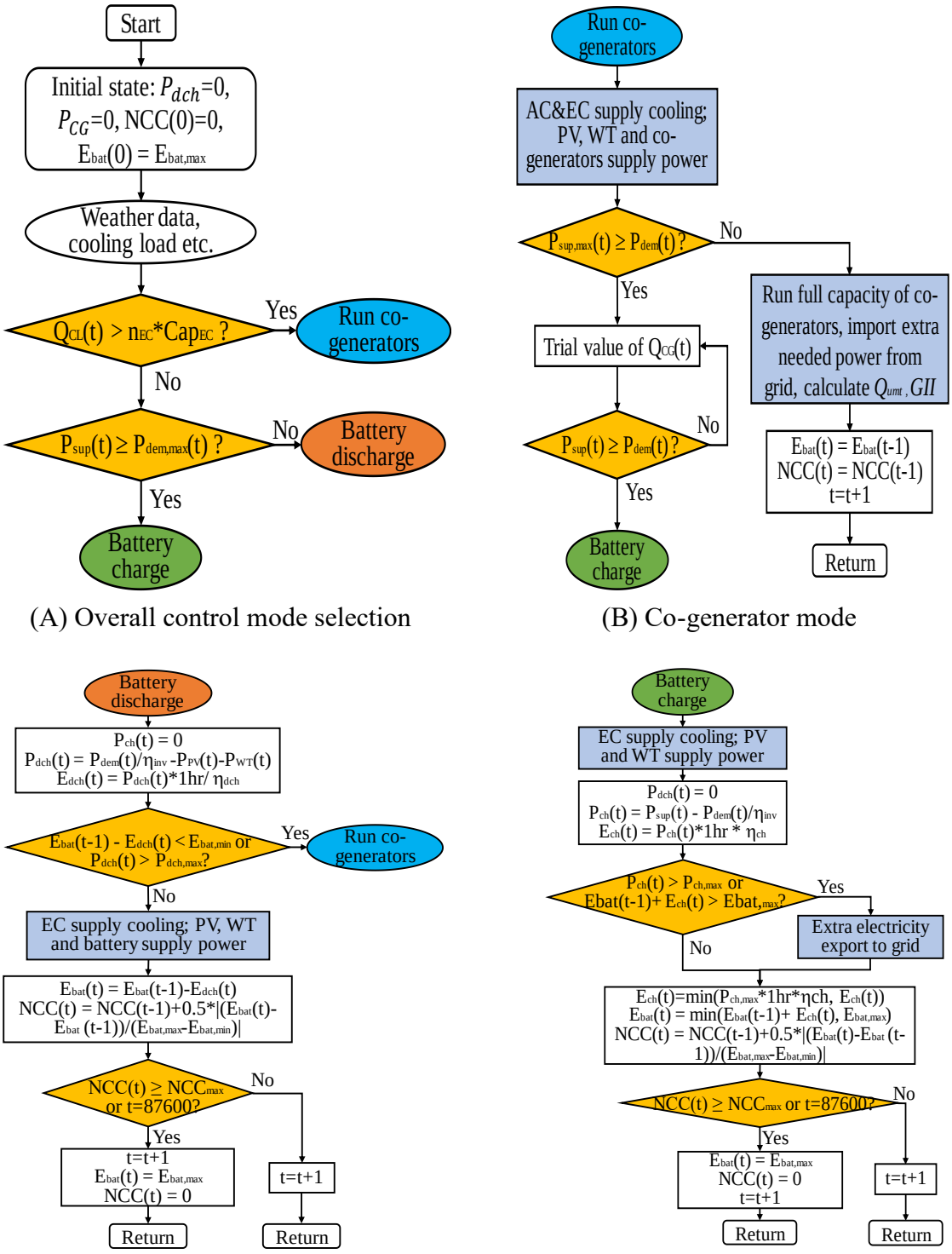

(A) Overall control mode selection

(B) Co-generator mode

(C) Battery discharge mode

(D) Battery charge mode

Figure 5.2 Control strategies of energy systems at a sampling step for grid-connected buildings

Battery discharge mode: At this mode, the deficit of power supply by PV and wind turbines needs to supply by the discharge power of battery. If this deficit is higher than

the maximum discharge power or the energy storage at the end of the control interval after discharge is below its minimum limit, the system is changed to "co-generator mode". Otherwise, electric chillers are used for cooling supply, while PV, wind turbines and the battery are used for power supply. The E_{bat} and NCC of battery are updated. If the NCC or the calendar life of the battery reaches its upper limit, the battery is replaced, and the E_{bat} and NCC are reset to their initial settings.

Battery charge mode: At this mode, electric chillers are used for cooling supply while PV and wind turbines are used for power supply. The surplus power provided by PV and wind turbines after satisfying the electricity demand is used to charge the battery. If the surplus power is higher than its maximum charge power, the charge power is set as its maximum limit. In this situation or if the energy storage at the end of this control interval after charging is over its maximum limit, the extra electricity is exported to the grid. For standalone buildings, the extra electricity is wasted. The E_{bat} and NCC are updated. If the NCC or the calendar life reaches its upper limit, the battery is replaced, and the E_{bat} and NCC are reset to their initial settings.

5.3 Identification of coordinating design variables and preprocessing of design optimization

5.3.1 The needs of coordinated design and identification of coordinating design variables

This subsection illustrates why the interactions between the envelope design and energy system design optimizations (especially the impacts of energy system design optimization on the envelope design optimization) should be considered in the building design optimization, how the energy system design optimization influences the envelope design optimization in the validation case, and the identification of the coordinating design variables. Figure 5.3 shows the variation of building cooling load and PV power

generation of the building configuration concerned under different building orientations. The building orientation corresponding to the maximum PV power generation is 15° (from north to east), while the building orientation corresponding to the minimum building cooling load is 270°. It can be seen that the envelope design optimization if considering the minimization of energy demand only would lead to low efficiency of PV power generation and thus lead to higher cost of energy systems. Therefore, there is a need to consider the impacts of the building envelope design on the power generation of PV when optimizing the building envelope design. In fact, it has been considered in the existing multi-stage design optimization of building envelope and energy systems.

Similarly, the design optimization of building energy systems also affects the design optimization of building envelope. For instance, for the building configuration concerned in the validation case, a northern building orientation (i.e., around 0°) may be preferred if the PV area is large, since the benefit of increasing PV power generation efficiency could be higher than the cost of increasing building energy demand. In contrary, an eastern or western building orientation (i.e., around 90° or 270°) may be preferred if the PV area is small, since the loss of decreasing PV power generation efficiency could be lower than the benefit of decreasing building energy demand. Therefore, there is also a need to consider the impacts of energy system design optimization (where the PV design is optimized) on the envelope design when optimizing the building envelope design. However, it is not considered in the existing multi-stage design optimization of building envelope and energy systems.

Coordinated optimal design, which considers the interactions between the building envelope design optimization and energy system design optimization, is therefore needed for buildings. Other examples are the buildings with façade integrated PV or/and solar

window. For the cases of buildings without system design variables which have significant impacts on energy system design optimization, coordinated optimal design is not essential as the existing multi-stage optimization methods would provide the same optimization outputs in these cases. Based on the above analysis, the system design variable A_{PV} (i.e., PV area) is eventually selected as the only coordinating design variable in this study.

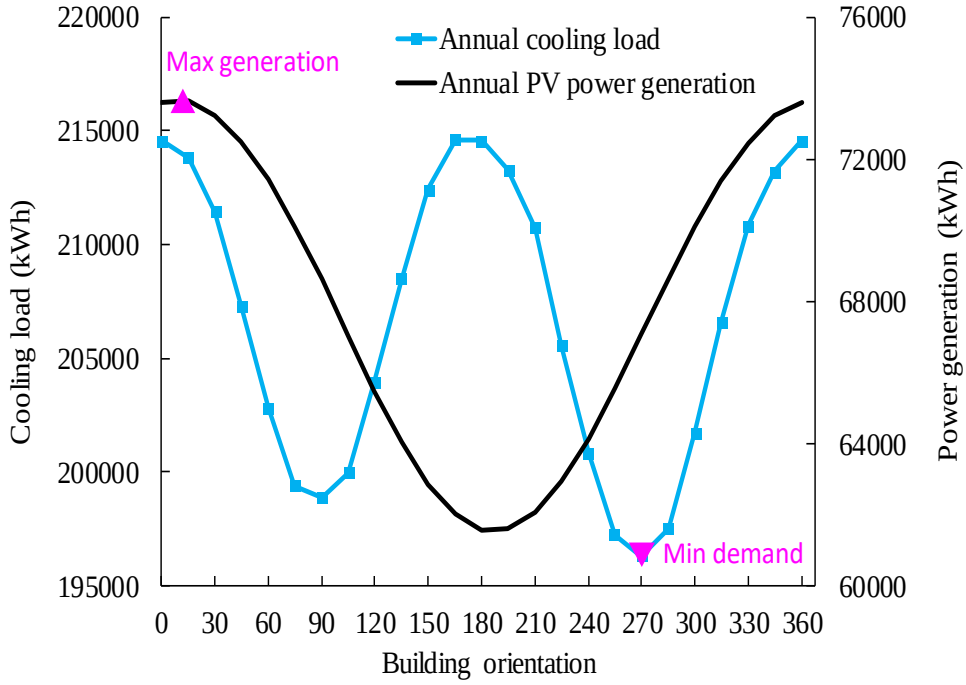

Figure 5.3 Impacts of building orientation on building cooling load and PV power generation

5.3.2 Training and validation of ANN building performance model

An ANN model is developed for building performance simulation in the envelope design optimization process in this study. The ANN model structure and model parameters (weights) are both optimized according to the method introduced in Subsection 3.2.2. MSE (mean squared error) is used to evaluate the performance of ANN model. The inputs of this ANN model are shown in Table 5.1, including the key envelope design variables listed in Table 4.4 (but excluding window solar heat gain coefficient) and the coordinating

design variable (i.e., PV area). The outputs are the corresponding building performance (i.e., annual building electricity load excluding that for cooling load, annual building cooling load, and annual winter thermal discomfort) simulated using EnergyPlus under the TMY weather data in Hong Kong.

Table 5.1 Inputs and outputs of ANN model for coordinated optimal design

Category		**Design variable**	**Abbreviation**	**Range**	**Unit**
Model inputs	Envelope design variables	Building orientation	BO	[0,360]	°
		Roof solar absorptance	RSA	[0.1,0.9]	-
		Window-to-wall ratio	WWR	[0.2,0.6]	-
		Wall solar absorptance	WSA	[0.1,0.9]	-
		Overhang projection ratio	OPR	[0.05,0.5]	-
	Coordinating design variable	PV area	A_{PV}	[100,1032]	m^2
Model outputs		Annual building electricity load excluding that for cooling load	-	-	kWh
		Annual building cooling load	-	-	kWh
		Annual winter thermal discomfort	-	-	-

At the first step, 12,000 sets of training data and 120 sets of validation test data are prepared. A large amount of training data is prepared in order to make sure the consistency between the building performance given by ANN model and that given by EnergyPlus, and thus to assure the reliability of envelope design optimization results.

At the second step, the optimal ANN model structure is identified using 10-fold cross-validation (Kohavi, 1995). Different numbers of hidden layers (1 or 2 hidden layers) and different numbers of neurons in different hidden layers (1-72 neurons when using 1 hidden layer, 1-6 neurons for each layer when using 2 hidden layers) are tested. The training results show that the optimal ANN model structure, which has the minimum average MSE in the cross-validation, is one hidden layer with 72 neurons. Its average MSE is 7.95×10^{-5}.

At last, the optimal ANN model is obtained by further optimizing the parameters (weights) of ANN model with the optimal model structure. Test data are then used to validate the optimal ANN model obtained. It can be seen from Figure 5.4 that the ANN model outputs well match the corresponding target outputs of the test data given by EnergyPlus. Their coefficients of linear regression are all up to 0.999. The consistencies between the impacts of different design variables on the building performance outputs estimated by the ANN model and EnergyPlus are also validated. As an example, Figure 5.5 shows the comparisons between the building performance outputs given by ANN model and EnergyPlus when the building orientation varies. It can be seen that the annual electricity loads, cooling loads and winter thermal discomfort given by ANN model and EnergyPlus match very well respectively. In summary, the optimized ANN model has very good accuracy in estimating the building performance including the impacts of individual design variable.

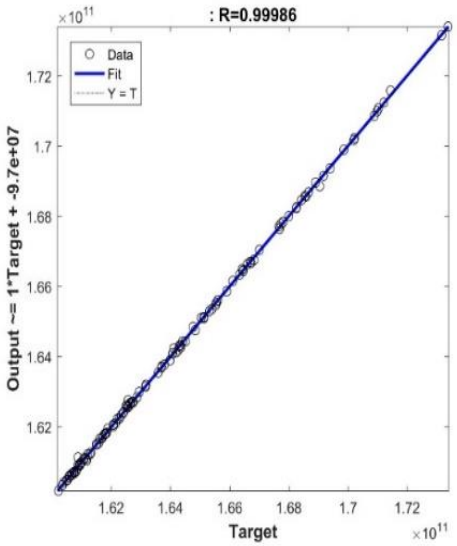

(A) Annual electricity load excluding that for cooling load

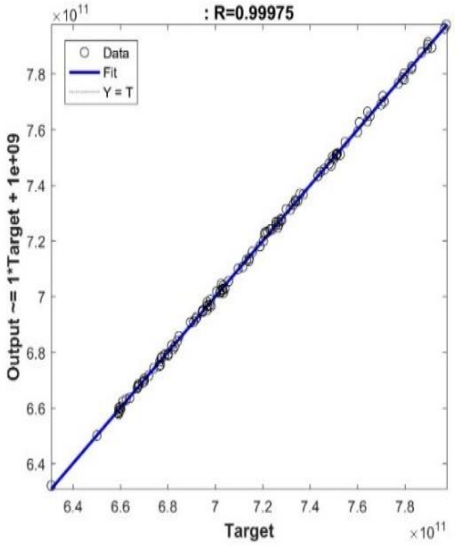

(B) Annual cooling load

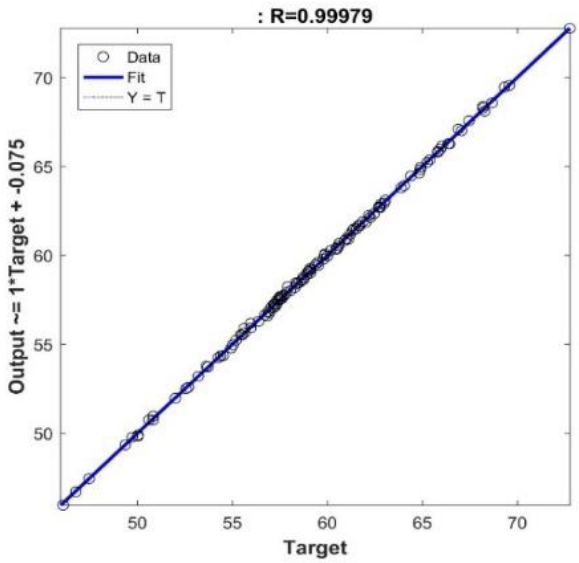

(C) Annual winter thermal discomfort

Figure 5.4 Outputs of optimal ANN model *vs* target outputs during model validation using test data

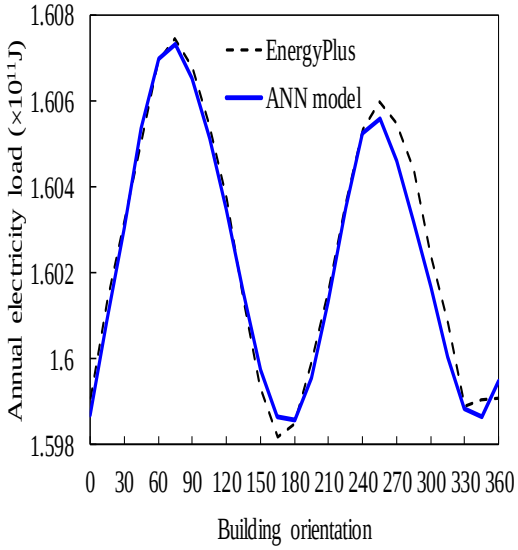

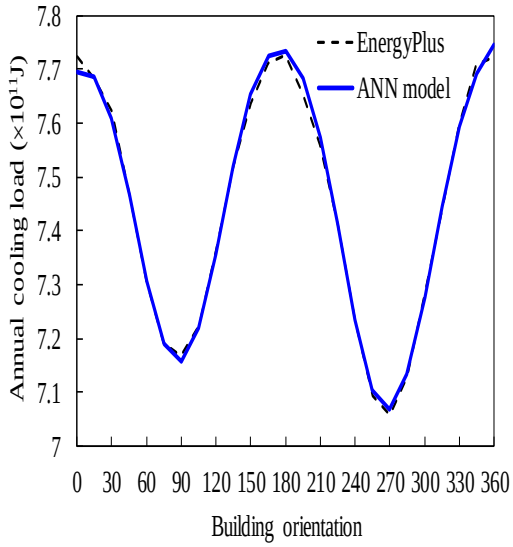

(A) Annual electricity load excluding that for cooling load (B) Annual cooling load

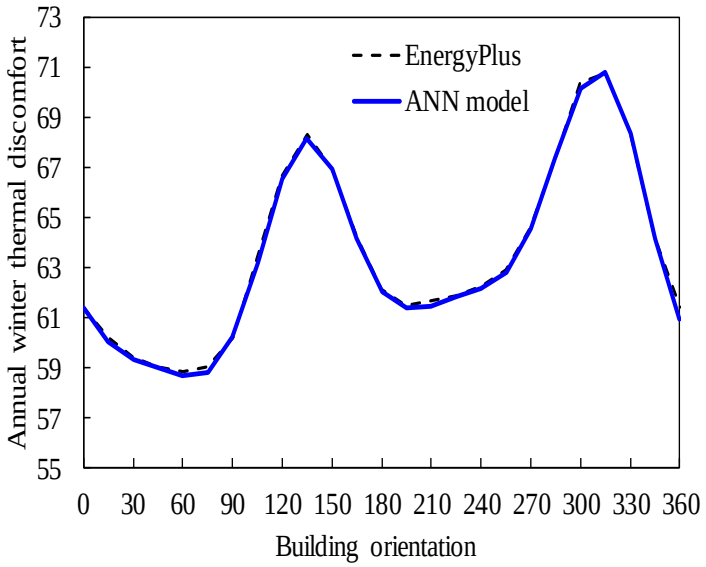

(C) Annual winter thermal discomfort

Figure 5.5 Outputs of optimal ANN model and EnergyPlus *vs* building orientation

5.3.3 Selection of penalty ratios for objective functions

The penalty ratio *a*, assigned to winter thermal discomfort in the optimization objective function of building envelope design, is set as 100 as explained in Section 4.2. Different *a1* and *a2* are tested in order to identify proper penalty ratios for the optimization objective function of standalone zero/low energy building energy systems (the design optimization of low energy building energy systems are taken as an example). A penalty

ratio, which can maintain the corresponding performance indicator within an acceptable level, is considered as a proper penalty ratio. For instance, the bigger the penalty ratio *a1*, the less the accumulated unmet power over the life cycle. A proper *a1* is set to make the accumulated unmet power less than a preset level (for example, 1,000 kWh accumulated throughout the building life cycle of 30 years). *a1* is set as different integral multiples of the unit electricity price in Hong Kong (i.e., about 0.15 USD/kWh), while *a2* is assumed to be one third of *a1* in this study by considering an overall COP of 3 for cooling supply. The basic data of energy system models are set according to Table 3.2 and 30 years of building life cycle is considered. The optimal system design and its corresponding system performance achieved under different penalty ratios are shown in Table 5.2. It can be seen that the total cost of the optimal energy system increases with the increase of penalty ratios, while its unmet cooling load decreases. The unmet power of the optimal energy system associated with the penalty ratio *a1* of 0.15 is larger than that associated with the penalty ratio *a1* of 0 (i.e., without considering penalties for unmet power and unmet cooling load). But the unmet power decreases when the penalty ratios further increase. A proper penalty ratio of 9 is finally assigned to the unmet power (i.e., $a1$=9), and a penalty ratio of 3 is assigned to the unmet cooling load (i.e., $a2$=3), since the total cost (TC), the accumulated unmet power (ΣP_{umt}) and the accumulated unmet cooling load (ΣQ_{umt}) of the corresponding optimal energy system design are within acceptable levels. For the grid-connected zero/low energy buildings, the penalty ratio for grid impact index is determined by assuming that one unit of grid impact index has a cost penalty equivalent to 30% of the total electricity cost in a typical month in this study, i.e., $a3$=240.

Table 5.2 Optimal energy system designs and their corresponding performance of the standalone low energy building under different penalty ratios

No.	a1	a2	Optimal energy system design										Energy system performance		
			A'_{PV}	Cap_{WT}	n_{WT}	Cap_{CG}	n_{CG}	Cap_{AC}	n_{AC}	Cap_{EC}	n_{EC}	Cap_{bat}	TC	ΣP_{umt}	ΣQ_{umt}
1	0	0	342.2	36.6	0	30.0	1	20.0	1	20.0	1	99.4	549,049	17,514	2,389,859
2	0.15	0.05	346.9	7.0	0	30.0	1	39.2	1	48.0	1	98.5	594,689	61,602	394,879
3	2.25	0.75	460.7	19.9	0	40.0	1	52.2	1	73.4	1	87.4	677,154	5,986	5,297
4	4.5	1.5	436.1	12.7	1	41.0	1	53.6	1	75.1	1	80.5	690,348	2,104	2,664
5	9	3	437.5	12.7	1	42.0	1	54.9	1	76.5	1	80.5	698,599	921	1,332
6	18	6	461.9	15.1	1	44.0	1	57.5	1	77.8	1	84.7	708,100	221	359

Note: The units of variables and objectives refer to that in Table 4.4 and Eq. (5.5) respectively.

5.4 Results of coordinated optimal design case studies and building performance analysis

5.4.1 Case 1 - Optimal design of a standalone low energy building

Coordinated optimal design is conducted for the validation building with the design intention of standalone low energy building. Two initial PV area settings (1,032 m^2 and 100 m^2) for envelope design optimization are tested in this case study to verify the effectiveness and robustness of coordinated optimal design method. Table 5.3 shows the "optimal" design solutions of all optimization loops in these two coordinated design tests. When the initial PV area for envelope design optimization is set as 1,032 m^2 (i.e., the maximum PV area), three optimization loops are needed to reach the convergence as shown in Table 5.3A. When a PV area of 1,032 m^2 is assumed for the envelope design optimization, the cost-optimal PV area given by the system design optimization in order to satisfy the energy demand of the optimized envelope design is 438 m^2 only, which

deviates significantly from the PV area assumed in envelope design optimization. Therefore, the envelope design achieved is not optimal under the smaller PV area actually given by the system design optimization. A new optimization loop is needed. In this new loop, the PV area is set as 438 m^2 in envelope design optimization, which is the optimized PV area given by the system design in the first optimization loop. Under a smaller PV area, the optimal building orientation and overhang projection ratio increase noticeably, leading to the decrease of the PV power generation efficiency and the energy demand. The optimal PV area given by the system design optimization for the new optimized envelope is 461 m^2, which still deviates from the PV area setting used in the latest envelope design optimization for over 2%. The third optimization loop is then activated. In this loop, the PV area is set as 449 m^2 in envelope design optimization to accelerate the convergence, which is the average of the PV areas used in envelope design optimization and optimized by the system design optimization in the second optimization loop. The optimal PV area given by system design optimization for the new optimized envelope in the third loop is 444 m^2, which has a deviation of 1.11%, i.e., within the convergence tolerance of 2%, thus the design optimization converges. The final optimal outputs of the coordinated design optimization under an initial PV area of 1,032 m^2 are the outputs of Loop 3 as listed in Table 5.3A.

When the initial PV area for envelope design optimization is set as 100 m^2, four optimization loops are needed to achieve the convergence. The optimal values of both envelope design variables and energy system design valuables are listed in Table 5.3B. Where, the outputs of Loop 4 are the final optimal outputs of the coordinated design optimization. It can be seen that the optimal design values achieved under the initial PV area setting of 100 m^2 are very close to that achieved under the initial PV area setting of 1,032 m^2. This indicates that the proposed coordinated optimal design is robust in

providing consistent optimal design solutions regardless of the initial settings though different iteration times are needed. In addition, it is practical to achieve the optimal design solution using the coordinated optimal design method. The computation cost is not increased too much (i.e., 3 or 4 times only) compared with the uncoordinated design method (i.e., existing multi-stage design optimization methods).

In contrary, the optimal design solutions achieved by uncoordinated design method under different initial PV area settings are very different, same as the outputs listed in the first row in Table 5.3A and 5.3B. The optimal building orientation obtained under a small initial PV area setting is close to east, while the optimal overhang projection ratio is much smaller (about half). The component capacities of the obtained optimal energy system design are obviously larger. This indicates that the uncoordinated design method is not robust in obtaining consistent optimal design solutions under different initial settings. Figure 5.6 presents a comparison between the energy performance of the optimal system design solutions obtained using coordinated design method and uncoordinated design method respectively under an initial PV area setting of 100 m^2. It can be seen that the optimal design given by coordinated design method provides 4.1% (30,190 USD) less total cost, 22.0% (286 kWh) less accumulated unmet cooling load (ΣQ_{umt}) and 3.3% (24,044 USD) less energy system design objective value ($F_{sys,AL}$) than that given by uncoordinated design method. Though its accumulated unmet power (ΣP_{umt}) is much higher (by 778 kWh), it is still within acceptable level. This indicates that coordinated design method can provide global optimal design solutions, while the optimal design solution achieved by uncoordinated design method is “local” optimum.

Table 5.3 Optimization loops of coordinated optimal design and optimal design solutions of coordinated and uncoordinated design methods - standalone low energy building

(A) Initial PV area for building envelope design optimization: 1,032 m^2

Loop no.	A_{PV}	Optimal envelope design					Optimal energy system design									
		BO	RSA	WWR	WSA	OPR	A'_{PV}	Cap_{WT}	n_{WT}	Cap_{CG}	n_{CG}	Cap_{AC}	n_{AC}	Cap_{EC}	n_{EC}	Cap_{bat}
1*	1032	7.75	0.10	0.20	0.10	0.44	438	12.7	1	42.0	1	54.9	1	76.5	1	80.5
2	438	8.15	0.10	0.20	0.10	0.45	461	14.0	1	44.0	1	57.5	1	76.6	1	99.9
3 *(final)*	***449***	***8.05***	***0.10***	***0.20***	***0.10***	***0.45***	***444***	***12.4***	***1***	***42.0***	***1***	***54.9***	***1***	***77.6***	***1***	***80.9***

(B) Initial PV area for building envelope design: 100 m^2

Loop no.	A_{PV}	Optimal envelope design					Optimal energy system design									
		BO	RSA	WWR	WSA	OPR	A'_{PV}	Cap_{WT}	n_{WT}	Cap_{CG}	n_{CG}	Cap_{AC}	n_{AC}	Cap_{EC}	n_{EC}	Cap_{bat}
1*	100	77.95	0.10	0.29	0.10	0.21	499	9.0	1	44.0	1	57.5	1	77.9	1	91.6
2	499	8.05	0.10	0.20	0.10	0.45	421	6.8	1	44.0	1	57.5	1	74.8	1	87.0
3	460	8.15	0.10	0.20	0.10	0.45	424	6.4	1	44.0	1	57.5	1	75.0	1	87.2
4 *(final)*	***442***	***8.25***	***0.10***	***0.20***	***0.10***	***0.45***	***443***	***12.4***	***1***	***42.0***	***1***	***54.9***	***1***	***77.0***	***1***	***80.7***

** Note: uncoordinated design method also gives the same design solution. The units of variables refer to that in Table 4.4.*

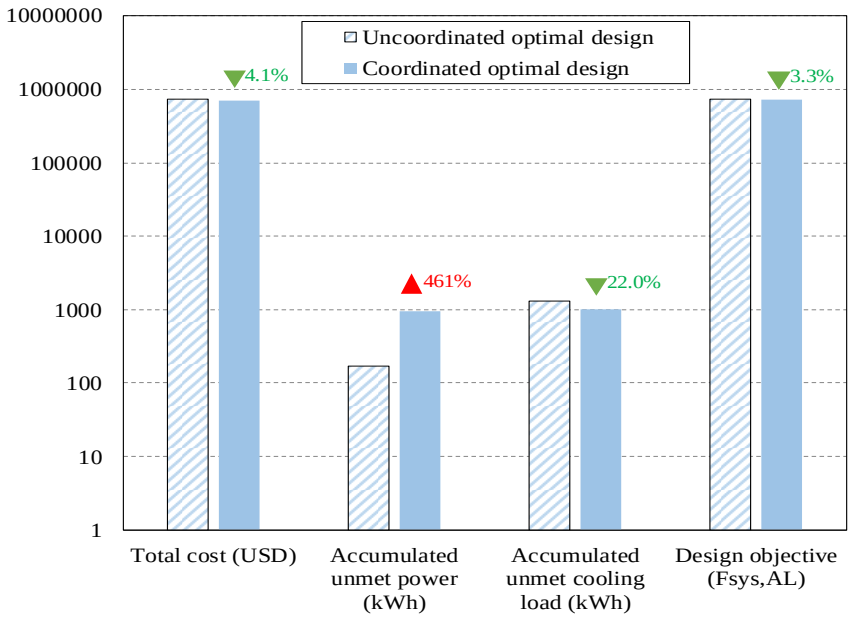

Figure 5.6 Comparison between energy performance of optimal designs given by coordinated and uncoordinated design methods - standalone low energy building

5.4.2 Case 2 - Optimal design of a grid-connected low energy building

The optimal design of a grid-connected low energy building is also studied using the coordinated design method and uncoordinated design method respectively. The optimal design solutions are listed in Table 5.4. Compared with the optimal design solution of the standalone low energy building given by the coordinated design method, smaller capacities of the energy system components are needed for the grid-connected low energy building though their optimal envelope design are similar. This is because it is not economic-efficient to supply electricity using the building-integrated power generation systems than importing electricity from grid when the capacities of energy system components are over certain level.

The optimal design solutions given by uncoordinated design method under different initial PV area settings are also very different for grid-connected low energy building as shown in Table 5.4. The optimal building envelope design obtained under a smaller PV area setting has much higher building orientation value (closer to east orientation), larger

WWR and much smaller overhang projection ratio. The capacities of optimal energy system components are larger except the battery capacity. The results indicate again that uncoordinated design method is not robust to obtain optimal design solutions under different initial settings. The energy performance of the optimal system design solutions given by coordinated design is compared with that given by uncoordinated design with an initial PV area setting of 100 m^2, as shown in Figure 5.7. It can be seen that the optimal design given by the coordinated design method has 3.2% (21,488 USD) less total cost, 28.8% (533 kWh) less accumulated unmet cooling load (ΣQ_{umt}) and 3.0% (20,520 USD) less energy system design objective value ($F_{sys,GC}$) compared with the uncoordinated design method, although its accumulated grid impact index (ΣGII) is 13.2% higher (11). This indicates again that coordinated design method can provide global optimal design solutions, while the design solutions given by uncoordinated design method are "local" optimum.

Table 5.4 Optimal design solutions of coordinated and uncoordinated design methods - grid-connected low energy building

Design method	A_{PV}	Optimal envelope design					Optimal energy system design									
		BO	RSA	WWR	WSA	OPR	A'_{PV}	Cap_{WT}	n_{WT}	Cap_{CG}	n_{CG}	Cap_{AC}	n_{AC}	Cap_{EC}	n_{EC}	Cap_{bat}
Uncoordinated design	1032	7.55	0.1	0.2	0.10	0.44	386	7.8	1	30.0	1	39.0	1	93.0	1	77.2
	100	83.75	0.1	0.29	0.1	0.20	447	14.1	1	30.0	1	39.2	1	94.3	1	57.4
Coordinated design	-	8.35	0.1	0.20	0.10	0.45	394	25.0	0	32.0	1	41.9	1	89.7	1	50.1

Note: The units of variables refer to that in Table 4.4.

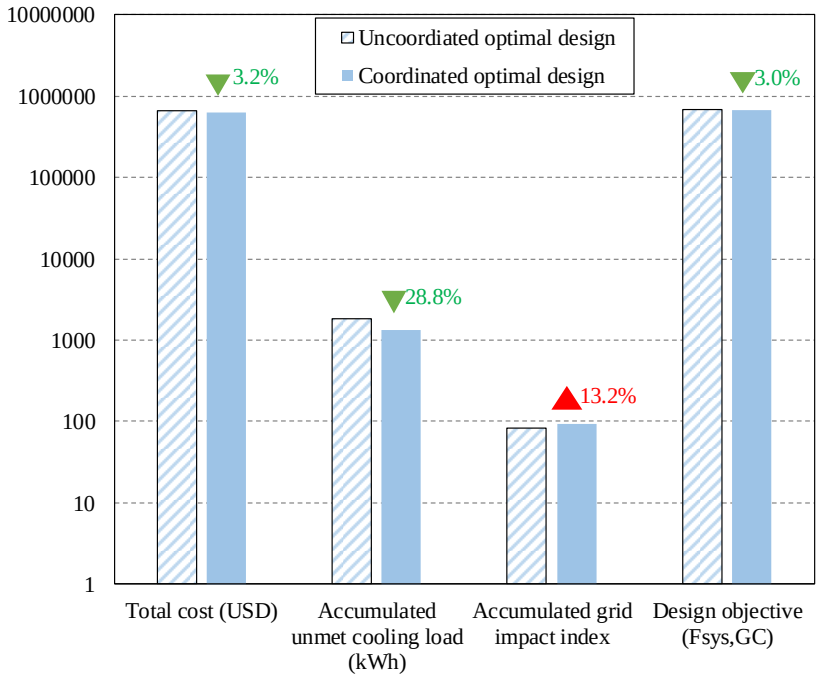

Figure 5.7 Comparison between energy performance of optimal design solutions given by coordinated and uncoordinated design methods - grid-connected low energy building

5.4.3 Case 3 - Optimal design of a grid-connected zero energy building

The optimal design of a grid-connected zero energy building is also studied using the coordinated design method and uncoordinated design method respectively. The optimal design solutions are shown in Table 5.5. The optimal design solutions given by uncoordinated design method under different initial PV area settings are very different. The optimal building envelope design of grid-connected zero energy building is the same as that of grid-connected low energy building (i.e., Case 2). The optimal energy system design for the optimal envelope design achieved under smaller initial PV area setting has larger capacities for the energy system components except the battery capacity. The results also indicate that uncoordinated design method is not robust to obtain optimal design solutions under different initial settings. The energy performance of optimal system design solutions given by coordinated design is compared with that given by uncoordinated design with the initial PV area setting of 100 m^2, as shown in Figure 5.8.

It can be seen that the optimal design given by coordinated design method has 4.7% (31,796 USD) less total cost, 25.2% (430 kWh) less accumulated unmet cooling load (ΣQ_{umt}) and 4.6% (31,893 USD) less energy system design objective value ($F_{sys,GC}$) compared with the uncoordinated design method, although its accumulated grid impact index (ΣGII) is 5.7% higher (5). This indicates again that coordinated design method can provide global optimal design solutions, while the optimal design solutions provided by uncoordinated design method are "local" optimum.

Table 5.5 Optimal design solutions of coordinated and uncoordinated design methods - grid-connected zero energy building

Design method	A_{PV}	Optimal envelope design					Optimal energy system design									
		BO	RSA	WWR	WSA	OPR	A'_{PV}	Cap_{WT}	n_{WT}	Cap_{CG}	n_{CG}	Cap_{AC}	n_{AC}	Cap_{EC}	n_{EC}	Cap_{bat}
Uncoordinated design	1032	7.55	0.1	0.2	0.10	0.44	467	16.6	0	30.0	1	39.2	1	92.7	1	61.6
	100	83.75	0.1	0.29	0.1	0.20	498	13.8	0	32.0	1	41.8	1	92.1	1	54.2
Coordinated design	-	8.65	0.10	0.2	0.1	0.45	395	8.9	0	32.0	1	41.8	1	89.8	1	50.4

Note: The units of variables refer to that in Table 4.4.

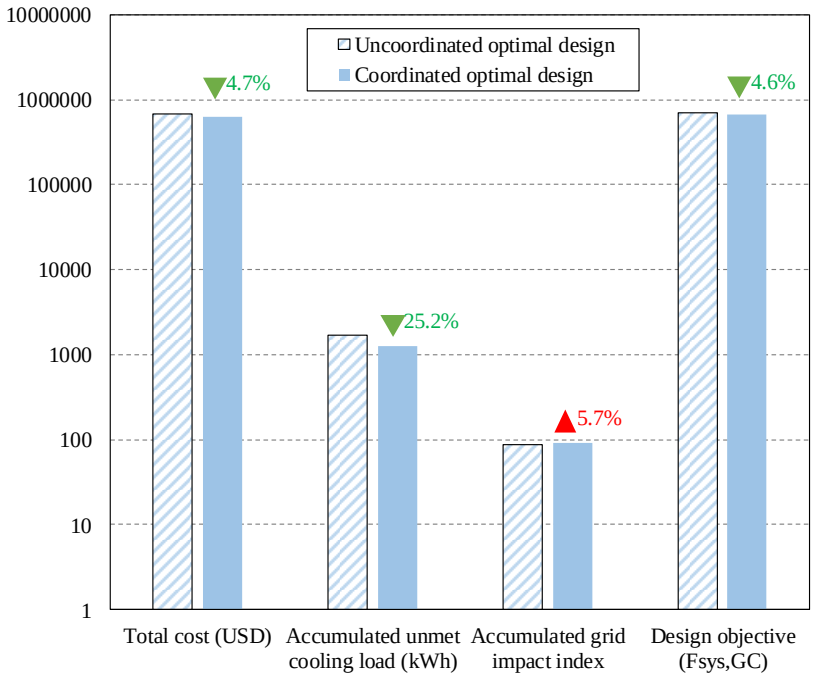

Figure 5.8 Comparison between energy performance of optimal design solutions given by coordinated and uncoordinated design methods - grid-connected zero energy building

5.5 Optimization complexity and computation cost of coordinated design optimization

The complexity of optimization and computation cost are other important issues as they are critical especially when a large number of design variables are optimized and simulation software tools are needed to assess the building performance and energy system performance. To achieve the global optimal design solution of a building, the design optimizations of its building envelope and energy systems need to be considered as a whole, which is typically achieved by simultaneous optimization methods. For example, when simultaneous optimization methods are used for the validation case, EnergyPlus or other building simulation software is needed for building performance evaluation. This is because hourly data are required for the energy system performance evaluation while the ANN model cannot provide hourly performance data. The computation time for the GA-based simultaneous optimization of the building envelope

and energy systems, using EnergyPlus (instead of ANN building model), is estimated to be about 500 hours if assuming the same evaluation times (i.e. 20,000 times = 100 generations × 200 populations, for the energy system optimization in the above case studies) are needed. This estimated minimum computation time is 5 times of that using the coordinated design method (23.5 hours on a regular PC). The actual computation time could be much longer as it would actually need much more evaluation times as 15 design variables (instead of 10 design variables for system design optimization) are involved. In such case and other cases involving more design variables, the computation time of simultaneous optimization method would be impractically long and unaffordable. Compared with the existing simultaneous design optimization methods, the coordinated design method proposed in this study can achieve the global optimal design solution approximately with significantly reduced computation cost and optimization complexity.

5.6 Summary

In this chapter, a coordinated optimal design method is developed for the entire zero/low energy buildings on the basis of multi-stage design optimization method, to consider the interactions between the designs of building envelope and energy systems. An iterative optimization approach is developed to identify the most cost-efficient and energy-efficient design solution by coordinating the design optimizations of building envelope and energy systems. Based on the results and experiences from the case studies, conclusions can be made as follows.

- The optimizations of building envelope design and energy system design need to be integrated as a coordinated design process when some of the system design variables have significant impacts on the envelope design optimization.
- The proposed coordinated design method is robust in providing optimal design

solutions for zero/low energy buildings and their energy systems. The case studies show that coordinated optimal design can always converge to the same optimal design solution under different initial settings although different iteration times may be needed, while design solutions of uncoordinated design method could be very different under different initial settings.

- The proposed coordinated design method can provide "global" optimal design solutions for standalone/grid-connected zero/low energy buildings and their energy systems, while the optimal design solutions given by the uncoordinated design method could be "local" optimum. For the validation case, the total cost and design objective value of the optimal energy systems given by the coordinated design method are about 4% less compared with the uncoordinated design method, and their accumulated unmet cooling loads decrease by over 22%.
- The proposed coordinated optimal design method can efficiently achieve the global optimal design solution that needs to consider building envelope and building energy systems as a whole in the optimization. This is typically achieved by simultaneous design optimization method while the proposed method could achieve similar effect with much reduced optimization complexity and computation cost. The experience of the case studies shows that the actual computation cost is about 3 or 4 times of that of multi-stage design optimization method but is estimated to be much less than simultaneous optimization methods, which might need impractically long and unaffordable computation time. The proposed method has essential advantage particularly when the numbers of design variables are large and the performance of building envelope and energy systems needs to be evaluated using simulation tools in their design optimizations.

CHAPTER 6 ROBUST OPTIMAL DESIGN OF BUILDING ENVELOPE CONSIDERING UNCERTAINTIES AND THE IMPACTS OF OBJECTIVE FUNCTIONS

This chapter presents the procedure and method of robust design optimization for zero/low energy buildings considering uncertainties and the impacts of alternative optimization objective functions on robust design optimization. An ANN (artificial neural network) model is trained and validated using the building performance data under uncertain scenarios and used for building performance evaluation. The robust optimal envelope design of zero/low energy buildings is studied and used as an example to identify the proper objective function for robust optimal design in building energy field. Three case studies using different objective functions are conducted to study the robust optimal envelope design of zero/low energy buildings. The performance of the robust optimal building designs obtained using different optimization objective functions are compared to identify the proper optimization objective function for robust design optimization in building energy field.

6.1 Procedure and method of robust design optimization

6.1.1 Approach and steps of robust design optimization

Figure 6.1 illustrates the detailed steps of robust design optimization. The design optimization is implemented on the MATLAB platform. LHS (Latin hypercube sampling) method is used for uncertainty propagation, since it requires smaller sample size than other Monte-Carlo-based sampling methods (Helton et al., 2005). Main uncertain design inputs, which have significant impacts on building performance, are identified beforehand. *In the first step*, the GA (genetic algorithm)/non-dominated sorting genetic

algorithm II (NSGA-II) optimizer is used to generate trial values of the design parameters (i.e., one possible design option). *In the second step*, the identified uncertain design inputs of significant impacts are sampled using the LHS method according to their probability density distributions, to generate all possible uncertain scenarios. *In the third step*, the performance indicators of the trial design option for each uncertain scenario is obtained using building simulation model. *In the fourth step*, the objective value(s) under all possible uncertain scenarios is/are calculated and evaluated by the GA/NSGA-II optimizer. These steps are repeated until the objective(s) is/are minimized while reaching the convergence tolerance. The design option(s) corresponding to the minimized evaluation objective(s) is/are identified as the optimal design option(s). This design method is suitable for both new and retrofitted buildings while less uncertainties will be involved in retrofitting cases. It is worth noticing that the optimization algorithms (i.e., GA/NSGA-II) and the uncertainty propagation method (i.e., LHS) shown in the Figure 6.1 are alternative options and used in this study. Other methods are also suitable based on the detailed cases.

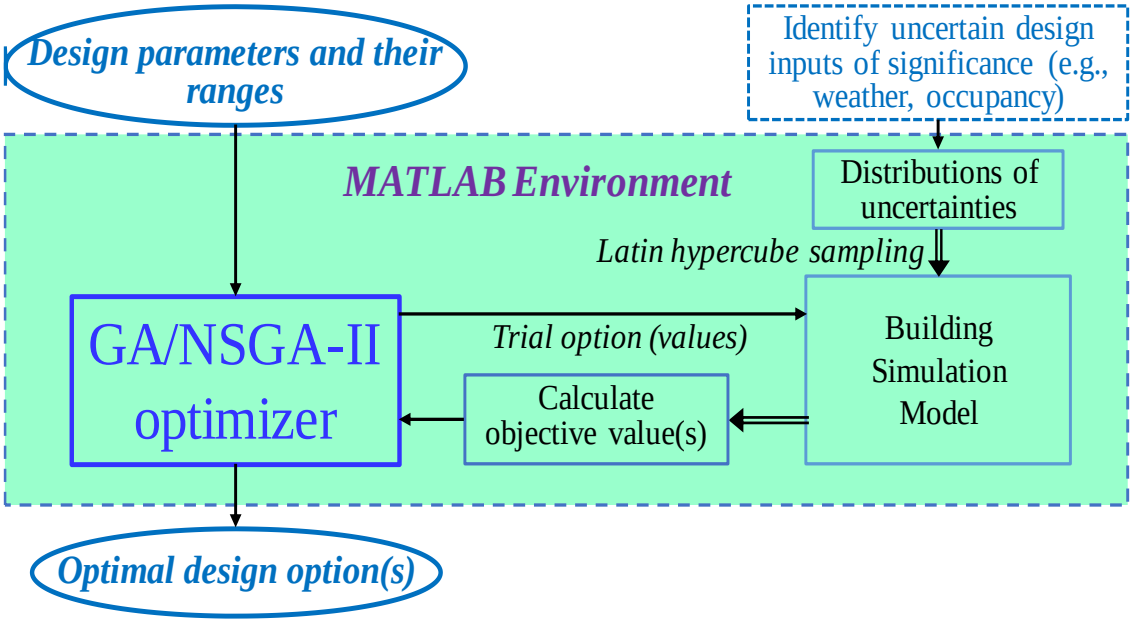

Figure 6.1 Procedure and steps of robust design optimization

6.1.2 Alternative objective functions for robust design optimization

It can be seen from the literature review in Chapter 2 that the mean of performance indicator under all uncertain scenarios, the standard deviation of performance indicator under all uncertain scenarios and the infeasibility/performance penalty are the three terms generally considered in the objective functions for robust design optimization. When adopting them in building design optimization applications, these three terms are also used to generate alternative optimization objective functions with different combination of them, as shown in Eq. (6.1-6.3). 'Objective 1' involves the mean and the standard deviation of the performance indicator under all uncertain scenarios, which is the most widely-used objective in robust design optimization in aerospace and structural engineering fields and in most previous studies on building robust design optimization (Nguyen et al., 2014; Yao et al., 2011). 'Objective 2' involves the mean of the performance indicator under all uncertain scenarios only. 'Objective 3' involves the mean of the performance indicator and the mean of the performance penalty under all uncertain scenarios.

In this study, robust optimal envelope design is taken as an example of the robust optimal design in building energy field to identify the proper objective function. The annual average energy consumption in the building life-cycle (30 years in this study) is considered as the performance indicator as shown in Eq. (4.2). The annual average discomfort index in the building life-cycle is considered as the performance penalty as shown in Eq. (4.3-4.4). The discomfort index (winter discomfort) is considered to avoid a severely cold indoor environment in the winter season in subtropical regions without heating provision. For the heating dominated regions without cooling provision, discomfort due to overheating in summer is recommended as the penalty.

Objective 1: $$\tilde{F}(X,p) = \frac{w}{s_{\mu f}}\mu_f(X,p) + \frac{1-w}{s_{\sigma f}}\sigma_f(X,p) \quad (6.1)$$

Objective 2: $$\tilde{F}(X,p) = \mu_f(X,p) \quad (6.2)$$

Objective 3: $$\tilde{F}(X,p) = \mu_f(X,p) + a\mu_D(X,p) \quad (6.3)$$

where, $\tilde{F}$ is the robust optimization objective. *X* is the vector of design variables. *p* is the vector of design parameters/inputs, which can be uncertain. *f* is the performance indicator concerned. μ_f is the mean of performance indicator under all uncertain scenarios. σ_f is the standard deviation of performance indicator under all uncertain scenarios. *w* is the weight for the mean of performance indicator. $s_{\mu f}$ is scaling factor of the mean of performance indicator. $s_{\sigma f}$ is scaling factor of the standard deviation of performance indicator. *a* is penalty ratio for the infeasible performance. μ_D is the mean of performance penalty under all uncertain scenarios. *D* is the infeasible performance.

6.2 Training and validation of ANN building performance model

An ANN model is developed to evaluate the building performance of different envelope design under each uncertain scenario for robust design optimization. The inputs of the ANN model are listed in Table 6.1, which include the key building envelope design parameters identified in Section 4.3 and the main uncertain design inputs of significant impacts identified in Section 4.5. The outputs are the corresponding building performance data, i.e., annual average energy consumption and annual average discomfort index in the building life cycle.

Sampling size is a basic issue affecting the model accuracy and computation efforts in preparing the training data. Matala (2008) recommended 10 times the variable numbers as the acceptable number of training data sets for LHS sampling. According to this rule, the recommended sampling size is 90. To ensure the ANN model accuracy and to check

the impact of the sampling size, 180 sets of training data and 32 sets of test data were prepared and tested. The training and optimization processes of ANN model using 180 sets of training data are presented as follows.

Table 6.1 Inputs and outputs of ANN model for robust design optimization

Category		Parameters	Range/distribution	Unit
Model inputs	Envelope design variables	Building orientation	[0,360]	°
		Roof solar absorptance	[0.1,0.9]	-
		Window-to-wall ratio	[0.25,0.8]	-
		Wall solar absorptance	[0.1,0.9]	-
		Window solar heat gain coefficient	[0.1,0.9]	-
		Overhang projection ratio	[0.05,0.5]	-
	Uncertain design inputs	Climate change trend	U(0,0.048)	K/year
		Occupancy density	Factor: Tri(0.3,1.2,0.9)	-
		Lighting load		-
		Equipment load		-
		Infiltration air mass flow rate	U(0.0025,0.0075)	kg/(s·m)
Model outputs		Annual average energy consumption in building life-cycle	-	kWh
		Annual average discomfort index in building life-cycle	-	-

First, the structure of the ANN model is optimized, and 99 different ANN model structures are tested by using different numbers of hidden layers (i.e., 1 or 2 hidden layers) and different numbers of neurons in the hidden layers (i.e., 1-18 neurons when using 1 hidden layer, 1-9 neurons in each layer when using 2 hidden layers). The performance of each model structure is trained and tested using 10-fold cross validation 10 times. The

test results are shown in Figure 6.2A. The first value in the *x*-axis is the number of neurons in the first hidden layer and the second value is the number of neurons in the second hidden layer. The zero number in the second hidden layer, i.e. (*x*,*0*), means there is only one hidden layer. The model structure, which uses only one hidden layer with six neurons (6, 0), is found to have the minimum average MSE (mean squared error) and the minimum average relative error. Its average MSE is 0.00125 and the average relative error is 1.74%. The MSEs of models using different model structures (one hidden layer only) in the cross-validation study are shown in Figure 6.2B. The model with six neurons in one hidden layer is found to have the best and the most stable performance. Its MSE is within a range between 0.0003 and 0.0027. Therefore, the optimal structure of the ANN model for the building concerned in this chapter is one hidden layer with six neurons.

Second, the parameters of the ANN model are optimized using the optimal model structure identified above. To eliminate the impact of random initialization of the model training process, the ANN model is trained and tested 100 times using the above 180 sets of training data and 32 sets of test data, respectively. Out of the 100 models obtained by training, the model with the minimum MSE in the model test is eventually selected as the optimal ANN model for further design optimization. Figure 6.3 shows the fitting between the outputs of the optimal ANN model and the target outputs using test data. The ANN model outputs are found to be very close to the corresponding target outputs of the test data. Their coefficients of linear regression are both up to 0.99. The *R* values are as high as 0.99695 and 0.99732 for annual average energy consumption and the discomfort index, respectively. The MSE of the optimal ANN model in the test is as low as 0.000698. This indicates that the optimal ANN model has very good accuracy in representing the building performance in the life-cycle.

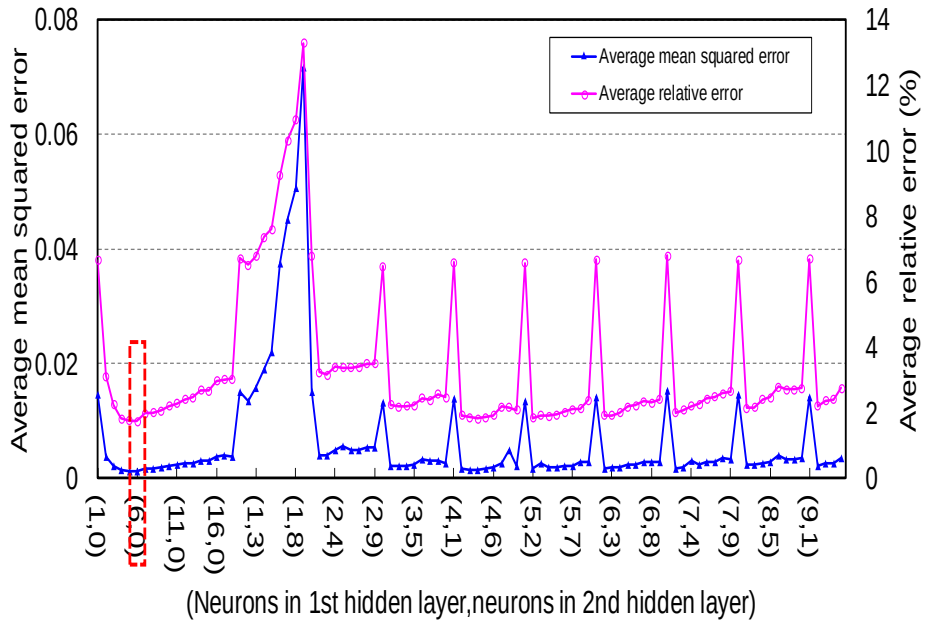

(A): Average MSE and relative errors of models with different structures

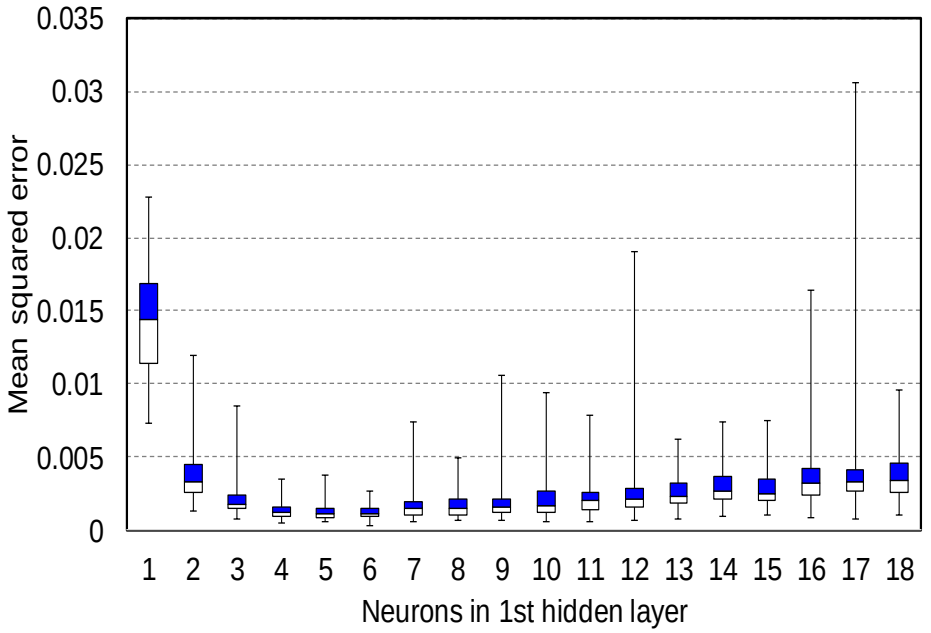

(B): MSEs of models with different structures (one hidden layer only)

Figure 6.2 ANN model structure *vs* model performance

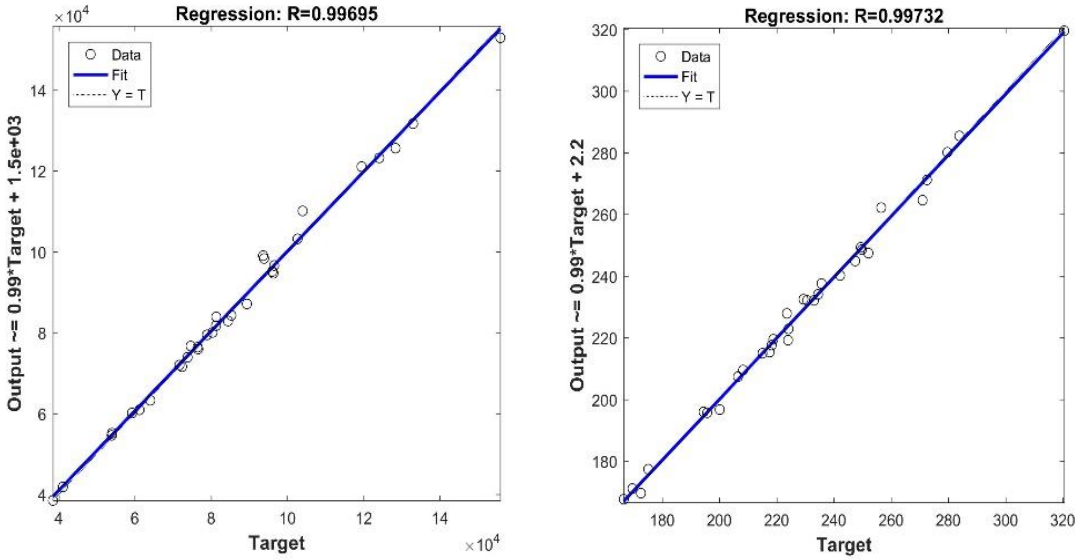

(A):Annual average energy consumption (kWh) (B):Annual average discomfort index

Figure 6.3 Comparison of outputs of optimal ANN model and test data during model validation

6.3 Results of robust optimal design case studies using different objective functions

Robust optimal envelope designs are performed using the three objective functions as defined in Subsection 6.1.2. The performance of buildings optimized using these three different objective functions is evaluated and compared in this section to identify the proper objective function for robust design optimization in building energy field. As it is a time consuming task to try different weights/penalties to make a trade-off between the two terms of the objective function in single-objective optimization, multi-objective optimization is conducted in assessing the impacts of involving standard deviation and performance penalty in the optimization objective function (i.e., 'Objective 1' and 'Objective 3').

6.3.1 Optimization case using 'Objective 2' vs optimization case using 'Objective 1'

Robust optimal envelope design is performed using the ANN model, obtained in Section 6.2, as the building performance model. 100 possible uncertain scenarios are generated

by sampling the uncertain design inputs according to their probability distributions using LHS method and considered in the three optimization cases. Multi-objective optimization is conducted using the two terms (i.e., mean and standard deviation) of 'Objective 1' as two optimization objectives. Different population sizes are tested to ensure that the convergence of optimization. The results show that a population size of 100 is sufficient as the results do not improve obviously when the population size is increased further. The pareto front obtained using a population size of 100 is shown in Figure 6.4. 35 pareto-optimal design solutions are identified. The mean of annual average energy consumption of the pareto-optimal solution increases with the decrease of its standard deviation. The mean varies in the range between 51,266 kWh and 55,125 kWh, while the standard deviation varies between 8,337 kWh and 9,901 kWh. The decision-makers can then select the best design options based on the relative weightings of the mean and deviation. A single objective optimization is conducted using single item (i.e., mean) of 'Objective 2' as the optimization objective. The mean of annual energy consumption of the achieved optimal design is 50,560 kWh and the calculated corresponding standard deviation is 10,009 kWh as marked in Figure 6.4.

The pareto-optimal design solutions of the multi-objective optimization and the design solution of the single objective optimization are presented in Table 6.2, where the solution of multi-objective optimization are listed in an increasing order according to the mean of annual average energy consumption under all uncertain scenarios. For the multi-objective optimization involving standard deviation, the optimal building orientation has a clear trend of changing from north-east oriented to south-east oriented with slight fluctuation. The optimal roof solar absorptance, window to wall ratio and window solar heat gain coefficient generally fluctuate around their lower limits of their preset searching ranges. The optimal wall solar absorptance fluctuates around 0.6 when the mean of annual energy

consumption is lower than 54,266 kWh (i.e., the pareto-optimal solutions above design solution 31 in Table 6.2). Then it decreases with the increase of the mean of annual average energy consumption when the mean of annual energy consumption is larger than 54,266 kWh (i.e., the pareto-optimal solutions below design solution 31). The optimal overhang projection ratio has a clear increasing trend when the mean of annual average energy consumption increases. The optimal building orientation, roof solar absorptance, window to wall ratio, wall solar absorptance, window solar heat gain coefficient and overhang projection ratio of the optimal design obtained by single objective (without involving standard deviation) optimization using 'Objective 2' are 0, 0.1, 0.25, 0.9, 0.1 and 0.05, respectively.

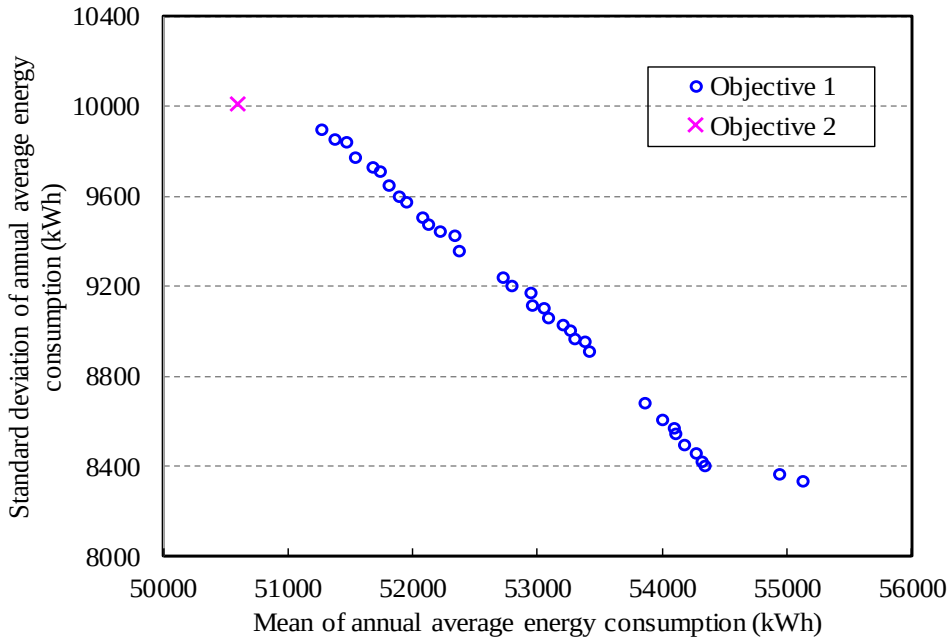

Figure 6.4 Mean and standard deviation of annual average energy consumption of pareto-optimal design solutions using Objective 1 (with standard deviation) and Objective 2 (without standard deviation)

Table 6.2 Pareto-optimal design solutions of optimization considering standard deviation (Objective 1) and optimal design solution without considering standard deviation (Objective 2)

Solution No.	**Optimal design parameters**						**Optimal objectives**	
	Building orientation	Roof solar absorptance	Window to wall ratio	Wall solar absorptance	Window solar heat gain coefficient	Overhang projection ratio	Mean of E_{tot} (kWh)	Standard deviation of E_{tot} (kWh)
Multi-objective optimization considering standard deviation (Objective 1)								
1	***29.2***	***0.10***	***0.25***	***0.59***	***0.10***	***0.08***	***51,266***	***9,901***
2	42.9	0.10	0.25	0.60	0.10	0.08	51,373	9,857
3	47.5	0.10	0.25	0.59	0.10	0.09	51,470	9,839
4	51.1	0.11	0.25	0.60	0.10	0.10	51,534	9,774
5	68.9	0.10	0.25	0.60	0.10	0.10	51,679	9,733
6	69.5	0.11	0.25	0.62	0.10	0.11	51,734	9,712
7	94.0	0.10	0.25	0.62	0.10	0.11	51,806	9,653
8	105.2	0.10	0.25	0.60	0.10	0.11	51,891	9,598
9	110.3	0.11	0.25	0.60	0.10	0.11	51,944	9,575
10	132.4	0.10	0.25	0.60	0.10	0.12	52,073	9,504
11	139.0	0.10	0.25	0.60	0.10	0.12	52,125	9,478
12	141.2	0.11	0.25	0.56	0.10	0.13	52,211	9,446
13	115.2	0.11	0.25	0.60	0.10	0.17	52,331	9,425
14	151.6	0.10	0.25	0.62	0.10	0.15	52,368	9,361
15	135.2	0.11	0.25	0.60	0.10	0.21	52,719	9,239
16	145.3	0.11	0.25	0.60	0.10	0.22	52,795	9,201
17	95.5	0.11	0.25	0.59	0.10	0.28	52,938	9,175
18	151.7	0.10	0.25	0.59	0.10	0.24	52,953	9,114
19	128.7	0.11	0.25	0.60	0.10	0.27	53,049	9,104
20	*145.0*	*0.11*	*0.25*	*0.62*	*0.10*	*0.27*	*53,079*	*9,061*
21	***143.8***	***0.11***	***0.25***	***0.61***	***0.10***	***0.29***	***53,206***	***9,031***
22	134.3	0.11	0.25	0.60	0.10	0.30	53,261	9,004
23	152.9	0.11	0.25	0.59	0.10	0.30	53,289	8,970
24	135.1	0.11	0.25	0.60	0.10	0.32	53,371	8,953
25	149.0	0.11	0.25	0.57	0.10	0.32	53,414	8,911
26	152.2	0.11	0.25	0.59	0.10	0.41	53,859	8,682
27	152.9	0.11	0.25	0.46	0.10	0.42	54,003	8,611
28	145.4	0.11	0.25	0.62	0.10	0.46	54,087	8,571
29	149.4	0.11	0.25	0.60	0.10	0.46	54,106	8,547
30	167.2	0.11	0.25	0.60	0.10	0.46	54,173	8,499
31	159.6	0.11	0.25	0.57	0.10	0.48	54,266	8,461
32	165.1	0.11	0.25	0.44	0.10	0.48	54,319	8,420
33	165.1	0.11	0.25	0.40	0.10	0.48	54,341	8,405
34	165.2	0.17	0.25	0.28	0.10	0.49	54,932	8,369
35	***165.2***	***0.19***	***0.25***	***0.22***	***0.10***	***0.49***	***55,125***	***8,337***
Single-objective optimization without considering standard deviation (Objective 2)								
-	0	0.1	0.25	0.9	0.1	0.05	50,560	10,009

It can be observed that the mean of annual average energy consumption of the single-objective optimization solution without involving its standard deviation is 1.3% lower than the lowest mean among the solutions obtained by the multi-objective optimization involving its standard deviation. Its standard deviation of annual average energy consumption is 1.1% higher than that of the lowest mean solution. A lower mean of annual average energy consumption means a lower total electricity demand under all the possible design scenarios (noted: a fixed COP of air-conditioning system is assumed). This means that the optimal design considering the mean as the optimization objective only (i.e., Objective 2) will have a lower electricity demand than that considering both the mean and standard deviation (i.e., Objective 1).

The detailed hourly cooling load probability density distributions of three typical pareto-optimal design solutions (1, 21 and 35) with very different weightings for standard deviation and the optimal solution of single-objective design are presented to analyze the impacts of involving the standard deviation as shown in Figure 6.5. Where, the hourly cooling load during the office hour in the life-cycle under all uncertain scenarios is included. It is observed that the shapes of the probability density distributions of these four design solutions are similar. It is hard to determine exactly which design solution is optimal to maintain high efficiency for energy systems in operation as it depends on the design of the energy systems and its partial load efficiencies. Therefore, robust design optimization aiming at reducing the variance in annual average energy consumption does not help in improving energy efficiency of energy systems in operation, but instead result in increased total energy demand.

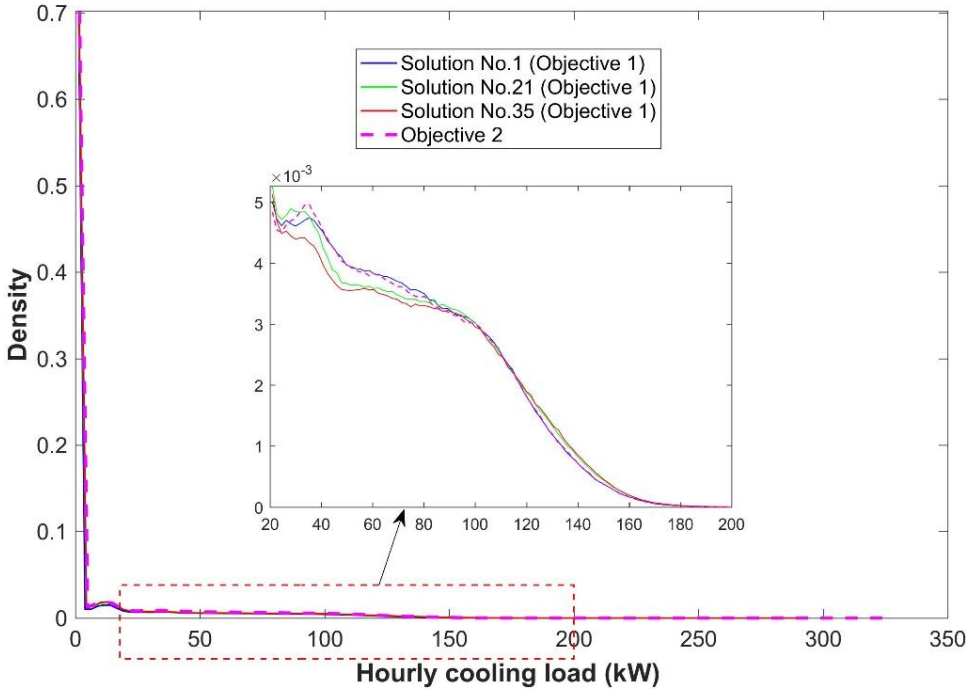

Figure 6.5 Probability density distribution of hourly cooling load for design solution 1, 21, 35 obtained using 'Objective 1' and the optimal design obtained using 'Objective 2'

In addition, as presented in Table 6.3, the design solution with a smaller standard deviation of annual average energy consumption tends to have a higher peak cooling load (50 unmet hour according to ASHRAE standard (ASHRAE, 2005)), which means that larger capacity of energy system is required and thus higher initial cost. For instance, the design solution No.35 with the lowest standard deviation has a higher peak cooling load compared with design solution No.1 and the design solution without considering standard deviation (i.e. using 'Objective 2'), which has much higher standard deviation. In summary, design optimization considering the standard deviation as one of the objectives would lead to a higher cooling energy demand/consumption and might lead to a higher initial cost of building air-conditioning systems.

Table 6.3 Peak cooling loads of typical pareto-optimal solutions considering standard deviation (Objective 1) and optimal design solution without considering standard deviation (Objective 2)

Design solution	**Peak cooling load (kW)**
No.1 (Objective 1)	210.7
No.21 (Objective 1)	236.3
No.35 (Objective 1)	242.1
Objective 2	213.1

6.3.2 Optimization case using 'Objective 3' vs optimization case using 'Objective 2'

Multi-objective optimization is also conducted using the two terms of 'Objective 3' as the objectives. The same population size of 100 is used and the results are shown in Figure 6.6. 35 pareto-optimal design solutions are identified. The mean of annual average energy consumption of the pareto-optimal design solutions increases with the decrease of the mean of annual average discomfort index. The mean of annual average discomfort index under all uncertain scenarios varies in the range between 162 and 287, while the mean of annual average energy consumption under all uncertain scenarios varies between 52,282 kWh and 165,652 kWh. The decision-makers can then select the best design options based on the relative weightings of energy consumption and thermal discomfort index. A single objective optimization is also conducted using single item of 'Objective 2' as the optimization objective. The mean of annual average energy consumption of the achieved optimal design is 50,560 kWh and the mean of calculated corresponding annual average discomfort index is 295 as marked in Figure 6.6.

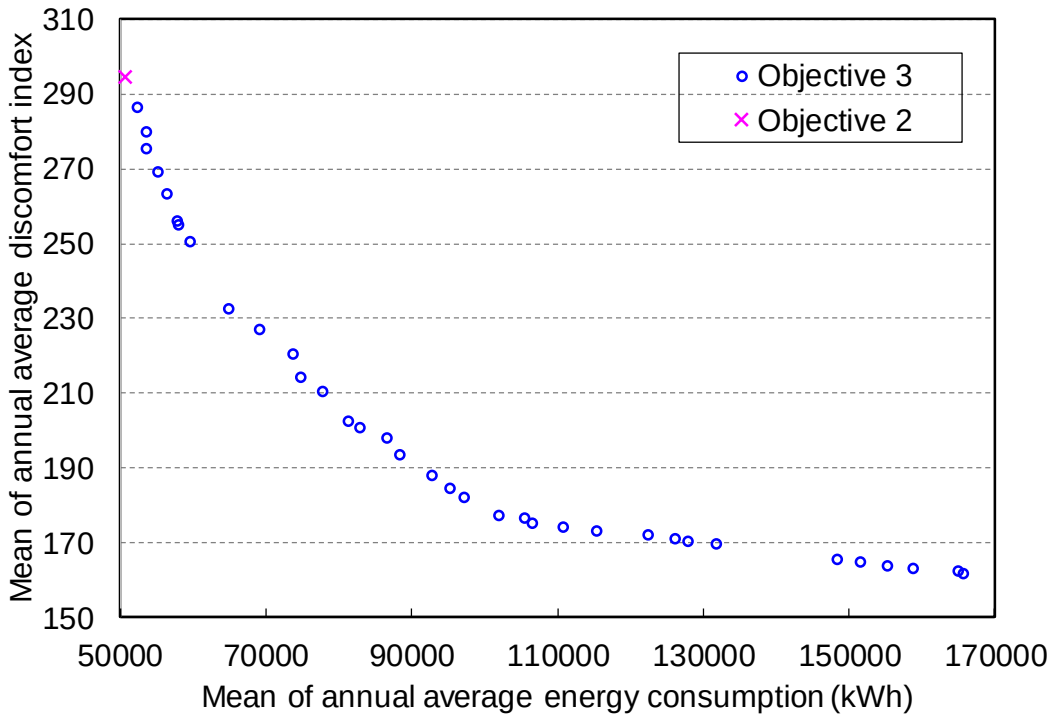

Figure 6.6 Mean of annual average energy consumption and annual average discomfort index of pareto-optimal design solutions using Objective 2 (without discomfort penalty) and Objective 3 (with discomfort penalty)

The pareto-optimal design solutions obtained when considering discomfort penalty are presented in Table 6.4, which are listed in an increasing order according to the mean of annual average energy consumption under all uncertain scenarios. The optimal roof solar absorptance, WWR and window solar heat gain coefficient are all found to increase with the increase in the energy consumption, while the building orientation has a clear trend of changing from east-oriented to south-oriented with fluctuations. The optimal wall solar absorptance fluctuates near the upper limit of its pre-set searching range (i.e., 0.9). The optimal overhang projection ratio fluctuates within a small range between 0.07 and 0.12.

The mean of annual average energy consumption of the optimal design without considering discomfort penalty (Objective 2) is 3.2% lower than the lowest mean annual average energy consumption achieved by robust design optimization considering discomfort penalty (Objective 3). But its mean of annual average discomfort index is

2.8% higher than that of the solution with lowest mean annual average energy consumption. If the increase in the mean of annual average energy consumption required to mitigate thermal discomfort using an alternative envelope design option is much higher than that using direct electrical heating during a 'cold' winter hour, it is obviously not worthwhile to further decrease the discomfort index by optimizing the building envelope. As the calculated heating load of the reference building in the coldest day is about 100 kWh, the penalty ratio for discomfort is about 100, when it is considered to be economically worthwhile to remove the winter discomfort by paying the electricity cost of direct electrical heating. The optimal design is close to the design solution 2 in Table 6.4. The corresponding annual average discomfort index and energy consumption are 281 and 52,438 kWh, respectively, while 14 hours (4.7%) of discomfort reduction is achieved by an increase of 1,878 kW (3.7%) in energy consumption, compared with the optimal design without considering discomfort penalty (Objective 2). If it is considered to be economically worthwhile to remove the winter discomfort by double cost of direct electrical heating, the penalty ratio for discomfort is about 200 and the optimal design will be then close to the design solution 5 in Table 6.4. It can be seen that robust optimal design using 'Objective 3' considering the winter discomfort penalty can make a better trade-off between energy consumption and thermal discomfort.

Table 6.4 Pareto-optimal design solutions using Objective 3 (with discomfort penalty) and Objective 2 (without discomfort penalty)

Solution No.	**Optimal design parameters**						**Optimal objectives**	
	Building orientation	Roof solar absorptance	Window to wall ratio	Wall solar absorptance	Window solar heat gain coefficient	Overhang projection ratio	Mean of D_{dis}	Mean of E_{tot} (kWh)
Multi-objective optimization considering discomfort penalty (Objective 3)								
1	77.0	0.12	0.26	0.88	0.13	0.07	287	52,282
2	77.0	0.12	0.26	0.88	0.19	0.07	275	53,441
3	77.7	0.13	0.27	0.7	0.17	0.08	280	53,523
4	99.1	0.25	0.26	0.83	0.21	0.08	269	55,089
5	79.8	0.24	0.27	0.77	0.26	0.08	263	56,261
6	89.7	0.21	0.26	0.74	0.32	0.08	256	57,629
7	*79.9*	*0.17*	*0.27*	*0.82*	*0.33*	*0.08*	*255*	*57,944*
8	109.1	0.36	0.27	0.77	0.34	0.09	251	59,460
9	85.5	0.13	0.26	0.87	0.5	0.08	233	64,842
10	135.7	0.67	0.29	0.80	0.49	0.09	227	68,991
11	112.9	0.53	0.31	0.82	0.55	0.11	221	73,599
12	112.7	0.44	0.27	0.78	0.62	0.1	214	74,677
13	137.4	0.17	0.28	0.73	0.66	0.09	210	77,672
14	92.0	0.52	0.26	0.86	0.7	0.08	203	81,195
15	92.2	0.28	0.27	0.8	0.73	0.09	201	82,864
16	108.4	0.63	0.29	0.72	0.73	0.08	199	86,577
17	93.2	0.28	0.27	0.83	0.78	0.09	194	88,191
18	117.5	0.41	0.27	0.76	0.82	0.1	188	92,752
19	123.2	0.42	0.27	0.82	0.85	0.1	185	95,099
20	143.7	0.44	0.27	0.82	0.87	0.1	182	97,103
21	*149.1*	*0.73*	*0.27*	*0.89*	*0.89*	*0.12*	*178*	*101,932*
22	126.1	0.85	0.29	0.82	0.88	0.09	177	105,452
23	145.4	0.88	0.29	0.86	0.89	0.08	175	106,419
24	148.9	0.86	0.33	0.83	0.89	0.09	174	110,743
25	143.9	0.85	0.37	0.84	0.89	0.09	173	115,347
26	150.2	0.74	0.43	0.81	0.89	0.09	172	122,397
27	147.2	0.84	0.45	0.8	0.89	0.09	171	125,985
28	150.2	0.85	0.46	0.83	0.89	0.09	170	127,728
29	150.2	0.85	0.5	0.77	0.89	0.09	169	131,724
30	157.7	0.8	0.64	0.81	0.89	0.09	166	148,222
31	158.9	0.85	0.67	0.79	0.89	0.1	165	151,540
32	127.3	0.82	0.7	0.85	0.89	0.09	164	155,137
33	159.0	0.89	0.73	0.79	0.89	0.1	163	158,724
34	159.0	0.85	0.8	0.67	0.89	0.1	163	164,926
35	158.9	0.85	0.8	0.79	0.89	0.1	162	165,652
Single-objective optimization without considering discomfort penalty (Objective 2)								
-	0	0.1	0.25	0.9	0.1	0.05	295	50,560

6.4 Discussion on the impacts and selection of objective functions

Having observed the above results and comparisons, one would ask some fundamental questions. *Is there a need to consider the variance, such as standard deviation, of performance indicator in robust design optimization in building energy field? What are the meaning and benefits of a lower variance of performance indicator?* The answers to these questions could be given and elaborated with reference to the original intention of involving the variance of performance indicator in robust design optimization in pioneer fields, and particularly the characteristics of building performance and building energy/HVAC systems.

The variance of performance indicator was introduced in the robust design optimization on the basis of stochastic linear programming, which considers the mean of performance indicator only. It is because, as stated by Mulvey et al. (1995), stochastic linear programming "*ignores higher moments of the distribution, and the decision maker's preferences toward risk. These aspects are particularly important for asymmetric distributions and for risk averse decision makers. Furthermore, aiming at expected value, optimization implicitly assumes an active management style whereby the control (i.e., recourse) variables are easily adjusted as scenarios unfold*". Robust optimization "*minimizes higher moments as well, e.g., the variance of the distribution of* ξ_s. *Hence, it assumes a more passive management style*". The consideration of variance in robust design optimization is indeed important and achievable in the fields or situations, where there are high-risk decisions under uncertainty or the variation of performance under uncertainty is preferably controlled within a small range. For instance, introducing a variance minimization term in the cost objective function for power system capacity expansion produces cost structures that are less volatile over time, and, hence, are easier to defend in front of administrative and legislative boards (Mulvey et al., 1995). Another

example is concerned with structure design, where the typical optimization objectives are nodal displacement and stiffness (Doltsinis et al., 2015; Asadpoure et al., 2011) and their standard deviations are included as the optimization objectives. In this case, there is a higher probability of failure when the variations of these performance are larger. Therefore, robust design optimization involving variance of performance indicators is necessary and worthwhile in these fields or addressing such problems.

However, the results and comparison of this study show that there are situations when involving the standard deviation as an optimization objective in the robust design optimization would lead to higher energy demand and even higher initial cost of energy systems in the building field when annual energy consumption is taken as the performance indicator. In fact, Nguyen et al. (2014) has raised their doubt on the necessity of robust design optimization involving standard deviation/variance of performance indicators in building energy field, without further elaboration or analysis. Rezvan et al. (2012) also found that the net present value and CO_2 emission cost increase and the primary energy saving of building energy generation systems decreases when reducing standard deviation of their combination. But they did not further provide the justification or elaboration on the benefits or consequences of reducing such standard deviation.

Indeed, a smaller variation of building hourly (or instantaneous) cooling load or energy demand would be preferable for energy system design and/or better energy efficiency in operation, meaning that aiming at smaller variation of hourly load/demand (note: not annual average) in robust design optimization is meaningful if possible. However, in practice, building cooling load/demand would change greatly due to the inherent patterns/changes of weather condition and building use in daily, weekly and seasonal basis. That makes narrowing down the variation of load/demand to a small range an

impossible or costly task. To cope with the large range of load/demand for high energy efficiency, building cooling systems are usually designed to have multiple or variable-speed devices (such as multiple/variable-speed chillers and pumps, and variable-speed fans). This further makes the reduction of standard deviation/variance of energy demand less important.

In summary, it is not beneficial to adopt the standard deviation/variance of building annual average cooling/energy demand as an optimization objective. It is also not necessary nor impractical to adopt the standard deviation/variance of building hourly cooling/energy demand as an optimization objective. If the variance of hourly load is concerned, the maximum hourly load could be considered as a cost (or penalty) term since it determines the design capacity of the HVAC system of a building. Therefore, "Objective 3" involving the mean of energy performance indicator, the penalty associated to winter/summer discomfort and possibly the cost/penalty associated to peak cooling/energy load (which relates to system design capacity) is recommended as the optimization objective function for robust design optimization of buildings. It comes to another question. Is there the need of robust design optimization in building design? If the use of the standard deviation (or other strict variance index) of the performance indicator is a pre-requisite, the answer is "no need". "Uncertainty-based design optimization" is recommended and applicable for design optimization of buildings considering uncertainties. If robustness in the building field means the capability of keeping relative high performance in all possible weather and working conditions or scenarios, the concept of robust design optimization is preferable and recommendable with loose definition of performance variance term in the objective function. For example, variance term could consider the range of hourly cooling/heating load by introducing cost

of system design capacity associated to peak cooling/heating demand or penalty of winter/summer discomfort in cases without heating/cooling provision.

6.5 Summary

In this chapter, different objective functions for robust design optimization are analyzed and compared to investigate their applicability and benefits in the building energy field. Robust optimal design of building envelope for zero/low energy buildings is taken as the example. An ANN model is used as the building performance model in the optimization process to reduce the computing time. Based on the results and experiences from the case studies, the following conclusions can be made.

It is not beneficial to adopt the standard deviation or variance of annual cooling/energy demand of a building as an optimization objective. The robust design optimization involving the standard deviation of annual average energy consumption in an optimization objective would lead to higher average building energy demand and even higher initial cost of cooling/energy systems. It is also not necessary nor impractical to adopt the standard deviation of building hourly cooling/energy demand as an optimization objective, due to inherent changes of building cooling/energy demand. The optimization objective function involving the mean of energy performance indicator, penalty associated to winter/summer discomfort and cost/penalty associated to peak cooling/energy load are recommended for robust design optimization in building energy field.

CHAPTER 7 COORDINATED ROBUST OPTIMAL DESIGN OF BUILDING ENVELOPE AND ENERGY SYSTEMS CONSIDERING UNCERTAINTIES

This chapter presents the procedure and methods of the coordinated robust design optimization method for the entire zero/low energy buildings concerning uncertainties. This method is proposed on the basis of coordinated design optimization method proposed in Chapter 5 and the proper robust design optimization method in building energy field identified in Chapter 6. Point estimate method is used for uncertainty propagation to significantly reduce the uncertain scenarios which need to be considered. An ANN (artificial neural network) model is trained/validated using the life-cycle building performance data under sampled uncertain scenarios and used for building performance evaluation in the envelope design optimization. A case study is conducted to test and validate the coordinated robust design optimization method.

7.1 Procedure and methods of coordinated robust design optimization considering uncertainties

7.1.1 Methodology and procedure

The proposed coordinated robust optimal design method coordinates the robust design optimizations of building envelope and energy systems to consider the interactions between building envelope and energy system design optimizations in order to achieve the robust global optimal solution under uncertainties. It is further enhanced to ensure the optimized buildings and energy system designs with more robust performance under possible uncertain scenarios, compared with the coordinated optimal design method presented in Chapter.5. Point estimate method (Bordbari et al., 2018) is used for the

quantification of uncertainties in cooling load and electrical power load to largely reduce the uncertain scenarios that need to be considered and thus to reduce computing time. Unlike the Monte Carlo method and LHS (Latin hypercube sampling) method which involve hundreds or even thousands of uncertain scenarios to represent the uncertainties, only a few uncertain scenarios (double of the number of uncertainty parameters concerned) are needed using the point estimate method. The coordinated robust design optimization method involves two steps, i.e., the *identification of coordinating design variables* and the *coordinated robust design optimization*. *At the first step*, the coordinating design variables (S) are identified. They are energy system design variables, which have impacts on building envelope optimization. These variables are considered at the stage of building envelope robust optimal design and optimized at the stage of system robust optimal design.

At the second step, an iterative approach is adopted to coordinate the multi-stage robust design optimizations. Each iteration (optimization loop) is, in fact, a multi-stage robust design optimization, consisting of robust design optimizations for building envelope and energy systems at two stages as elaborated below.

At the first stage, an initial set of values (S_i) is assumed for the coordinating design variables to be used in the performance assessment for robust design optimization of building envelope in order to make a trade-off between building envelope and energy system design optimizations. Possible uncertain scenarios are generated using the point estimate method according to the probability distributions of uncertain design inputs concerned. The design variables of building envelope are optimized to identify the robust optimal envelope design which has the minimum optimization objective value of building envelope under these scenarios.

At the second stage, the hourly cooling load and electrical power load (excluding the power load for cooling) profiles of the robust optimal envelope design under these uncertain scenarios are calculated using building simulation software. These profiles are used for robust design optimization of building energy systems. The energy system design variables, including the coordinating design variables, are optimized, under all the possible cooling and electrical power load profiles associated to the robust optimal envelope design, to identify the robust optimal energy system design. The optimization objective of energy system design is therefore minimized while satisfying the cooling and electricity demands of concern.

If the obtained optimal coordinating design variables given by robust design optimization of energy systems (S_i') deviates significantly from the value set in the robust design optimization of building envelope (S_i), a new trial of robust design optimization of building envelope will be performed after setting a new S_{i+1} based on the S_i and S_i' at last optimization loop. The new S_{i+1} can be determined as the S_i' at the last optimization loop or the average of the S_i and S_i' at last optimization loop in order to accelerate the convergence. The robust design optimizations of building envelope and energy systems are then conducted again under the updated setting. The optimization loop continues until the deviation between S_i and S_i' in the same loop is less than a preset threshold, ε. ε is set as 2% in this chapter by assuming that 2% deviation has negligible impacts on building and system performance. The robust optimal envelope design and robust optimal energy system design, achieved eventually, constitute the robust optimal design solution for the entire building.

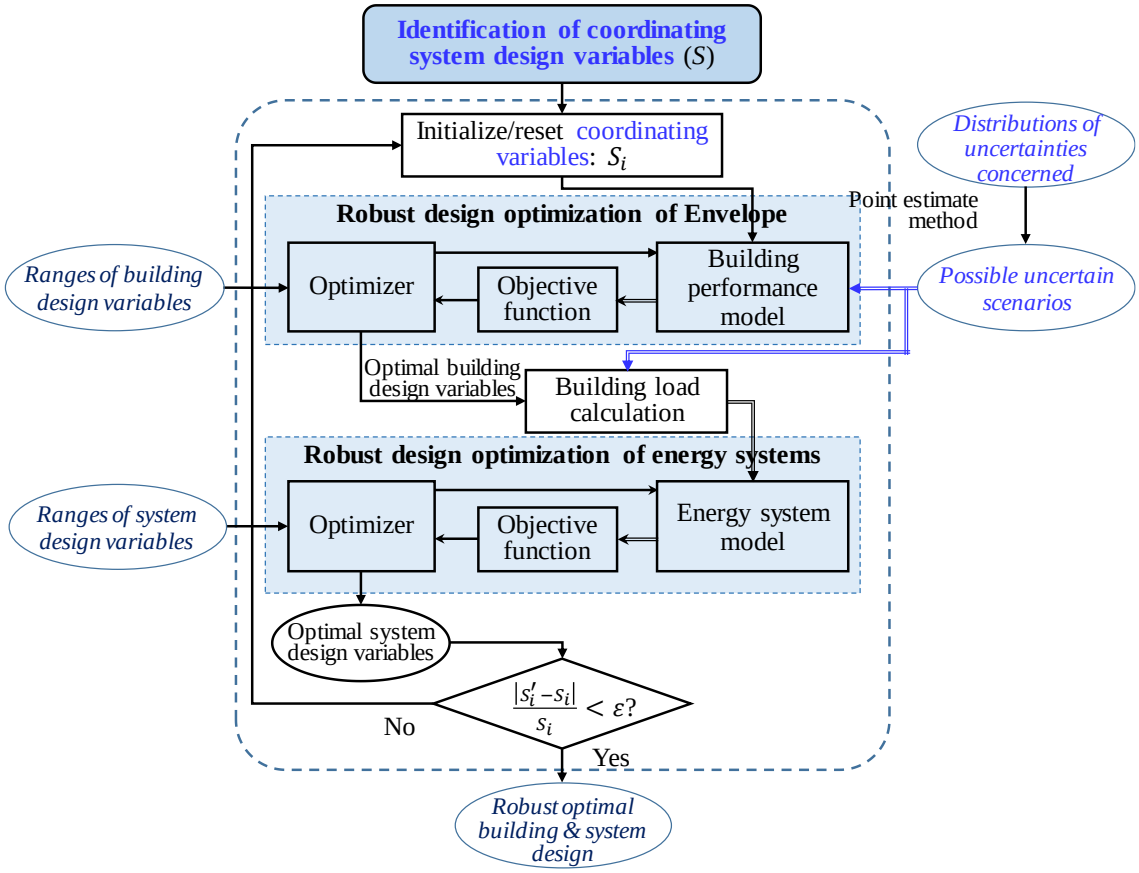

Figure 7.1 Outline of the coordinated robust optimal design method

7.1.2 Formulation of the optimization problems

The robust design optimizations of building envelope and energy systems are formulated as Eq. (7.1) and Eq. (7.2) respectively, according to the robust design optimization method recommended in Chapter 6. The robust design optimization of building envelope minimizes the objective function involving the mean of building performance indicator, the mean of building performance penalty and the mean of performance of the system component(s) associated with the coordinating design variables S under all uncertain scenarios. The robust design optimization of energy systems minimizes the objective function involving the mean of the system performance indicator, and the mean of the system performance penalty under all uncertain scenarios. Where, $\tilde{F}$ is the objective of robust design optimization. f is the performance indicator. D is the infeasible performance.

μ is the mean, which refers the weighted average in this part of study because of the characteristics of the uncertainty quantification method adopted. *X* is the vector of design variables. *p* is the vector of design inputs, which can be uncertain. The subscript "*env*" refers to envelope, while subscript "*sys*" refers to energy systems. *a* and *a'* are penalty ratios for infeasible performance. The design variables of building envelope are optimized within their searching ranges. The design variables of energy systems are optimized within their searching ranges subject to some equality and inequality design constraints.

Robust design optimization of building envelope:

$$\text{Minimize: } \tilde{F}_{env}(X_{env}, p_{env}, S) = \mu_{f_{env}} + a * \mu_{D_{env}} - \mu_{f_S} \tag{7.1}$$

$$\text{subject to: } X_{env,min} \leq X_{env} \leq X_{env,max}$$

Robust design optimization of energy systems:

$$\text{Minimize: } \tilde{F}_{sys}(X_{sys}, p_{sys}) = \mu_{f_{sys}} + a' * \mu_{D_{sys}} \tag{7.2}$$

$$\text{subject to: } X_{sys,min} \leq X_{sys} \leq X_{sys,max}$$

$$g(X_{sys}, p_{sys}) = 0$$

$$h(X_{sys}, p_{sys}) \leq 0$$

7.1.3 Uncertainty quantification using point estimate method

The 2-point estimate method (2PEM), as a modified point estimate method, is employed in this part of study to quantify the uncertainties in building cooling and electrical power loads. Based on the 2PEM method (Bordbari et al., 2018), the uncertainty in the *i*th uncertain design input (i.e., p_i, $\forall i = 1, 2, \ldots, M$. Where, *M* is the total number of uncertain design inputs concerned.) can be represented by two points (i.e., $p_{i,j}$, and $j = 1, 2$.), together with a weight factor for each point (i.e., $w_{i,j}$). Each representing point and its weigh factor are calculated using Eqs. (7.3-7.6) and Eq. (7.7), respectively. All weight factors should

be between 0 and 1, and the sum of the weight factors for all the points representing the uncertain design inputs should be 1. The mean of performance or penalty performance under uncertain scenarios is calculated using Eqs. (7.8-7.9) by summing the performance or penalty performance under a representing point of a uncertain design input multiplied by its corresponding weight factor, while setting the other uncertain design inputs as the mean of their distribution. Where, $\xi_{i,j}$ represents the standard location of the *j*th concentration of p_i. $\gamma_{i,3}$ represents the coefficient of skewness. $Prb(p_{i,j})$ is the probability of occurrence $p_{i,j}$ according the probability distribution of the *i*th uncertain design input.

$$p_{i,j} = \mu_{p_i} + \xi_{i,j}\sigma_{p_i} \tag{7.3}$$

$$\xi_{i,j} = \frac{\gamma_{i,3}}{2} + (-1)^{3-j}\sqrt{M + (\frac{\gamma_{i,3}}{2})^2} \tag{7.4}$$

$$\gamma_{i,3} = \frac{E[(p_i - \mu_{p_i})^3]}{(\sigma_{p_i})^3} \tag{7.5}$$

$$\mathrm{E}\left[(p_i - \mu_{p_i})^3\right] = \sum_{j=1}^{2} prb(p_{i,j})(p_{i,j} - \mu_{p_i})^3 \tag{7.6}$$

$$w_{i,j} = \frac{1}{M}(-1)^j \frac{\xi_{i,3-j}}{2\sqrt{M + (\frac{\gamma_{i,3}}{2})^2}} \tag{7.7}$$

$$\mu_f \cong \sum_{i=1}^{M}\sum_{j=1}^{2} f(i,j) * w_{i,j} \tag{7.8}$$

$$f(i,j) = f(x, \mu_{p_1}, \mu_{p_2}, \cdots, p_{i,j}, \cdots, \mu_{p_M}) \tag{7.9}$$

7.2 An overview of the validation case

7.2.1 Optimization objective functions and design constraints

The optimization objective ($\tilde{F}_{env}$) of the robust design optimization of building envelope is calculated using Eq. (7.10). Where, the optimization objective of building envelope under each uncertain scenario F_{env} is calculated according to Eq. (5.3). The annual

average cost for the building energy consumption in the life-cycle is considered as the performance indicator in this part of study. The annual average penalty cost for winter thermal discomfort in the building life cycle is considered as the infeasibility performance. The winter discomfort is considered to avoid a severely cold indoor environment in the winter season in subtropical regions without heating provision. The cost for selling the electricity generated by PV is taken as the system performance to be considered in envelope design optimization, since the PV area is identified as the only coordinating design variable in Subsection 5.3.1. The penalty ratio for winter thermal discomfort is set as 100 in this study (i.e., a=100), as explained in Section 4.2.

$$\tilde{F}_{env} = \sum_{i=1}^{M} \sum_{j=1}^{2} F_{env}(i,j) * w_{i,j} \tag{7.10}$$

The optimization objective ($\tilde{F}_{sys}$) of the robust design optimization of building energy systems is calculated using Eq. (7.11). Where, the optimization objective of energy system under each uncertain scenario F_{sys} is calculated according to Eq. (5.7), since the grid-connected zero energy building is concerned only in the validation case. The total cost in the building life cycle is considered as the system performance indicator. The cost penalty of the accumulated unmet cooling load over the building life cycle due to insufficient cooling capacity, and the cost penalty of accumulated monthly grid impact index over the building life cycle are taken as the infeasibility performance. The penalty ratio for unmet cooling load is set as 3 in this study (i.e., $a1$=3), and the penalty ratio for grid impact index is set as 240 (i.e., $a2$=240), as explained in Subsection 5.3.3.

$$\tilde{F}_{sys} = \sum_{i=1}^{M} \sum_{j=1}^{2} F_{sys,GC}(i,j) * w_{i,j} \tag{7.11}$$

The constraints for robust design optimization of building energy systems include the battery charge and discharge rate limits, and the battery storage limit, as shown in Eq. (5.9-5.11). In addition, the energy generated from renewable resources over the building

life cycle should be equal to or larger than the energy demand of energy systems over the building life cycle.

7.2.2 Energy system control strategy

A typical control strategy is implemented, as an ideal control, for the performance assessment of system design optimization same as that used in the coordinated optimal design in Chapter 5. The priority (high to low) of power supply is: PV & wind turbines, battery, co-generators and grid. Absorption chillers have higher priority to supply cooling than electric chillers when co-generators are put into operation. At this situation, electric chillers are put into operation when cooling demand cannot be satisfied using absorption chillers only. Only electric chillers are used when co-generators are not in operation. The detailed control strategy of the entire energy system for grid-connected buildings is explained in Subsection 5.2.2, including an overall control mode selection and three alternative operation modes.

7.3 Training and validation of ANN building performance model

An ANN model is developed for the building performance assessment in the robust design optimization of building envelope in order to reduce the computing time. The inputs of the ANN model are listed in Table 7.1, which include the envelope design variables listed in Table 4.4, the coordinating design variable identified in Subsection 5.3.1, and the uncertain design inputs (excluding the uncertainty in variation of weather condition, but including the uncertainty in climate change trend) listed in Table 4.5. The model outputs are the corresponding building performance (i.e., cooling load, electricity load, winter thermal discomfort in the building life cycle) obtained by building simulation using EnergyPlus under the randomly-ordered measured weather data in Hong Kong together with the corresponding sampled climate change trend.

Table 7.1 Inputs and outputs of ANN model for coordinated robust optimal design

Category		Parameters	Range/distribution	Unit
Model inputs	Envelope design variables	Building orientation	[0,360]	°
		Roof solar absorptance	[0.1,0.9]	-
		Window-to-wall ratio	[0.25,0.8]	-
		Wall solar absorptance	[0.1,0.9]	-
		Overhang projection ratio	[0.05,0.5]	-
	Uncertain design inputs	Climate change trend	U(0,0.048)	K/year
		Occupancy density	Factor: Tri(0.3,1.2,0.9)	-
		Lighting load		-
		Equipment load		-
		Infiltration air mass flow rate	U(0.0025,0.0075)	kg/(s·m)
	Coordinating design variable	PV area	[100,1032]	m^2
Model outputs		Electricity load in building life-cycle	-	J
		Cooling load in building life-cycle	-	J
		Thermal discomfort index in building life-cycle	-	-

The ANN model structure and model parameters (weights) are both optimized in the training process. MSE (mean squared error) is used to evaluate the performance of ANN model. *At the first step*, 2,400 sets of training data and 120 sets of validation test data are prepared. A large number of training data are prepared in order to make sure the consistency between the building performance given by ANN model and that given by EnergyPlus, and thus to assure the reliability of envelope design optimization results.

At the second step, the optimal ANN model structure is identified using 10-fold cross-

validation (Kohavi, 1995). Different numbers of hidden layers (1 or 2 hidden layers) and different numbers of neurons in different hidden layers (1-27 neurons when using 1 hidden layer, 1-9 neurons for each layer when using 2 hidden layers) are tested. The training results show that the optimal ANN model structure, which has the minimum average MSE in the cross-validation, is one hidden layer with 27 neurons. Its average MSE is 1.19×10^{-4}.

At last, the optimal ANN model is obtained by further optimizing the parameters of ANN model with the optimal model structure. Test data are then used to validate the optimal ANN model obtained. It can be seen from Figure 7.2 that the ANN model outputs well match the test data given by EnergyPlus. Their coefficients of linear regression are all up to 0.999. The consistencies between the impacts of different design variables on the building performance outputs estimated by the ANN model and EnergyPlus are also validated. As an example, Figure 7.3 shows the comparisons between the building performance outputs given by ANN model and EnergyPlus when the building orientation varies. It can be seen that the annual average electricity loads, cooling loads and winter thermal discomfort given by ANN model and EnergyPlus match very well respectively. In summary, the optimized ANN model has very good accuracy in estimating the building performance including the impacts of individual design variable.

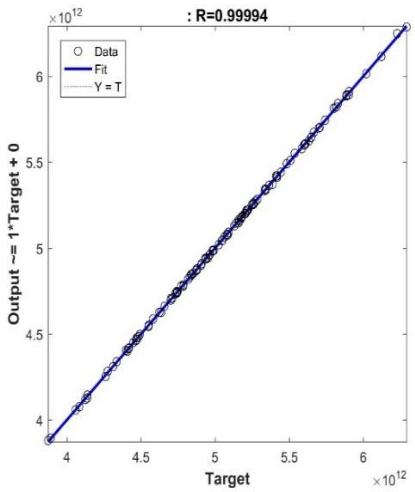

(A) Electricity load in building life cycle

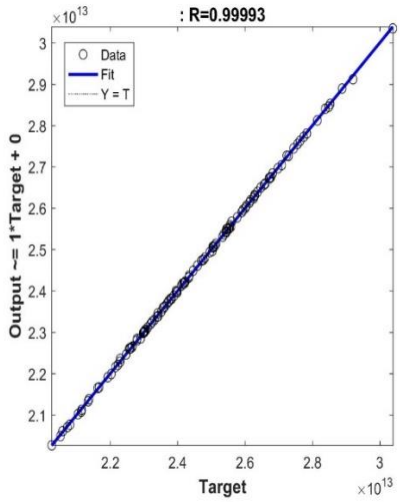

(B) Cooling load in building life cycle

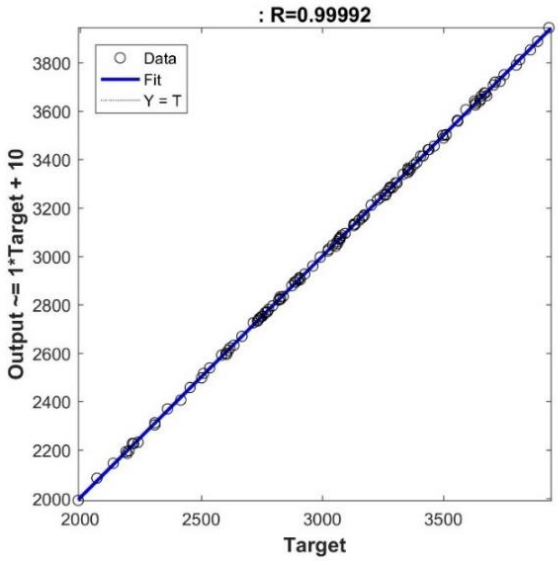

(C) Thermal discomfort in building life cycle

Figure 7.2 Comparison of outputs of optimal ANN model and test data during model validation

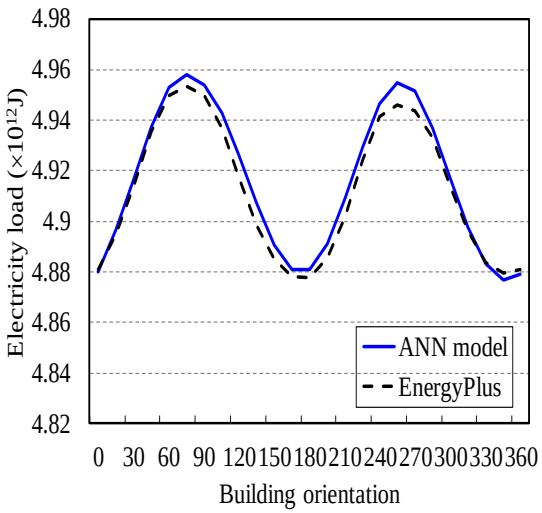

(A) Electricity load in building life cycle

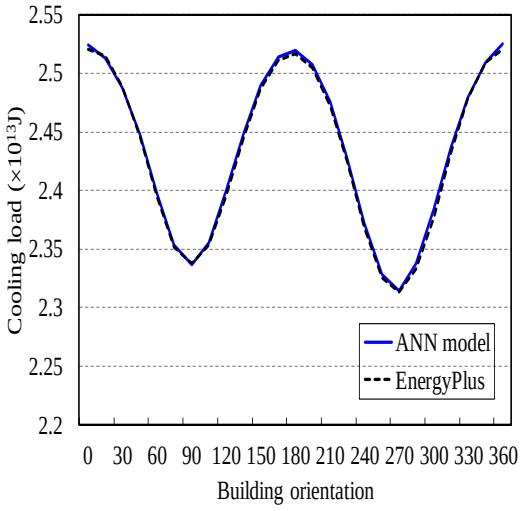

(B) Cooling load in building life cycle

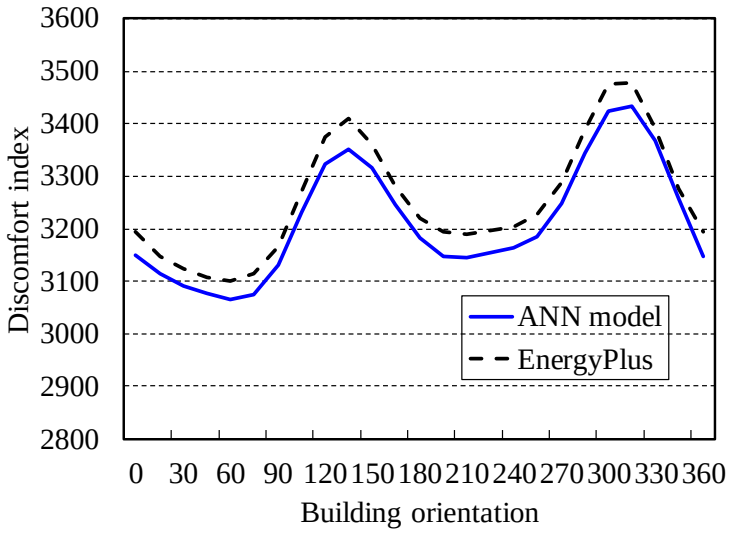

(C) Thermal discomfort in building life cycle

Figure 7.3 Outputs of optimal ANN model and EnergyPlus *vs* building orientation

7.4 Results of coordinated robust optimal design case study

The design optimization is performed for the reference building (introduced in Section 3.2) using the proposed method with a design intention of grid-connected zero energy building. GA (genetic algorithm) is used as the optimization algorithm. The design results at each optimization loop (iteration) are shown in Table 7.2. It can be seen that five optimization loops are needed to reach the convergence when the initial PV area for envelope design is set as 1,032 m^2. When an initial PV area of 1,032 m^2 is set for the

envelope design, the actual cost-optimal PV area given by the robust design optimization of energy systems is 458 m^2 only, which deviates significantly from the preset initial PV area in the robust design optimization of building envelope. Then a new optimization loop starts by setting the PV area as 458 m^2 for the robust design optimization of building envelope. This design process is repeated until the PV area for envelope design is set as 419 m^2. The corresponding optimized PV area given by robust design optimization of energy systems is 416 m^2, which is within the convergence tolerance (2%). The optimal design obtained in optimization loop 5 is eventually identified as the robust optimal design for the grid-connected zero energy building.

Table 7.2 Optimization loops of the design case using coordinated robust optimal design method

Loop nos.	A_{PV}	Robust optimal envelope design					Robust optimal system design									
		BO	RSA	WWR	WSA	OPR	A'_{PV}	Cap_{WT}	n_{WT}	Cap_{CG}	n_{CG}	Cap_{AC}	n_{AC}	Cap_{EC}	n_{EC}	Cap_{bat}
1	1032	0	0.1	0.2	0.1	0.39	458	17	0	30	1	50	1	130	1	43
2	458	0	0.1	0.2	0.1	0.41	430	10	0	30	1	50	1	129	1	58
3	444	0	0.1	0.2	0.1	0.41	419	27	0	30	1	50	1	128	1	67
4	432	0	0.1	0.2	0.1	0.41	419	35	0	30	1	50	1	128	1	67
5 (final)	***419***	***0***	***0.1***	***0.2***	***0.1***	***0.41***	***416***	***29***	***0***	***30***	***1***	***50***	***1***	***126***	***1***	***68***

** Note: The units of variables refer to that in Table 4.4.*

Compared with the optimal designs (as shown in Table 5.4) given by both coordinated and uncoordinated design optimization methods, it can be seen that the optimal design given by the coordinated robust design optimization method requires larger absorption chiller, electric chiller and battery. The optimal PV area given by coordinated robust design optimization method is larger than the optimal PV area given by coordinated optimal design method, but is smaller than the optimal PV area given by uncoordinated optimal design method (i.e., existing multi-stage design optimization method). This may

be due to more cooling and electrical power load is required considering possible uncertainties compared with the presumed design condition.

The system performance under uncertain scenarios of optimal system design solutions given by these three methods (i.e., coordinated robust optimal design method, coordinated optimal design method and uncoordinated optimal design method with an initial PV area setting of 100 m^2) are compared as shown in Figure 7.4. It can be seen that the robust optimal design given by coordinated robust optimal design method has 1.9% (i.e., 9,841 USD) less total cost in average under uncertain scenarios, compared with that given by the uncoordinated design method. The accumulated unmet cooling load is reduced by 97.0% (i.e., 132,320 kWh). The accumulated grid impact index is reduced by 3.0% (i.e., 5). And the energy system design objective value is reduced by 41.6% (i.e., 408,031 USD).

The optimal design given by coordinated optimal design method has 0.4% (i.e., 2,021 USD) less total cost in average under uncertain scenarios, compared with that given by the uncoordinated design method. The accumulated unmet cooling load is reduced by12.3% (i.e., 16,816 kWh). The accumulated grid impact index is reduced by 4.8% (i.e., 8), and the energy system design objective value is reduced by 5.5% (i.e., 54,444 USD). This indicates that the robust optimal design method is more robust in sustaining the possible uncertainties in operation compared with the coordinated and uncoordinated optimal design methods. The coordinated optimal design method outperforms the uncoordinated optimal design method in maintaining good performance under possible uncertainties.

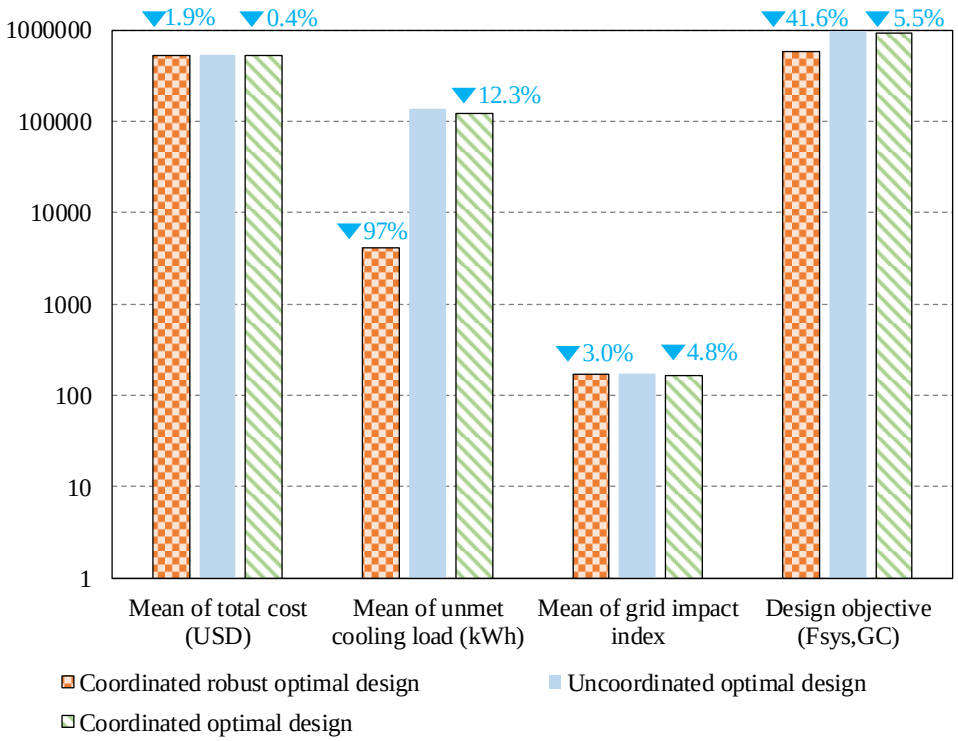

Figure 7.4 Comparison between system performance of optimal design solutions given by three optimal design methods under uncertain scenarios

7.5 Summary

In this chapter, a coordinated robust design optimization method is proposed for the entire zero/low energy buildings concerning uncertainties. Point estimate method is used for uncertainty quantification, which significantly reduces the uncertain scenarios to be considered. An ANN model is used as building performance model to reduce evaluation time. One case study is conducted to validate the proposed method. Based on the results of the case study, conclusions can be made as follows.

Among the coordinated robust, coordinated and uncoordinated optimal design methods, the coordinated robust optimal design method is the most robust in sustaining the possible uncertainties in operation followed by coordinated optimal design method. The coordinated robust optimal design achieved has 97% less accumulated unmet cooling load and 42% less system design objective value in average under possible uncertain

scenarios, compared with existing multi-stage design methods without considering uncertainties. The accumulated unmet cooling load of the optimal design provided by coordinated optimal design method is reduced by 12% and the system objective value is reduced by 6% in average.

CHAPTER 8 COORDINATED ONLINE MULTI-OBJECTIVE OPTIMAL CONTROL OF ENERGY SYSTEMS BASED ON A GAME THEORY APPROACH

This chapter presents a coordinated online multi-objective optimal control strategy for the predictive scheduling and real-time optimal control of the energy systems in zero/low energy buildings. The strategy consists of an online multi-objective predictive scheduling scheme and a real-time multi-objective optimal control scheme. A cooperative game theory-based approach is adopted for the online multi-objective optimizations of both predictive scheduling and real-time optimal control. The optimal control strategy and control optimization schemes are tested and evaluated on the energy systems in the reference building supplemented with battery storage.

8.1 Coordinated online optimal control strategy using a game theory approach

8.1.1 Outline of the online optimal control strategy for energy systems with energy storages

As shown in Figure 8.1, the online multi-objective optimal control strategy includes an online multi-objective predictive scheduling scheme and a real-time multi-objective optimal control scheme. As shown in Figure 8.1(A), at the start of each predictive scheduling optimization interval (one day in this study), the storage charge/discharge schedule or the schedule of power imported/exported from/to the power grid (named as "power import/export" hereafter), for all scheduling control action intervals (one hour in this study) within the scheduling interval, is optimized under predicted operation conditions. When low operation energy cost has higher priority, the storage charge/discharge is selected for predictive scheduling. When low grid impact has higher

priority, the power import/export is selected for predictive scheduling. The other control variables of energy systems at the same time intervals are also optimized simultaneously as the optimization of the storage charge/discharge or power import/export schedule can be achieved only at optimized settings of all other control variables concerned although only the predictive optimal charge/discharge or power import/export schedule is used eventually.

In operation, the settings of all other control variables concerned, are optimized at each supervisory optimization/action interval under current operation condition, given that the storage charge/discharge or power import/export is controlled according to its optimal schedule determined by the above predictive scheduling, as shown in Figure 8.1(B). Where, the optimization/action interval (5 minutes is used in this study) of real-time optimal control is much shorter than the optimization and action intervals of predictive scheduling.

Another major means of coordination between two control optimization schemes is the refinement of the storage charge/discharge schedule in the actual real-time control when the optimal schedule of storage charge/discharge is used in real-time optimal control. It is needed due to the fact that the actual surplus renewable power generation in the building could be more than that predicted. In this situation, the actual charge/discharge control is refined, according to the surplus renewable power generation and the limits (including charge/discharge limit and storage limit) of energy storage system, to reduce the waste of renewable energy and/or selling/buying electricity to/from the power grid. The online multi-objective optimization of both control optimization schemes are achieved using the game theory-based optimization method described in detail in the following subsection.

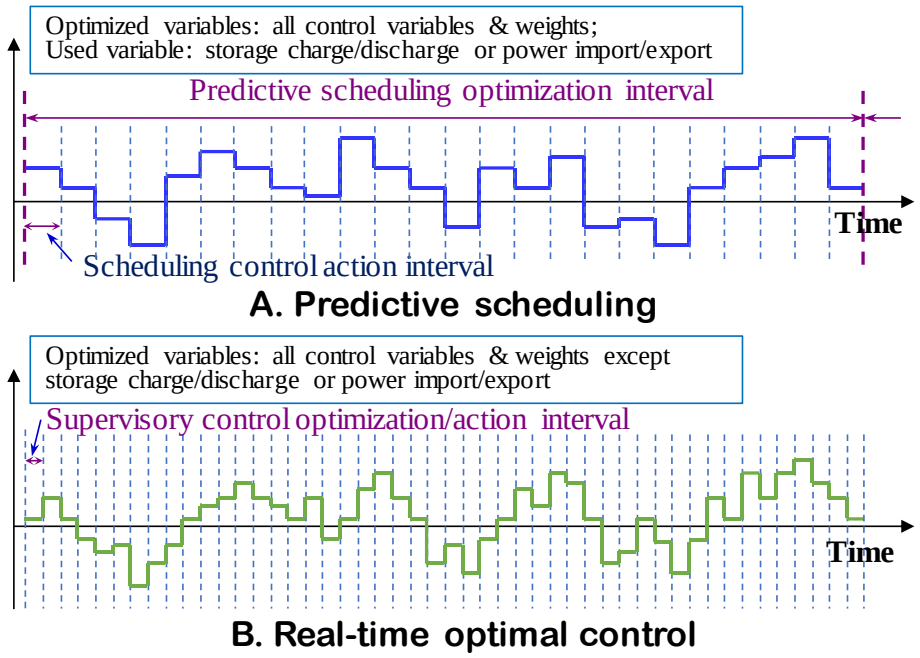

Figure 8.1 Illustration of the coordinated online optimal control strategy

8.1.2 Multi-objective predictive optimal scheduling and real-time optimal control schemes adopting a game theory method

The problems of multi-objective predictive scheduling and the real-time multi-objective optimal control can be formulated as Eq. (8.1) and Eq. (8.2) respectively. In the predictive scheduling, the control variables of building energy systems at each "control action interval" over a scheduling "optimization interval" are optimized to minimize the accumulated sum of the values of the combined objective (i.e., combined from the multiple objectives concerned) during the entire scheduling optimization period (interval). In the real-time optimal control, the control variables of building energy systems at current control interval are optimized to minimize the combined objective with the predictive optimal control value of the coordinating control variable, which can be the storage charge/discharge or power import/export, as a given input. Where, F is the function combining multiple objectives concerned. The subscript PS refers to predictive scheduling, while the subscript RT refers to real-time optimal control. f is the objective concerned. N is the number of objectives concerned. X is the vector of control variables

in predictive scheduling. *p* is the vector of control inputs. *C* and *C'* are the constraint for predictive scheduling and real-time optimal control respectively. *Y* is the vector of control variables in real-time optimal control. *S* is the coordinated control variable which is optimized in predictive scheduling and used as an input in real-time optimal control. It is worth noticing that *S* refers to the refined charge/discharge control value of the energy storage system when the storage charge/discharge schedule is used to coordinate the two control optimization schemes.

$$\text{Minimize: } F_{PS} = \sum F(f_1(X_{PS,\Delta T}, p_{\Delta T}), f_2(X_{PS,\Delta T}, p_{\Delta T}), \dots f_N(X_{PS,\Delta T}, p_{\Delta T})) \quad (8.1)$$

$$\text{subject to: } X_{PS} \in \mathrm{C}$$

$$\text{Minimize: } F_{RT} = F(f_1(X_{RT,\Delta t}, p_{\Delta t}, S), f_2(X_{RT,\Delta t}, p_{\Delta t}, S), \dots f_N(X_{RT,\Delta t}, p_{\Delta t}, S) \quad (8.2)$$

$$\text{subject to: } X_{RT} \in \mathrm{C}'$$

A cooperative game theory approach proposed by Rao and Freiheit (1990) is used to solve the online multi-objective optimization problems in the study. Optimization objectives are envisioned as players cooperating with each other to improve the solution as a whole. The cooperative game theory approach enables to distribute the resources such that all players are as far from their worst cases as possible. Using this approach, the objective function for the multi-objective optimization can be formulated as Eq. (8.3), involving the weighted sum of all objectives and a supercriterion *Z*. Where, w_i is the weight factor for the *i*th objective. The supercriterion is introduced as a penalty to avoid the objectives being too close to their worst cases, as shown in Eq. (8.4). The approach follows three main steps as below.

$$\mathrm{F} = \sum_{i=1}^{N} w_i * f_{ni}(X) - Z \quad (8.3)$$

$$\mathrm{Z} = \prod_{i=1}^{N} (1 - f_{ni}(X)) \quad (8.4)$$

- Minimize each objective separately, record the values of all the objectives at the optimal design solutions obtained by minimizing each objective, and identify the worst value of each objective from the corresponding values recorded before.
- Normalize each objective (according to Eq. (8.5)) using the identified minimum and worst values of the corresponding objective. Where, 0 means the objective reaches its minimum value, and 1 means the objective reaches its worst value. f_{ni} is the normalized value of the *i*th objective. $f_{i,min}$ is the minimum value of the *i*th objective. $f_{i,wst}$ is the worst value of the *i*th objective.

$$f_{ni}(X) = \frac{f_i(X) - f_{i,min}}{F_{i,wst} - f_{i,min}} \tag{8.5}$$

- Minimize the combined objective which combines the weighted sum of all objectives and the supercriterion *S*, as shown in Eq. (8.3). The control variables and the weights of all objectives are optimized.

8.2 Implementation in the online control optimization of energy systems

8.2.1 Description of the energy systems concerned

The online optimal control strategy is implemented on the online optimal control of energy systems introduced in Section 3.3 to test its effectiveness and benefits. The energy systems include PV panels, a co-generator, a heat recovery unit, a duty absorption chiller, two duty electric chillers, a battery and associated cooling system components. Table 8.1 shows the capacities and numbers of the system components. EnergyPlus building performance model of the reference building is built, which refers to ZCB as introduced in Subsection 3.2.1, to generate the electrical power load and cooling load profiles for the case studies. The building is connected to the power grid, allowing the electricity being exported/imported to/from the power grid.

Table 8.1 Specification of building energy systems used in case studies

Parameter	Symbol	Value	Unit
PV area	A_{PV}	480	m^2
Capacity of co-generator	Cap_{CG}	40	kW
Number of co-generators	n_{CG}	1	-
Capacity of absorption chiller	Cap_{AC}	40	kW
Number of absorption chillers	n_{AC}	1	-
Capacity of electric chiller	Cap_{EC}	70	kW
Number of electric chillers	n_{EC}	2	-
Capacity of battery	Cap_{bat}	50	kWh

8.2.2 Online optimization procedure of optimal control strategy

The online optimal control strategy consists of two control optimization schemes, which are implemented at two stages sequentially as introduced earlier. The procedure of the online optimal control strategy using the battery charge/discharge schedule as the coordinating control variable of the two control optimization schemes is taken as an example and illustrated in Figure 8.2. The *first stage* is the implementation of the predictive scheduling scheme. The control optimization interval is set as one day. At this stage, the hourly cooling load (Q_{CL}), electrical power load (P_{EL}) and PV power generation (P_{PV}) in the scheduling optimization interval are estimated using the EnergyPlus building performance model and PV model, and used as the inputs for the predictive scheduling under the electricity price profile of the power grid. The control variables to be optimized are the power imported from grid (P_{grid}), power generation of the co-generator (P_{CG}), power discharged by battery (P_{bat}), cooling supply of electric chillers (Q_{EL}) and cooling supply of absorption chiller (Q_{AC}). A negative value of P_{grid} means that the power is exported to the power grid. A negative value of P_{bat} means that the battery is charged.

These five control variables at each hour in the next 24 hours and the weights of the two objectives (i.e. totally 122 values to be optimized) are optimized to minimize the combined objective given by Eq. (8.1) using the game theory method. OPTI solver is used as the optimizer since it is capable to solve large scale mixed-integer nonlinear optimization problem. The optimization is subject to the balances of power supply/demand and cooling supply/demand, battery storage limits and the charge/discharge rate limits. The actual effective output of the predictive scheduling scheme is the optimal schedule of battery charge/discharge, which is used for the real-time optimal control.

The *second stage* is the implementation of the real-time optimal control scheme. At this stage, the control variables are optimized at an interval of 5 minutes. The measured cooling load (Q_{CL}), electrical power load (P_{EL}), PV power generation (P_{PV}) and the current electricity price, as well as the refined battery charge/discharge control value (P'_{bat}), are used as the inputs for the optimal control optimization. The control variables (except battery charge/discharge) and the weights for the objectives are optimized to minimize the combined objective given by Eq. (8.2) using the game theory method. Prior to optimization, the charge/discharge control of the battery (P_{bat}) is refined by checking if the battery storage has reached its upper/lower limits and if there is surplus electricity generated by PV after satisfying all the current energy demands. If the battery storage has reached its upper limit, no further charge is allowed. If the battery storage has reached its lower limit, no further discharge is allowed. If there is surplus electricity generated by PV, all this surplus electricity will be charged to the battery or less power is discharged by fully use of the electricity generated by PV while satisfying the charge/discharge limits of battery. The “fmincon” solver in Matlab is used as the optimizer. The optimization is also subject to the balances of power supply/demand and cooling supply/demand.

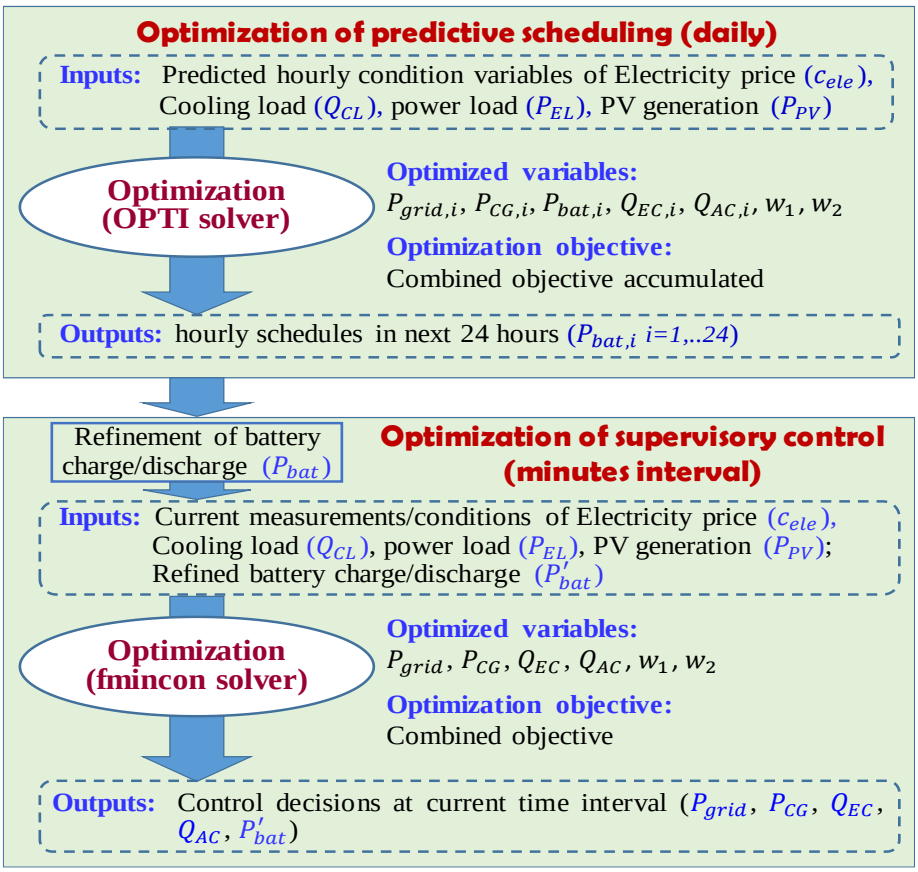

Figure 8.2 Procedure of the online optimal control strategy using battery charge/discharge schedule as the coordinating control variable

8.2.3 Optimization objectives

Two objectives are considered for the optimization in this study, including the operation energy cost (*OC*) and grid impact index (*GII*). The operation energy cost at each control action interval is calculated using Eq. (8.6) – Eq. (8.7). It consists of the fuel cost for the co-generator and the cost for buying/selling the electricity from/to the grid. Time-varying price given by the power grid is used in this study. The grid impact index is quantified using Eq. (8.8). It is worth noticing that the standard deviation of power import/export over a month is used to quantify the grid impact of a building in design optimization, while the absolute deviation of current power import/export from its moving average over the last 24 hours is used here for online control optimization, considering the feasibility and convenience of online applications.

$$\mathrm{OC(t)} = c_{grid} * P_{grid}(t) * \Delta t + c_{fuel} * FC_{CG}(t) * \Delta t \tag{8.6}$$

$$c_{grid} = \begin{cases} c_{ele}, & if \;\; P_{grid}(t) \geq 0 \\ c_{tif,} & if \;\; P_{grid}(t) < 0 \end{cases} \tag{8.7}$$

$$\mathrm{GII(t)} = \left| P_{grid}(t) - \sum_{i=1}^{H} P_{grid}(t-i) \,/H \right| \tag{8.8}$$

where, c_{fuel} is the fuel cost (USD/kWh). Δt is the time interval (h). FC_{CG} is the heat energy generated by fuel combustion (kW). H is the total number of control action time interval concerned in one day.

8.3 Evaluation of the optimal control strategies

8.3.1 Description of the test conditions

Evaluation tests are conducted on two selected days, including: a *sunny spring day* when the power generated by renewable sources is sufficient for power supply most of the time, and a *cloudy summer day* when the power generated by renewable sources is insufficient for power supply most of the time. The control period is between 21:00 PM of each day and 21:00 PM on the next day. The selection considers the simplicity for battery charge/discharge scheduling since the electricity price is low during the period between 21:00 PM and 8:00 AM. The online optimal control strategies using battery charge/discharge schedule and power import/export schedule as the coordinating control variable respectively are tested. The detailed test results of the online optimal control using battery charge/discharge schedule as the coordinating control variable are presented in Subsection 8.3.2 and Subsection 8.3.3 to show the performance of the proposed control strategy. The game theory-based approach is compared with the conventional weighted sum method using the fixed weights in Subsection 8.3.4 to evaluate its effectiveness and benefits. The actual performance under different control strategies is also compared to demonstrate the needs and impacts of coordinating predictive scheduling and real-time

optimal control in Subsection 8.3.5. The actual profiles of loads and weather condition used for the real-time operation tests are modified from that used for the predictive scheduling optimization to introduce the discrepancies between predicted and actual operation conditions as shown in Figure 8.3.

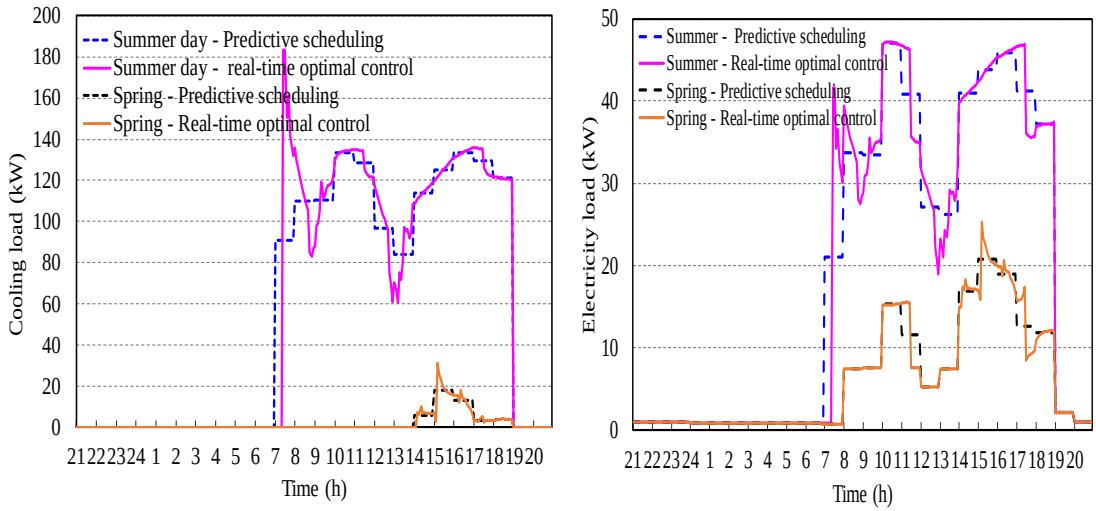

(A) Cooling load (B) Power load

Figure 8.3 Load profiles used for predictive scheduling and real-time optimal control on two test days

8.3.2 Test results in sunny spring day

The predictive optimal schedule of the energy systems obtained in the spring day is shown in Figure 8.4. It can be seen (from Figure 8.4A) that, during 21:00 PM and 6:00 AM, the co-generator was activated or battery was discharged to supply electricity since there was no PV generation. During 6:00 AM and 16:00 PM, the PV power generation was more than the electrical power load and the power required for the cooling supply using electric chillers. The surplus electricity was charged to the battery and sold to the grid. During 11:00AM-12:00PM and 15:00PM-16:00PM, the co-generator was used in order to reduce the impacts on the power grid. After 16:00 PM, the co-generator was used and/or the battery was discharged since the PV generation was insufficient or no PV generation was available. It can be seen that the power kept being exported to the grid on this day. This

is because the power export was more than the power import on previous day according to the profile used in this case study, and the power was then scheduled to export the grid in order to reduce the grid impact index.

It can be seen (from Figure 8.4B) that cooling was demanded only during 14:00 PM and 19:00 PM in that day. The cooling demand was less than the lower limit of electric chiller operation load (i.e., 20% of one electric chiller capacity) during this period except the period between 15:00PM and 16:00PM. During this period between 15:00PM-16:00PM, the cooling load was satisfied using an electric chiller and an absorption chiller. In the rest of the time during the cooling period, only one electric chiller (14:00PM-15:00PM and 18:00PM-19:00PM) or one absorption chiller (16:00PM-18:00PM) was used. The electric chiller operated at its lower limit load most of the time.

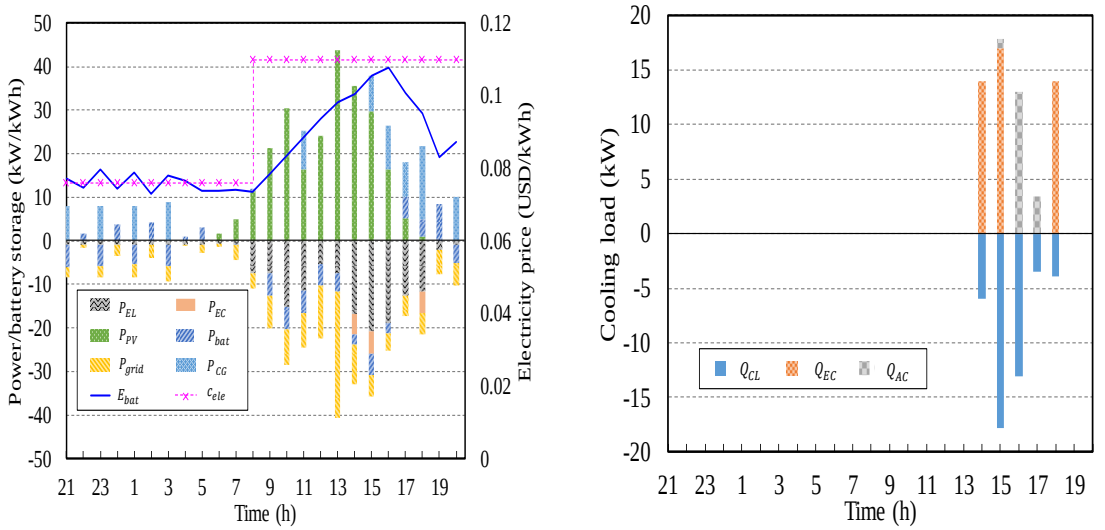

(A) Power demands and power generations (B) Cooling demand and cooling supply

Figure 8.4 Predictive optimal schedules of energy systems - Sunny spring day

Based on the day-ahead optimal schedule for battery charge/discharge, the real-time optimal control of the energy systems was then determined by the real-time optimal control scheme at an interval of 5 minutes. Figure 8.5A shows the actual power generations and power demands under the real-time optimal control. During 21:00PM

and 6:00AM, electricity was imported from the grid to satisfy the electricity demand and charge the battery most of the time, since there was no PV generation and the electricity price was low. This is different from the optimal schedule given by predictive scheduling scheme, which used the co-generator to generate electricity in order to supply the electricity demand and charge battery. It is due to that a lower operation energy cost was more profitable than a lower grid impact index to minimize the objective value at current time interval.

During the period between 6:00AM and 16:00PM (except a short time around 11:00AM), the PV power generation was more than electricity demand. The surplus electricity was charged to the battery and sold to the grid. Unlike the predictive scheduling which used the co-generator to reduce the impacts on grid sometimes, the co-generator was not used during this period. During the time around 11:00AM, the power was imported from the grid since the PV generation was reduced significantly and insufficient for power supply. After 16:00PM, the PV power generation was not sufficient to meet the electricity demand or no power was generated by PV. The battery was discharged or power was imported from the grid to meet the power demand. The co-generator was also activated when the absorption chiller was needed. It can be seen (from Figure 8.5B) that the cooling load was supplied using an electric chiller only or using an absorption chiller only most of the time, which are similar to that given by predictive scheduling.

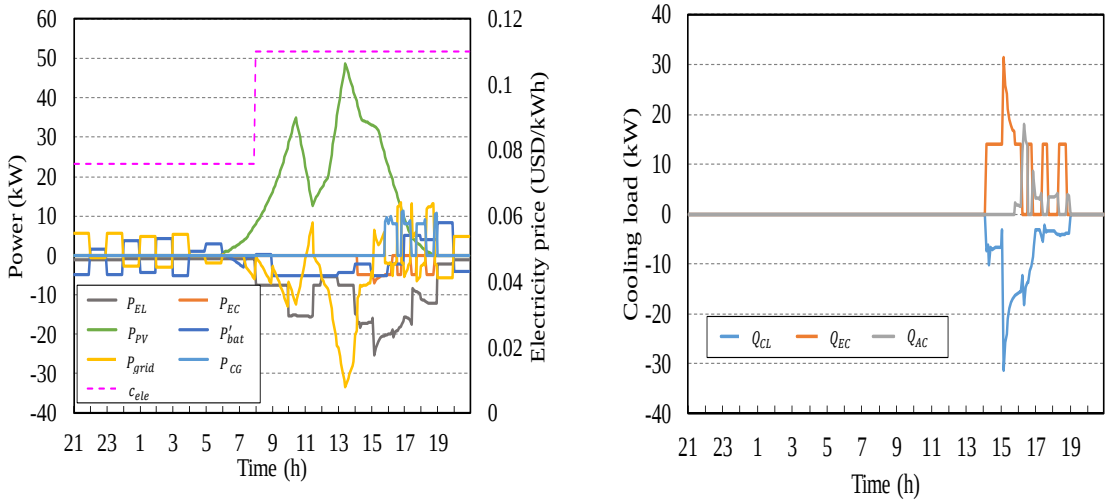

(A) Power demands and power generations (B) Cooling demand and cooling supply

Figure 8.5 Actual profiles of control settings and other main variables under real-time optimal control - Sunny spring day

Figure 8.6 presents a comparison between the refined optimal control schedule and the predictive optimal schedule of battery charge/discharge. It can be seen that the control setting of battery charge/discharge during 6:00AM and 7:00AM was refined and different from the optimal schedule. The battery was charged with more power in actual operation since there was surplus electricity generated by PV and there was still available storage space in battery during that period. It is also worth noticing that, compared with the minor refinement of battery charge/discharge, other control settings have more obvious differences from the corresponding optimal schedules given by the predictive scheduling optimization due to the difference of actual and predicted operation conditions, as shown by the results presented above.

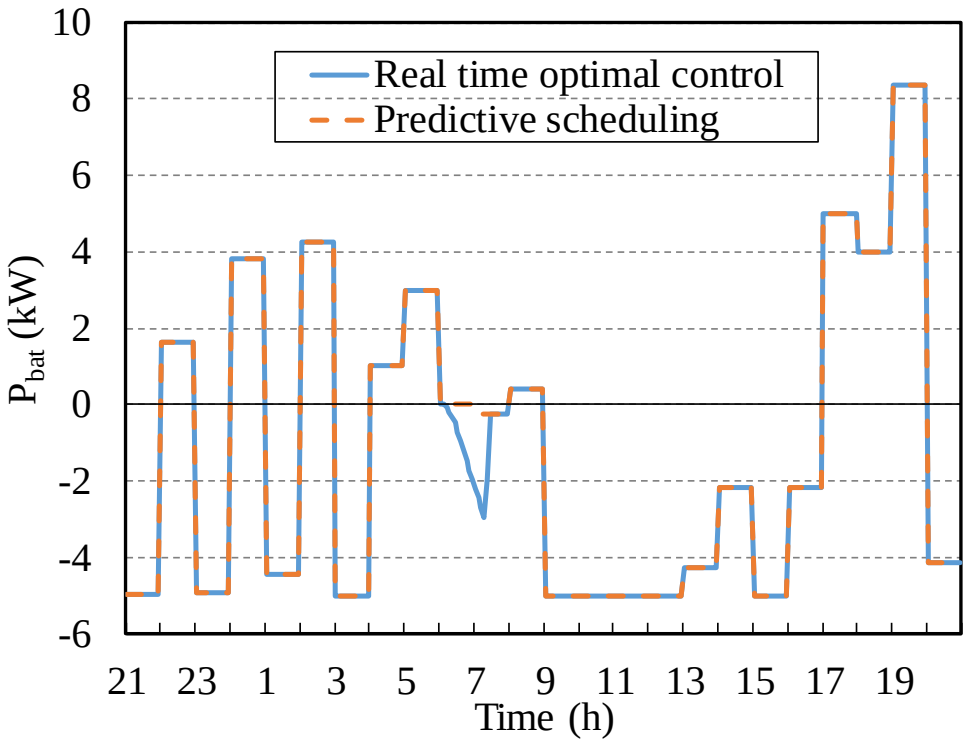

Figure 8.6 Comparison between battery charge/discharge schedules determined by the real-time optimal control and predictive scheduling schemes

8.3.3 Test results in cloudy summer day

The predictive optimal schedule of the energy systems on the selected cloudy summer day is shown in Figure 8.7. It can be seen that the electrical power demand and the cooling demand were much higher than that on the spring day. The PV power generation was insufficient to meet the power demand over the entire day. Electricity was imported from the grid to meet the high electrical power demand all the day. During 21:00PM and 7:00AM, the battery was charged until reaching its maximum storage limit since the electricity price was low. During 7:00AM and 19:00PM, the co-generator was activated and used to supply the power and cooling. The battery was discharged until reaching its lower storage limit since the electricity price was high. Between 19:00PM and 21:00PM, the co-generator was shut down, and the battery was charged using the power imported from the grid while satisfying the electricity demand. Where, extra power (i.e., more then

what need for meeting the power demand) was imported from the grid to charge battery since the impacts on the grid could be reduced. Figure 8.7B shows the optimal schedule of cooling supply given by predictive scheduling and the cooling demand. It can be seen that there was cooling demand in the office hour during 7:00AM and 19:00PM. The cooling load during the entire office hour was higher than the capacity of an electric chiller. Thus both the electric chiller(s) and the absorption chiller were used for the cooling supply.

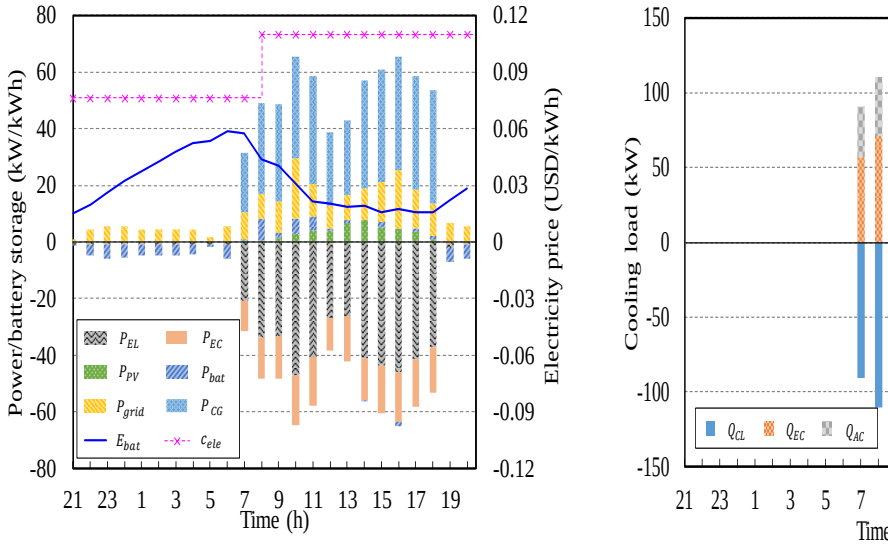

(A) Power demands and power generations (B) Cooling demand and cooling supply

Figure 8.7 Predictive optimal schedules of energy systems - Cloudy summer day

Figure 8.8 shows the profiles of the control settings for the energy systems determined by the real-time optimal control scheme. The electricity was imported from the grid over the entire day, and no electricity was exported to the grid. Between 21:00PM and 7:00AM, the battery was charged. Between 7:00AM and 19:00PM, the co-generator was used (except a short period around 13:00PM) and the battery was discharged. After 19:00PM, the co-generator was shut down, and the battery was charged using the power imported from the grid while satisfying the electricity demand. Both the electric chiller(s) and the absorption chiller were used to supply cooling in office hour, except a short period around

13:00PM. During this short period, only an electric chiller was used for cooling supply. The optimal control settings of the energy systems are mostly in consistency with their corresponding predictive optimal schedules with some obvious differences in magnitude.

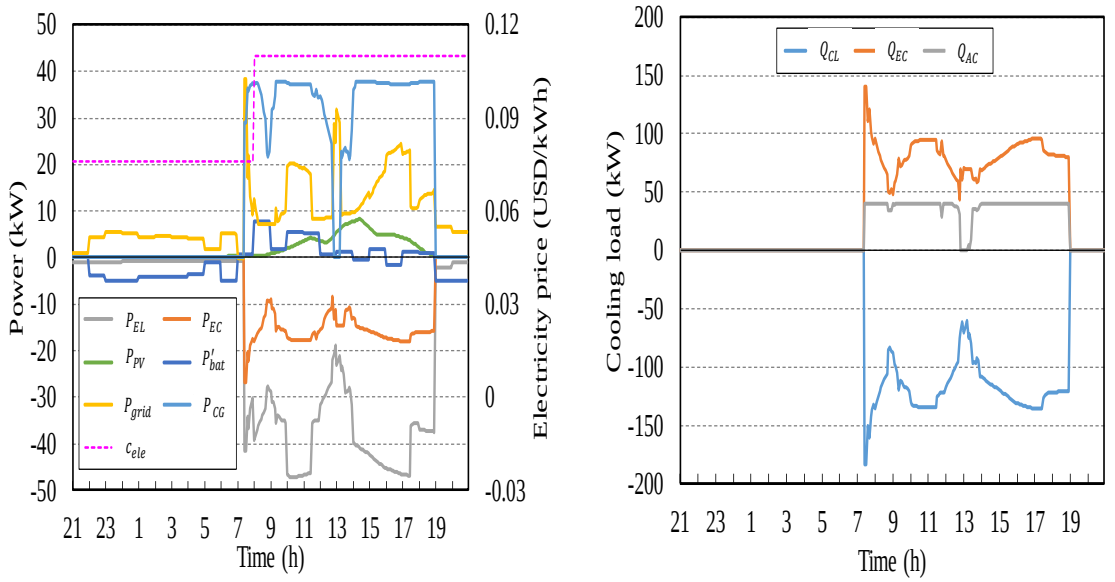

(A) Power demands and power generations (B) Cooling demand and cooling supply

Figure 8.8 Actual profiles of control settings and other main variables under real-time optimal control - Cloudy summer day

8.3.4 Comparison between multi-objective optimizations using game theory and weighted-sum methods

The game theory-based approach is compared with the weighted sum method using the fixed weights to validate its effectiveness. The predictive scheduling of the energy systems on the spring day is used as an example. Twelve sets of fixed weights for the objectives (i.e., operation energy cost and grid impact index) are tested using the weighted sum method. They are 0, 0.1, 0.25, 0.3, 0.4, 0.5, 0.6, 0.7, 0.75, 0.8, 0.9 and 1, respectively. The accumulated energy cost and grid impact index over the test day associated with the optimal schedules given by the game theory-based method and weighted sum method are shown in Fig. 11. It can be seen that the objective values given by the weighted sum method varied in a large range when different weights were used. The accumulated energy

cost in the test day varied between -1.6 and 93.1 USD, while the accumulated grid impact index in the test day varied between 64 and 146 kWh. The experience of the test also shows that it was difficult to determine proper weights for the energy cost and grid impact index based on the preference of the decision-makers. This is because a small change in the weights did not have significant impacts on the objective values in some cases, but did have significant impacts on the objective values in some cases. For instance, changing the weight of energy cost from 0.25 to 0.75 did not affect the values of energy cost and grid impact index significantly, but changing the weight of energy cost from 0.75 to 1 affects the value of energy cost greatly.

It can also be observed that the game theory method was efficient to find the optimal solution (i.e. schedules of control settings in scheduling optimization and control settings of real-time control optimization), which is in fact a solution having the objectives as far away from their worst values as possible without the need of trying different weights. The results show that the optimal operation energy cost and grid impact index obtained using game theory-based method was preferable as its grid impact index was very close its lowest value but its operation energy cost was still far away from its worst value. In addition, the game theory-based method was efficient to provide the online optimal control. It cost about 2-3 minutes for day-ahead predictive scheduling optimization, and cost about 0.1 second for real-time optimal control optimization. The computation time is close to that using weighted sum method.

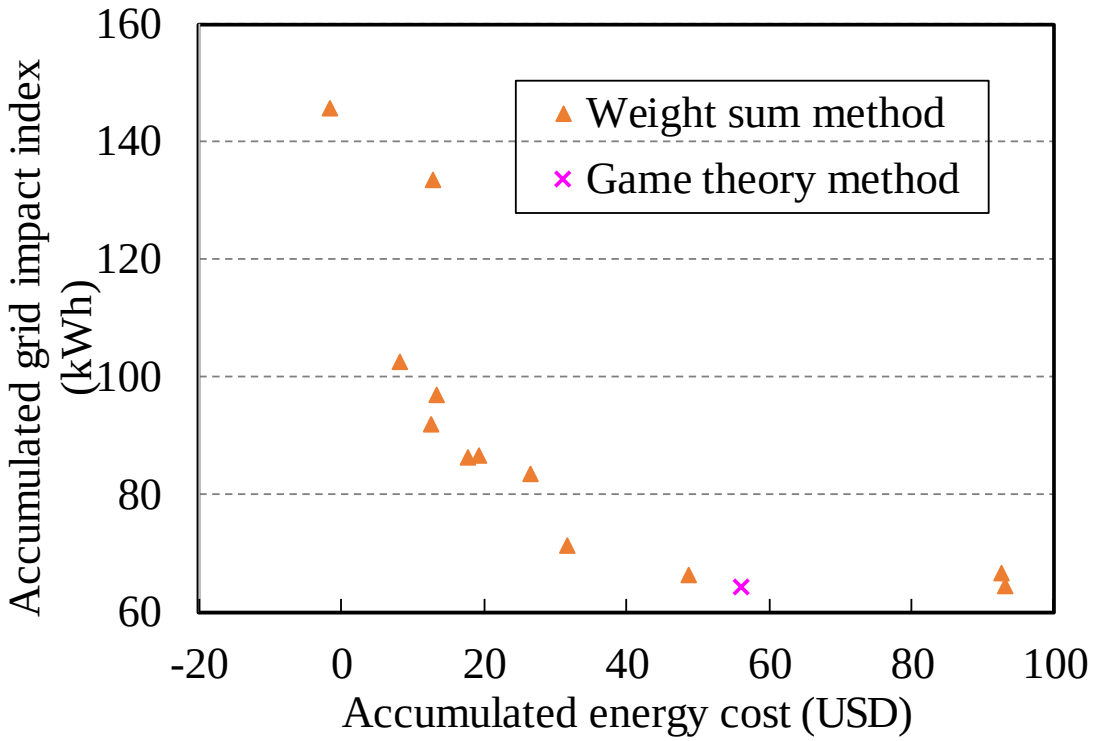

Figure 8.9 Comparison of the objective values of optimal schedules determined by game theory-based method and weighted-sum method – Sunny spring day

8.3.5 Analysis on the need and benefits of coordinating the predictive scheduling and real-time optimal control

To evaluate the need and benefits of coordinating the predictive scheduling and real-time optimal control, the performance of the proposed online optimal control strategy coordinating the predictive scheduling and real-time optimal control is compared with that solely using the predictive scheduling. The actual performance of the energy systems under the control of four different control strategies on the sunny spring test day is shown in Table 8.2.

The four control strategies include: *(1).* Coordinated optimal control using battery charge/discharge as the coordinating control variable, *(2).* Coordinated optimal control using the power import/export as the coordinating control variable, *(3).* Predictive scheduling with online refinement for satisfying the actual cooling and power demands,

(4). Predictive scheduling (without online refinement). It can be seen that it is not recommendable to use predictive scheduling directly without online refinement since there were significant unmet cooling and power loads in actual operation when the energy systems are strictly controlled according to the optimal schedule determined by the predictive scheduling. The accumulated unmet cooling load was 4.2 kWh and the accumulated unmet electrical power load was 14.7 kWh in the sunny spring test day. This is because the actual operation condition is different from that predicted. It is also observed that, although the cooling and power loads can be met when the energy systems were controlled using the predictive scheduling with online refinement, the operation energy cost was increased by 1.8% to satisfy the need of building services.

When any of the coordinated optimal control strategies was used, there was no unmet cooling nor power load. Compared with the optimal scheduling with online refinement, the coordinated optimal control strategy using the power import/export as the coordinating control variable achieved a lower energy cost (reduced by 4.0%) while it maintained the same low grid impact. The coordinated optimal control strategy using the battery charge/discharge as the coordinating control variable achieved much lower energy cost (reduced by 81.37%) while the grid impact index was much higher (increased by 109.7%). This is because the predictive optimal control of battery has higher priority on the minimization of the energy cost particularly under the time-varying electricity price. The above results show the need and benefits of combining and coordinating the predictive scheduling with real-time optimal control in order to satisfy the service need with the least “cost”. The proposed optimal control strategy involving two coordinated control optimization schemes can ensure the satisfaction of building service need and provide the best performance based on the priority of the decision-makers without need of specifying the weights of optimization objectives.

Table 8.2 Performance comparison of different control strategies – Sunny spring day

Control strategy	Accumulated energy cost (USD)	Accumulated grid impact index (kWh)	Accumulated unmet cooling load (kWh)	Accumulated unmet power load (kWh)
Predictive scheduling	56.2 (*-1.7%*)	63.9 (*1.3%*)	4.2	14.7
Predictive scheduling with online refinement	57.2 (-)	63.1 (-)	0	0
Coordinated optimal control (CCV: battery charge/discharge)	10.7 (*-81.3%*)	132.3 (*109.7%*)	0	0
Coordinated optimal control (CCV: power import/export)	54.9 (*-4.0%*)	63.9 (*1.3%*)	0	0

Note: CCV stands for coordinating control variable.

8.4 Summary

In this chapter, a coordinated online multi-objective optimal control strategy consisting of two control optimization schemes is proposed for the predictive scheduling and real-time optimal control of energy systems in zero/low energy buildings. A cooperative game theory method is adopted for the online multi-objective optimization of both predictive scheduling and real-time optimal control. This control strategy is tested and evaluated on the energy systems with battery storage in a grid-connected building under two typical working conditions. Based on the results and experiences from the case studies, conclusions can be made as follows.

- It is necessary and beneficial to coordinate predictive scheduling with real-time optimal control to provide satisfactory services with less “cost” in operation. Following predictive scheduling strictly cannot ensure the satisfaction of cooling and electrical power demands in operation. Although online refinement on the predicted

schedules can be made to satisfy the actual demands in operation, the energy cost might be increased obviously in operation. The proposed coordinated optimal control strategy can provide the satisfactory services with less cost compared with predictive scheduling with online refinement. The test results show that the proposed control strategy achieved a lower energy cost (reduced by 4.0%) while it maintained the same low grid impact, compared with the predictive scheduling with online refinement.

- The coordinated online optimal control has the flexibility to achieve a low value for the objective with higher priority while maintaining other objectives at reasonable levels by selecting the coordinating control variable properly. For example, when low energy cost has higher priority, the battery charge/discharge should be selected as the coordinating control variable of the coordinated optimal control strategy, which could achieve much lower energy cost (reduced by 81.3%) compared with solely using predictive scheduling with online refinement.
- The proposed game theory-based online optimization approach is effective to find optimal control settings for energy systems without the need of specifying weights for multiple optimization objectives. That provides an effective means for online multi-objective optimal control since it is often difficult or impractical to determine the proper weights for different objectives to convert the multi-objective optimization problems to single objective optimization problems. The test results also show that the proposed game theory-based online optimization approach is computationally effective and can fulfill the needs of online optimization for online optimal control applications. It took about 2-3 minutes for the optimization of day-ahead predictive scheduling, and about 0.1 second for the optimization of the real-time optimal control, which are close to that for optimizations using the weighted sum method.

CHAPTER 9 CONCLUSIONS AND FUTURE WORK

In this chapter, the main contributions of this thesis are summarized, followed by the main conclusions made based on the study presented in this thesis. Recommendations for future work are presented at the end.

9.1 Main contributions of this study

This PhD study proposed a coordinated optimal design method for the building envelope and energy systems of zero/energy buildings, a coordinated robust optimal design method for the building envelope and energy systems of zero/energy buildings concerning uncertainties, and an online multi-objective optimal control strategy for the energy systems in zero/low energy buildings. The main contributions can be summarized as follows:

1. A new multi-stage sensitivity analysis method is developed for holistic sensitivity analysis to avoid missing of important parameters. The impacts of design parameters and uncertain design inputs on the performance of zero/low energy buildings in subtropical regions are studied comprehensively. The key design parameters and main uncertain design inputs of zero/low energy buildings in subtropical regions are identified.
2. A coordinated optimal design method is proposed for the entire zero/low energy buildings including building envelope and energy systems. This innovative method can achieve the global optimal design solution, which needs to consider building envelope and building energy systems as a whole in the optimization, with much less computing cost.

3. The impacts of alternative objective functions on robust design optimization are studied to identify the proper objective function for robust optimal design in building energy field. The applicability of the commonly-used objective functions in pioneer fields is analyzed comprehensively when used in the building energy field.

4. A coordinated robust optimal design method is proposed for the entire zero/low energy buildings, including both building envelope and energy systems, concerning uncertainties. This new method can provide better building and system performance under possible uncertain operation conditions/scenarios, compared with the existing design methods.

5. A coordinated online multi-objective optimal control strategy is proposed for predictive scheduling and real-time optimal control of energy systems in zero/low energy buildings based on a game theory-based method. The novel control strategy coordinates predictive scheduling with real-time optimal control, which can provide satisfactory services with less "cost" in operation. In addition, online multi-objective optimization can be achieved effectively without the need of specifying weights for different optimization objectives.

9.2 Conclusions and recommendations

Conclusions on sensitivity analysis

1. Six key envelope design parameters, which significantly affects the performance of buildings in subtropical regions are identified. They are building orientation, roof solar absorptance, window to wall ratio, wall solar absorptance, window solar heat gain coefficient and overhang projection ratio.

2. The outputs of the sensitivity analysis using different sensitivity analysis methods can be different and using a single sensitivity analysis method to identify the key design

parameters may result in missing some important design parameters. It is therefore recommended to combine more than one sensitivity analysis method to identify and determine the parameters to be optimized. For instance, the sensitivity analysis using regression method only would lead to missing two key design parameters, namely overhang projection ratio and building orientation, which are commonly considered as highly-sensitive parameters in previous studies for buildings in hot climate regions.

3. The consideration of winter thermal discomfort significantly affects outputs of sensitivity analysis for buildings without heating provision in subtropical regions and therefore the identification and selection of their key design parameters. In this study, the results of sensitivity analysis show that roof and wall solar absorptance are highly-influential parameters when winter thermal discomfort is concerned in the buildings without heating provision in subtropical regions. However, these two parameters are seldom selected as the key design parameters in previous studies, which are mainly concerned about energy consumption.
4. The uncertainties in the design inputs have significant effects on the choice of optimal design for zero/low energy buildings. It is necessary to consider the uncertainties in the building design optimization. The uncertain design inputs, which have significant impacts on the performance of buildings in subtropical regions, are weather conditions, infiltration and internal loads.

Conclusions on coordinated optimal design

1. The optimizations of building envelope design and energy system design need to be integrated as a coordinated design process when some system design variables have impacts on the design optimization of building envelope.
2. The proposed coordinated design method is robust in providing optimal design

solutions for the entire zero/low energy buildings. The case studies show that coordinated optimal design can always converge to the same optimal design solution under different initial settings although different iteration times may be needed, while design solutions of uncoordinated design method could be very different under different initial settings.

3. The proposed coordinated design method can provide "global" optimal design solutions for the entire zero/low energy buildings, while the optimal design solutions given by the uncoordinated design method could be "local" optimum. For the validation case, the total cost and design objective value of the optimal energy systems given by the coordinated design method are about 4% less compared with the existing multi-stage design optimization method, and their accumulated unmet cooling loads decrease by over 22%.

4. The proposed coordinated optimal design method can efficiently achieve the global optimal design solution that needs to consider building envelope and building energy systems as a whole in the optimization. This is typically achieved by simultaneous design optimization method while the proposed method could achieve similar effect with much reduced optimization complexity and computation cost. The experience of the case studies shows that the actual computation cost is about 3 or 4 times of that of multi-stage design optimization method but is estimated to be much less than simultaneous optimization methods, which might need impractically long and unaffordable computation time. The proposed method has essential advantage particularly when the numbers of design variables are large and the performance of building envelope and energy systems needs to be evaluated using simulation tools in their design optimizations.

Conclusions on robust optimal design

It is not beneficial to adopt the standard deviation or variance of annual cooling/energy demand of a building as an optimization objective. The robust design optimization involving the standard deviation of annual average energy consumption as one of the optimization objectives would lead to higher average building energy demand and even higher initial cost of cooling/energy systems. It is also not necessary nor impractical to adopt the standard deviation of building hourly cooling/energy demand as an optimization objective, due to inherent changes of building cooling/energy demand. The optimization objective function involving the mean of energy performance indicator, penalty associated to winter/summer discomfort and cost/penalty associated to peak cooling/energy load are recommended for robust design optimization in building energy field

Conclusions on coordinated robust optimal design

Among the coordinated robust, coordinated and uncoordinated optimal design methods, the coordinated robust optimal design method is the most robust in sustaining the possible uncertainties in operation, followed by the coordinated optimal design method. The coordinated robust optimal design achieved has 97% less accumulated unmet cooling load and 42% less system design objective value in average under possible uncertain scenarios, compared with uncoordinated optimal design (i.e., existing multi-stage optimal design) without considering uncertainties. The accumulated unmet cooling load of the optimal design provided by coordinated optimal design method is 12% less and the system objective value is 6% less in average.

Conclusions on multi-objective online optimal control

1. It is necessary and beneficial to coordinate predictive scheduling with real-time

optimal control to provide satisfactory services with less “cost” in operation. Following predictive scheduling strictly cannot ensure the satisfaction of cooling and electrical power demands in operation. Although online refinement on the predicted schedules can be made to satisfy the actual demands in operation, the energy cost might be increased obviously in operation. The proposed coordinated optimal control strategy can provide the satisfactory services with less cost compared with predictive scheduling with online refinement. The test results show that the proposed control strategy achieved a lower energy cost (reduced by 4.0%) while it maintained the same low grid impact, compared with the predictive scheduling with online refinement.

2. The coordinated online optimal control has the flexibility to achieve a low value for the objective with higher priority while maintaining other objectives at reasonable levels by selecting the coordinating control variable properly. For example, when low energy cost has higher priority, the battery charge/discharge should be selected as the coordinating control variable of the coordinated optimal control strategy, which could achieve much lower energy cost (reduced by 81.3%) compared with solely using predictive scheduling with online refinement.

3. The proposed game theory-based online optimization approach is effective to find optimal control settings for energy systems without the need of specifying weights for multiple optimization objectives. That provides an effective means for online multi-objective optimal control since it is often difficult or impractical to determine the proper weights for different objectives to convert the multi-objective optimization problems to single objective optimization problems. The test results also show that the proposed game theory-based online optimization approach is computationally effective and can fulfill the needs of online optimization for online optimal control

applications. It took about 2-3 minutes for the optimization of day-ahead predictive scheduling, and about 0.1 second for the optimization of the real-time optimal control, which are close to that for optimizations using the weighted sum method.

9.3 Recommendations for future work

This PhD study has made great efforts on developing robust design optimization method and optimal control strategy for zero/low energy buildings. In future studies, more efforts can be made on the following aspects to further enhance the methods and the convenience for practical applications.

1. The design optimization of building envelope in this study evaluates the design solution alternatives according to their energy consumption and thermal discomfort. The material and construction costs (such as the manufacturing cost, transportation cost and labor cost) is not considered, which significantly affects the final choice and is an important factor concerned in practice. Therefore, the life cycle cost of building envelope design needs to be considered in future studies.

2. The variations in the maximum values of occupant density, equipment load and lighting load in the building are considered in the robust optimal design and coordinated robust optimal design in this study. However, the stochastic variations of these design inputs at different time, which can also bring large variation of energy use, are not considered in this study. Therefore, the possible stochastic variations in these internal loads should be considered in robust optimal design of buildings in future studies.

3. In this study, only the uncertainties which affects the cooling load are considered. In fact, the uncertainties in the prices of electricity, fuel and system components can significantly affect the final choice of energy system design when life cycle cost is

considered to evaluate the design solution alternatives. Future studies on the robust design optimization of zero/low energy buildings should pay attention to the uncertainties in these costs.

4. In this study, the robust design optimization evaluates the design solution according to its mean of energy consumption and penalty of thermal discomfort. The risk of extreme situations (such as high peak cooling load), which is essential especially to achieve zero/low energy goal for zero/low energy buildings in operation, is ignored. In future studies, robust design optimization of zero/low energy buildings considering the risk of extreme situations needs to be investigated.
5. In this study, the online optimal control strategy considers the energy balance only at each time interval without considering the energy balance over the design period. Online optimal control strategies, which are capable to assure the zero/low energy goal in the operation of zero/low energy buildings need to be explored in the future.

REFERENCE

Adamski, M. 2007. Optimization of the form of a building on an oval base. Building and Environment 42: 1632–1643.

Asadi, S., S.S. Amiri, and M. Mottahedi. 2014. On the development of multi-linear regression analysis to assess energy consumption in the early stages of building design. Energy and Buildings 85: 246–255.

Asadpoure, A., M. Tootkaboni, and J.K. Guest. 2011. Robust topology optimization of structures with uncertainties in stiffness-Application to truss structures. Computers & Structures 89: 1131-1141.

Ascione, F., N. Bianco, C. De Stasio, G.M. Mauro, and G.P. Vanoli. 2016. Multi-stage and multi-objective optimization for energy retrofitting a developed hospital reference building: A new approach to assess cost-optimality. Applied energy 174: 37-68.

Ascione, F., N. Bianco, G. M. Mauro, and G.P. Vanoli. 2019. A new comprehensive framework for the multi-objective optimization of building energy design: Harlequin. Applied energy 241: 331-361.

Ascione, F., N. Bianco, R. F. De Masi, G.M. Mauro, and G.P. Vanoli. 2017. Resilience of robust cost-optimal energy retrofit of buildings to global warming: A multi-stage, multi-objective approach. Energy and Buildings 153: 150-167.

ASHARE. 2010. Standard 55 - Thermal environmental conditions for human occupancy. Atlanta: ASHRAE.

ASHRAE. 2005. ASHRAE handbook: HVAC systems and equipment. Atlanta: ASHRAE.

Back, T. 1996. Evolutionary Algorithms in Theory and Practice: Evolution Strategies, Evolutionary Programming, Genetic Algorithms. Oxford, UK: Oxford University Press.

Baker, N.V. 1987. Passive and low energy building design for tropical island climate. The

Commonwealth Secretariat.

Bernal-Agustín, J.L., and R. Dufo-Lopez. 2009. Simulation and optimization of stand-alone hybrid renewable energy systems. Renewable and Sustainable Energy Reviews 13(8): 2111-2118.

Bordbari, M.J., A.R. Seifi, and M. Rastegar. 2018. Porbabilistic energy consumption analysis in building using point estimate method. Energy 142: 716-722.

Burhenne, S., D. Jacob and G.P. Henze. 2010. Uncertainty analysis in building simulation with Monte Carlo techniques. Proceedings of SimBuild 2010: 4th National Conference of IBPSA-USA, New York, August 11-13.

Chen, X., H.X. Yang, and K. Sun. 2017. Developing a meta-model for sensitivity analyses and prediction of building performance for passively designed high-rise residential buildings. Applied Energy 194: 422-439.

Cheng, Q., S.W. Wang and C.C. Yan. 2016. Robust optimal design of chilled water systems in buildings with quantified uncertainty and reliability for minimized life-cycle cost. Energy and Buildings 126: 159-169.

Cheng, Q., S.W. Wang and C.C. Yan. 2016. Sequential Monte Carlo simulation for robust optimal design of cooling water system with quantified uncertainty and reliability. Energy 118: 489-501.

Cheng, Q., S.W. Wang, C.C. Yan, and F. Xiao. 2017. Probabilistic approach for uncertainty-based optimal design of chiller plants in buildings. Applied Energy 185: 1613-1624.

CIC. 2018. Zero Carbon Design. https://zcb.cic.hk/eng/story-of-zcb.

Clift, R. 2007. Climate change and energy policy: the importance of sustainability

arguments. Energy 30: 769-782.

Corrado, V., and H.E. Mechri. 2009. Uncertainty and sensitivity analysis for building energy rating. Journal of Building Physics 33(2): 125-156.

Crawley, D., S. Pless, and P. Torcellini. 2009. Getting to net zero. ASHRAE Journal 51(9): 18–25.

Crawley, D.B., L.K. Lawrie, F.C. Winkelmann, W.F. Buhl, Y.J. Huang, C.O. Pedersen, et al. 2001. EnergyPlus: creating a new-generation building energy simulation program. Energy and Buildings 33(4): 319-331.

D'Agostino, D., and D. Parker. 2018. A framework for the cost-optimal design of nearly zero energy buildings (NZEBs) in representative climates across Europe. Energy 149: 814-829.

Dall'O', G., V. Belli, M. Brolis, I. Mozzi, and M. Fasano. 2013. Nearly zero-energy buildings of the Lombardy region (Italy), a case study of high-energy performance buildings. Energies 6: 3506-3527.

Daud, A.K., and M.S. Ismail. 2012. Design of isolated hybrid systems minimizing costs and pollutant emissions. Renewable Energy 44: 215-224.

De Wit, S., and G. Augenbroe. 2002. Analysis of uncertainty in building design evaluations and its implications. Energy and Buildings 34 (9):951-8.

Diaf, S., M. Belhamel, M. Haddadi, and A. Louche. 2008. Technical and economic assessment of hybrid photovoltaic/wind system with battery storage in Corsica island. Energy Policy 36(2): 743-754.

Doltsinis, I., Z. Kang, and G.D. Cheng. 2015. Robust design of non-linear structures using optimization methods. Computer Methods in Applied Mechanics and Engineering 194:

1779-1795.

EMSD. 2016. Hong Kong energy end-use data. http://www.emsd.gov.hk/emsd/eng/pee/edata_1.shtml.

Environment Bureau. 2017. Hong Kong's Climate Action Plan 2030+.

Erdinc, O., and M. Uzunoglu. 2012. Optimum design of hybrid renewable energy systems: Overview of different approaches. Renewable and Sustainable Energy Reviews 16: 1412-1425.

Fan, C., G.S. Huang, and Y.J. Sun. 2018. A collaborative control optimization of grid-connected net zero energy buildings for performance improvements at building group level. Energy 164: 536-549.

Fanger, P.O. 1972. Thermal comfort: Analysis and applications in environmental engineering. McGraw-Hill.

Ferrara, M., E. Fabrizio, J. Virgone, and M. Filippi. 2014. A simulation-based optimization method for cost-optimal analysis of nearly Zero Energy Buildings. Energy ad Buildings 84: 442-457.

Fong, K.F., and C.K. Lee. 2012. Towards net zero energy design for low-rise residential buildings in subtropical Hong Kong. Applied Energy 93: 686-694.

Gang, W.J., G. Augenbroe, S.W. Wang, C. Fan and F. Xiao. 2016. An uncertainty-based design optimization method for district cooling systems. Energy 102: 516-527.

Gang, W.J., S.W. Wang, F. Xiao, and D.C. Gao. 2015. Robust optimal design of building cooling systems considering cooling load uncertainty and equipment reliability. Applied Energy 159: 265-275.

Gang, W.J., S.W. Wang, G. Augenbroe, and F. Xiao. 2016. Robust optimal design of

district cooling systems and the impacts of uncertainty and reliability. Energy and Buildings 122: 11-22.

Gang, W.J., S.W. Wang, K. Shan and D.C. Gao. 2015. Impacts of cooling load calculation uncertainties on the design optimization of building cooling systems. Energy and Buildings 94: 1-9.

Ge, H., and F. Baba. 2015. Dynamic effect of thermal bridges on the energy performance of a low-rise residential building. Energy and Buildings 105: 106-118.

Gelder, L.V., H. Janssen, and S. Roels. 2014. Probabilistic design and analysis of building performances: Methodology and application example. Energy and Buildings 79: 202-211.

Georges, L., C. Massart, G.V. Moeseke, and A.D. Herde. 2012. Environmental and economic performance of heating systems for energy-efficient dwellings: Case of passive and low-energy single-family houses. Energy Policy 40: 452-464.

Guglielmetti, R., D. Macumber, and N. Long. 2011. OpenStudio: an open source integrated analysis platform. Proceedings of Building Simulation 2011, Sydney, Australia, November 14-16.

Hamdy, M., A. Hasan, and K. Siren. 2013. A multi-stage optimization method for cost-optimal and nearly-zero-energy building solutions in line with the EPBD-recast 2010. Energy and Buildings 56: 189-203.

Hamdy, M., M. Palonen, and A. Hasan. 2012. Implementation of pareto-archive NSGA-II algorithms to a nearly-zero-energy building optimisation problem. First Building Simulation and Optimization Conference. Loughborough, UK, September 10-11.

Heiselberg, P., H. Brohus, A. Hesselholt, H. Rasmussen, E. Seinre, and S. Thomas. 2009.

Application of sensitivity analysis in design of sustainable buildings. Renewable Energy 34: 2030-2036.

Helton, J.C., and F.J. Davis. 2002. Latin hypercube sampling and the propagation of uncertainty in analyses of complex systems. New Mexico, USA: Sandia National Laboratories. SAND2001-0417.

Helton, J.C., and F.J. Davis. 2003. Latin hypercube sampling and the propagation of uncertainty in analyses of complex systems. Reliability Engineering & System Safety 81(1): 23-69.

Helton, J.C., F.J. Davis, and J.D. Johnson. 2005. A comparison of uncertainty and sensitivity analysis results obtained with random and Latin hypercube sampling. Reliability Engineering and System Safety 89: 305-300.

Hernandez, P., and P. Kenny. 2010. From net energy to zero energy buildings: Defining life cycle zero energy buildings (LC-ZEB). Energy and Buildings 42(6): 815-821.

Hoes, P., M. Trcka, J.L.M. Hensen, and B.H. Bonnema. 2011. Optimizing building designs using a robustness indicator with respect to user behaviour. Proceedings of the 12th International Building Performance Simulation Association, Sydney, November 14-16.

Hong Kong Observatory. 2015. Monthly Meteorological Normals for Hong Kong. http://www.hko.gov.hk/cis/normal/1981_2010/normals_e.htm#table4.

Hooke, R., and T.A. Jeeves. 1961. “Direct Search” solution of numerical and statistical problems. Journal of the ACM 8(2): 212–229.

Hopfe, C.J. and J.L.M. Hensen. 2011. Uncertainty analysis in building performance simulation for design support. Energy and Buildings 43(10): 2798-2805.

Huang, P., and Y.J. Sun. 2019. A collaborative demand control of nearly zero energy buildings in response to dynamic pricing for performance improvements at cluster level. Energy 174: 911-921.

Huang, P., G.S. Huang, and Y.J. Sun. 2018. A robust design of nearly zero energy building systems considering performance degradation and maintenance. Energy 163: 905-919.

Huang, Y., and J.L. Niu. 2016. Optimal building envelope design based on simulated performance: History, current status and new potentials. Energy and Buildings 117: 387-398.

Hui, S.C.M. 2010. Zero energy and zero carbon buildings: myths and facts. Proceedings of the International Conference on Intelligent Systems, Structures and Facilities (ISSF2010): Intelligent Infrastructure and Buildings, Hong Kong, China, January 12.

Hygh, J.S., J.F. DeCarolis, D.B. Hill, and R. Ranjithan. 2012. Multivariate regression as an energy assessment tool in early building design. Building and Environment 57: 165-175.

International Energy Agency (IEA). 2017. Key world energy statistics 2017. Paris: OECD/IEA.

International Energy Agency (IEA). 2018. World energy outlook 2018. Paris: OECD/IEA.

Ismail, M.S., M. Moghavvemi, and T.M.I. Mahlia. 2012. Design of a PV/diesel standalone hybrid system for a remote community in Palestine. Journal of Asian Scientific Research 2(11): 599-606.

Janssen, H. 2013. Monte-Carlo based uncertainty analysis: Sampling efficiency and sampling convergence. Reliability Engineering and System Safety 109: 123-132.

Johnson, M.H., Z.Q. Zhai, and M. Krarti. 2012. Performance evaluation of network

airflow models for natural ventilation. HVAC&R Research 18(3): 349-365.

Joint Research Center of the European Commission. 2011. SIMLAB, Version 2.2. Simulation environment for uncertainty and sensitivity Analysis. Joint Research Center of the European Commission, Italy.

José, L.B.A., and D.L. Rodolfo. 2009. Simulation and optimization of standalone hybrid renewable energy systems. Renewable and Sustainable Energy Reviews 13(8): 2111-2118.

Kaabeche, A., and R. Ibtiouen. 2014. Techno-economic optimization of hybrid photovoltaic/wind/diesel/battery generation in a stand-alone power system. Solar Energy 103: 171-182.

Kapsalaki, M., V. Leal, and M. Santamouris. 2012. A methodology for economic efficient design of Net Zero Energy Buildings. Energy and Buildings 55: 765-778.

Kohavi, R. 1995. A study of cross-validation and bootstrap for accuracy estimation and model selection. International Joint Conference on Artificial Intelligence 1995.

Kolokotsa, D., D. Rovas, E. Kosmatopoulos, and K. Kalaitzakis. 2011. A roadmap towards intelligent net zero-and positive-energy buildings. Solar Energy 85(12): 3067-3084.

Kumar, K.S., K.N. Tiwari, and M.K. Jha. 2009. Design and technology for greenhouse cooling in tropical and subtropical regions: A review. Energy and Buildings 41: 1269-1275.

Kurnitski, J., A. Saari, T. Kalamees, M. Vuolle, J. Niemelä, and T. Tark. 2011. Cost optimal and nearly zero (nZEB) energy performance calculations for residential buildings with REHVA definition for nZEB national implementation. Energy and

Buildings 43: 3279-3288.

Kurnitski, J., F. Allard, D. Braham, G. Goeders, P. Heiselberg, L. Jagemar, R. Kosonen, J. Lebrun, L. Mazzarella, J. Railio, O. Seppänen, M. Schmidt, and M. Virta. 2011. How to define nearly net zero energy buildings nZEB. REHVA Journal: 6-12.

Lam, J.C., and S.C.M. Hui. 1996. Sensitivity analysis of energy performance of office buildings. Building and Environment 31(1): 27-39.

Li, D.H., L. Yang, and J.C. Lam. 2013. Zero energy buildings and sustainable development implications–a review. Energy 54: 1-10.

Li, H.X., and S.W. Wang. 2017. Probabilistic optimal design concerning uncertainties and on-site adaptive commissioning of air-conditioning water pump systems in buildings. Applied Energy 202: 53-65.

Liu, M.X., Y. Shi, and F. Fang. 2012. A new operation strategy for CCHP systems with hybrid chillers. Applied Energy 95: 164-173.

Liu, Z.B., L. Zhang, G.C. Gong, H.X. Li, and G.F. Tang. 2015. Review of solar thermoelectric cooling technologies for use in zero energy buildings. Energy and Buildings 102: 207-216.

Lojuntin, S. 2018. Zero Energy Building in Malaysia by SEDA Malaysia. https://www.slideshare.net/asetip/zero-energy-building-in-malaysia-by-seda-alaysia.

Lu, Y.H., S.W. Wang, and K. Shan. 2015. Design optimization and optimal control of grid-connected and standalone nearly/net zero energy buildings. Applied Energy 155: 463-477.

Lu, Y.H., S.W. Wang, C.C. Yan, and K. Shan. 2015. Impacts of renewable energy system design inputs on the performance robustness of net zero energy buildings. Energy 93:

1595-1606.

Lu, Y.H., S.W. Wang, Y. Zhao, and C.C. Yan. 2015. Renewable energy system optimization of low/zero energy buildings using single-objective and multi-objective optimization methods. Energy and Buildings 89: 61-75.

Lu, Y.H., S.W. Wang, Y.J. Sun, and C.C. Yan. 2015. Optimal scheduling of buildings with energy generation and thermal energy storage under dynamic electricity pricing using mixed-integer nonlinear programming. Applied Energy 147: 49-58.

Ma, L., N. Liu, L.F. Wang, J.H. Zhang, J.Y. Lei, Z. Zeng, C. Wang, and M.Y. Cheng. 2016. Multi-party energy management for smart building cluster with PV systems using automatic demand response. Energy and Buildings 121: 11-21.

Macdonald, I., and P. Strachan. 2001. Practical application of uncertainty analysis. Energy and Buildings 33(3):219-27.

Macdonald, I.A. 2002. Quantifying the effects of uncertainty in building simulation. PhD dissertation, University of Strathclyde.

Maheri, A. 2014. Multi-objective design optimisation of standalone hybrid wind-PV-diesel systems under uncertainties. Renewable Energy 66: 650-661.

Marszal, A.J., and P. Heiselberg. 2011. Life cycle cost analysis of a multi-storey residential Net Zero Energy Building in Denmark. Energy 36: 5600-5609.

Marszal, A.J., P. Heiselberg, J.S. Bourrelle, E. Musall, K. Voss, I. Sartori, and A. Napolitano. 2011. Zero Energy Building – A review of definitions and calculation methodologies. Energy and Buildings 43: 971-979.

Martirano, L., and A. Giuseppi. 2018. Nearly Zero Energy Building model predictive control for efficient heating. Proceedings in 2019 IEEE Industry Applications Society

Annual Meeting, USA, Portland, September 23-27.

Martirano, L., and G. Greco. 2017. Demand side management in microgrids for load control in nearly zero energy buildings. IEEE Transactions on Industry Applications 53(3): 1769-1779.

Matala, A. 2008. Sample size requirement for Monte Carlo-simulations using Latin Hypercube Sampling. Helsinki University of Technology.

Matthies, H.G. 2007. Quantifying uncertainty: modern computational representation of probability and applications. Extreme Man-Made and Natural Hazards in Dynamics of Structures: 105-135.

McKay, M.D., R.J. Beckman, and W.J. Conover. 1979. A comparison of three methods for selecting values for input variables in the analysis of output from a computer code. Technometrics 21: 239-245.

McRae, G.J., J.W. Tilden, and J.H. Seinfeld. 1982. Global sensitivity analysis - a computational implementation of the Fourier Amplitude Sensitivity Test (FAST). Computers & Chemical Engineering 6: 15-25.

Mechri, H.E., A. Capozzoli, and V. Corrado. 2010. Use of the ANOVA approach for sensitive building energy design. Applied Energy 87: 3073-3083.

Morgan, M.G. 2009. Best practice approaches for characterizing, communicating and incorporating scientific uncertainty in climate decision making. DIANE Publishing.

Morris, M.D. 1991. Factorial sampling plans for preliminary computational experiments. Technometrics 33: 161-174.

Morrison Hershfield Limited. 2016. Building envelope thermal bridging guide. Vancouver: BC Hydro Power Smart.

Mulvey, J.M., R.J. Vanderbei, and S.A. Zenios. 1995. Robust optimization of large-scale systems. Operations Research 43(2): 264-281.

National Climate Change Secretariat. 2016. Singapore's Climate Action Plan: Take Action Today, For a Carbon-Efficient Singapore.

Natural Resources Canada. 2017. Build smart – Canada's buildings strategy: a key driver of the pan-Canadian framework on clean growth and climate change. Energy and Mines Ministers' Conference. St. Andrews by-the-sea, New Brunswick, Canada, August.

NDRC: National Development & Reform Commission of China. 2015. China's Intended Nationally Determined Contribution: Enhanced Actions on Climate Change. Beijing, China.

Nguyen, A.T., and S. Reiter. 2015. A performance comparison of sensitivity analysis methods for building energy models. Building Simulation 8(6): 651-664.

Nguyen, A.T., S. Reiter, and P. Rigo. 2014. A review on simulation-based optimization methods applied to building performance analysis. Applied Energy 113: 1043-1058.

Nottrott, A., J. Kleissl, and B. Washom. 2013. Energy dispatch schedule optimization and cost benefit analysis for grid-connected, photovoltaic-battery storage systems. Renewable Energy 55: 230-240.

Odonkor, P., and K. Lewis. 2015. Adaptive operation decisions in net zero building clusters. Proceedings of the ASME 2015 International Design Engineering Technical Conferences & Computers and Information in Engineering Conference, Boston, Massachusetts, USA, August 2-5.

Official Journal of the European Union. 2010. The Directive 2010/31/EU of the European

Parliament and of the Council of 19 May 2010 on the energy performance of buildings. http://eurlex.europa.eu/LexUriServ/LexUriServ.do?uri=OJ:L:2010:153:0013:0035:EN:PDF

Park, G.J., T.H. Lee, and K.H. Lee. 2006. Robust design: An overview. AIAA Journal 44(1): 181-191.

Peterson, S. and K.W. Bundgaard. 2014. The effect of weather forecast uncertainty on a predictive control concept for building systems operation. Applied Energy 116: 311-321.

Pikas, E., M. Thalfeldt, and J. Kurnitski. 2014. Cost optimal and nearly zero energy building solutions for office buildings. Energy and Buildings 74: 30-42.

Province of British Columbia. 2018. British Columbia Building Code 2018.

Rao, S.S., and T.I. Freiheit. 1990. A modified game theory approach to multiobjective optimization. Journal of Mechanical Design 113(3): 286-291.

Rezvan, A.T., N.S. Gharneh, and G.B. Gharehpetian. 2012. Robust optimization of distributed generation investment in buildings. Energy 48: 455-463.

Rodriguez-Ubinas, E., C. Montero, M. Porteros, S. Vega, I. Navarro, M. Castillo-Cagigal, et al. 2014. Passive design strategies and performance of Net Energy Plus Houses. Energy and Buildings 83: 10-22.

Rysanek, A.M., and R. Choudhary. 2012. A decoupled whole-building simulation engine for rapid exhaustive search of low-carbon and low-energy building refurbishment options. Building and Environment 50: 21-33.

Sanchez, D.G., B. Lacarrière, M. Musy, and B. Bourges. 2014. Application of sensitivity analysis in building energy simulations: Combining first- and second-order elementary

effects methods. Energy and Buildings 68: 741-750.

Sartori, I., and A.G. Hestnes. 2007. Energy use in the life cycle of conventional and low-energy buildings: A review article. Energy and Buildings 39(3): 249-257.

Schirrer, A., M. Brandstetter, I. Leobner, S. Hauer, and M. Kozek. 2016. Nonlinear model predictive control for a heating and cooling system of a low-energy office building. Energy and Buildings 125: 86-98.

Schnieders, J., T. Schulz, W. Feist, B. Kaufmann, S. Sheng, H.J. Jiang, S. Winkel, E. Buteikyte and C. Sifferlen. 2016. Passive houses in Chinese climates. Germany: Wolfgang Feist, Passive House Institute and University of Innsbruck, Unit for Energy Efficient Buildings.

Shaikh, P.H., N.B.M. Nor, P. Nallagownden, I. Elamvazuthi, and T. Ibrahim. 2014. A review on optimized control systems for building energy and comfort management of smart sustainable buildings. Renewable and Sustainable Energy Reviews 34: 409-429.

Shaikh, P.H., N.B.M. Nor, P. Nallagownden, I. Elamvazuthi, and T. Ibrahim. 2016. Intelligent multi-objective control and management for smart energy efficient buildings. International Journal of Electrical Power & Energy Systems 74: 403-409.

Singh, R., I.J. Lazarus, and V.V.N. Kishore. 2016. Uncertainty and sensitivity analyses of energy and visual performances of office building with external venetian blind shading in hot-dry climate. Applied Energy 184: 155-170.

Sowden, M. 2002. Oversized and underachieving. World Pumps 433: 38-41.

Spitz, C., L. Mora, E. Wurtz, and A. Jay. 2012. Practical application of uncertainty analysis and sensitivity analysis on an experimental house. Energy and Buildings 55: 459-470.

Stadler, M., A. Siddiqui, C. Marnay, H. Aki, and J. Lai. 2011. Control of greenhouse gas emissions by optimal DER technology investment and energy management in zero-net-energy buildings. European Transactions On Electric Power 21: 1291-1309.

Stein, M. 1987. Large sample properties of simulations using Latin hypercube sampling. Technometrics 29: 143-151.

Sun, Y. 2014. Closing the Building Energy Performance Gap by Improving Our Predictions. PhD Dissertation, Georgia Institute of Technology, United States.

Sun, Y.J. 2015. Sensitivity analysis of macro-parameters in the system design of net zero energy building. Energy and Buildings 86: 464-477.

Sun, Y.J., P. Huang, and G.S. Huang. 2015. A multi-criteria system design optimization for net zero energy buildings under uncertainties. Energy and Buildings 97: 196-204.

Sun, Y.M., L. Gu, C.F.J. Wu and G. Augenbroe. 2014. Exploring HVAC system sizing under uncertainty. Energy and Buildings 81: 243-252.

Svozil, D., V. Kvasnička, and J. Pospíchal. 1997. Introduction to multi-layer feed-forward neural networks. Chemometrics and Intelligent Laboratory Systems 39: 43-62.

Tavares, P., and A. Martins. 2007. Energy efficient building design using sensitivity analysis – a case study. Energy and Buildings 39(1): 23-31.

Thalfeldt, M., E. Pikas, J. Kurnitski, and H. Voll. 2013. Facade design principles for nearly zero energy buildings in a cold climate. Energy and Buildings 67: 309-321.

Tian, W. 2013. A review of sensitivity analysis methods in building energy analysis. Renewable and Sustainable Energy Reviews 20: 411-419.

Tian, W., and D.P. Wilde. 2011. Uncertainty and sensitivity analysis of building performance using probabilistic climate projections: A UK case study. Automation in

Construction 20: 1096-1109.

Tian, W., Y. Heo, P.D. Wilde, Z.Y. Li, D. Yan, C.S. Park, X.H. Feng, and G. Augenbroe. 2018. A review of uncertainty analysis in building energy assessment. Renewable and Sustainable Energy Reviews 93: 285-301.

Ting, C.K. 2005. On the mean convergence time of multi-parent genetic algorithms without selection. European Conference on Artificial Life: 403-412.

Torcellini, P., S. Pless, and M. Deru. 2006. Zero energy buildings: a critical look at the definition. National Renewable Energy Laboratory U.S. Department of Energy.

Walker, W.E., P. Harremoës, J. Rotmans, J. Sluijs, M. Asselt, P. Janssen, and M. Krauss. 2003. Defining uncertainty: a conceptual basis for uncertainty management in model-based decision support. Integrated assessment 4(1):5-17.

Wang, C.S., B.Q. Jiao, L. Guo, Z. Tian, J.D. Niu, and S.W. Li. 2016. Robust scheduling of building energy system under uncertainty. Applied Energy 167: 366-376.

Wang, L.P., J. Gwilliam, and P. Jones. 2009. Case study of zero energy house design in UK. Energy and Buildings 41: 1215-1222.

Wang, S.W., and Z.J. Ma. 2008. Supervisory and optimal control of building HVAC systems: A review. HVAC&R Research 14(1): 3-32.

Wang, S.W., C.C. Yan and F. Xiao. 2012. Quantitative energy performance assessment methods for existing buildings. Energy and Buildings 55: 873-888.

Wilcox, S., and W. Marion. 2008. Users Manual for TMY3 Data Sets. Colorado: National Renewable Energy Laboratory (NREL).

Wit, S.D. and G. Augenbroe. 2002. Analysis of uncertainty in building design evaluations and its implications. Energy and Buildings 34(9): 951-958.

Yan, C.C, S.W. Wang, and F. Xiao. 2012. A simplified energy performance assessment method for existing buildings based on energy bill disaggregation. Energy and Buildings 55: 563-574.

Yang, R., Z. Wang, and L.F. Wang. 2011. A GUI-based simulation platform for energy and comfort management in zero-energy buildings. Proceedings in 2011 North American Power Symposium, Boston, MA, USA, 4-6 August.

Yang, S., W. Tian, E. Cubi, Q.X. Meng, Y.L. Liu, and L. Wei. 2016. Comparison of sensitivity analysis methods in building energy assessment. Procedia Engineering 146: 174-181.

Yao, W., X.Q. Chen, W.C. Luo, M.V. Tooren, and J. Guo. 2011. Review of uncertainty-based multidisciplinary design optimization methods for aerospace vehicles. Progress in Aerospace Sciences 47: 450-479.

Yik, F.W.H., W.L. Lee, J. Burnett and P. Jones. 1999. Chiller plant sizing by cooling load simulation as a means to avoid oversized plant. HKIE Transactions 6(2): 19-25.

Yildiz, Y., and Z.D. Arsan. 2011. Identification of the building parameters that influence heating and cooling energy loads for apartment buildings in hot-humid climates. Energy 36: 4287-4296.

Yu, C.S., and H.L. Li. 2000. A robust optimization model for stochastic logistic problems. International Journal of Production Economics 64: 385-397.

Yu, J.H., C.Z. Yang, and L.W. Tian. 2008. Low-energy envelope design of residential building in hot summer and cold winter zone in China. Energy and Buildings 40(8): 1536-1546.

Yu, J.H., L.W. Tian, C.Z. Yang, X.H. Xu, and J.B. Wang. 2013. Sensitivity analysis of

energy performance for high-rise residential envelope in hot summer and cold winter zone of China. Energy and Buildings 64: 264-274.

Yu, Z., Y. Zhou, and A. Dexter. 2007. Hierarchical fuzzy rule-based control of renewable energy building systems. Renewables in a changing climate: 507-512.

Zero-energy building. https://en.wikipedia.org/wiki/Zero-energy_building

Zhang, S., P. Huang, and Y.J. Sun. 2016. A multi-criterion renewable energy system design optimization for net zero energy buildings under uncertainties. Energy 94: 654-665.

Zhang, Y. 2009. “Parallel” EnergyPlus and the development of a parametric analysis tool. Proceedings of the 11th International IBPSA Conference, Glasgow, Scotland, July 27-30.

Zhao, M., H.M. Künzel, and F. Antretter. 2015. Parameters influencing the energy performance of residential buildings in different Chinese climate zones. Energy and Buildings 96: 64-75.

Zhao, Y., Y.H. Lu, C.C. Yan, and S.W. Wang. 2015. MPC-based optimal scheduling of grid-connected low energy buildings with thermal energy storages. Energy and Buildings 86: 415-426.

Zhou, Z.H., L. Feng, S.Z. Zhang, C.D. Wang, G.Y. Chen, T. Du, Y.S. Li, and J. Zuo. 2016. The operational performance of “net zero energy building”: A study in China. Applied Energy 177: 716-728.